

FUNCTIONAL CHARACTERIZATION OF *TRIB1*, A GENE ASSOCIATED WITH MULTIPLE
CARDIOMETABOLIC TRAITS

Katherine Quiroz-Figueroa

A DISSERTATION

in

Cell and Molecular Biology

Presented to the Faculties of the University of Pennsylvania

in

Partial Fulfillment of the Requirements for the

Degree of Doctor of Philosophy

2021

Supervisor of Dissertation

Graduate Group Chairperson

Daniel J. Rader, MD

Daniel S. Kessler, PhD

Seymour Gray Professor of

Associate Professor of

Molecular Medicine

Cell and Developmental Biology

Dissertation Committee:

- Klaus H. Kaestner, Ph.D., Thomas and Evelyn Suor Butterworth Professor in Genetics.
- Warren S. Pear, M.D., Ph.D., Gaylord P. and Mary Louise Harnwell Professor of Pathology and Laboratory Medicine.
- Kiran Musunuru, M.D., Ph.D., M.P.H., M.L., Professor of Medicine.
- Benjamin F. Voight, Ph.D., Associate Professor of Systems Pharmacology and Translational Therapeutics.

*This thesis is dedicated to my family and friends,
without your love and support I would have not made it this far!*

ACKNOWLEDGMENTS

First, I would like to acknowledge my thesis advisor Dr. Daniel Rader for all his mentorship, guidance, and support. Thanks for giving me the opportunity to be part of such an amazing lab and allowing me to pursue a research area that was completely new, but greatly exciting for me. I also wish to acknowledge my thesis committee consisting of Drs. Klaus Kaestner (chair), Warren Pear, Kiran Musunuru and Benjamin Voight. Thank you for your thoughtful critiques, guidance and dedication to my mentorship.

I highly thank Dr. Nicholas Hand, who mentored and supported me through of my PhD. Thank you for helping me every step of the way, for always providing feedback for all my abstracts, posters, conference talks, grants, manuscripts, etc.! and for always listening and providing encouragement during difficult times.

I also want to thank all the member of the Rader Lab, both past and present. Each and everyone of you have helped me so much and I would not have done this without you! Deepti Abbey, thank you for introducing me to the lab as my rotation mentor and for continuing mentoring me even after my project had nothing to do with yours. Cecilia Vitali, thank for all the help figuring out my kinetics experiments, western blots and for always being there when I needed help. Donna Conlon, thank you always helping with apoB secretion experiments as well as discussing all aspects of my projects. Kate Townsend Creasy, thanks for helping me will glucose and glycogen metabolism experiments, for always having great constructive feedback and for always helping me when I needed it. Xin Bi, thank you for all your feedback and all the great conversations. I specially want to thank Sylvia Stankov for being the best bay mate and peer I could have asked for! Thanks for listening to all my rants, for encouraging me when I was down and always being down

to celebrate our minor accomplishments. You made my PhD experience so much more fun and hopefully I made yours a bit better too! I will miss you!

I also want to thank John Millar, Jeff Billheimer and Marie Guerraty for all the great discussions and all the feedback I received from them. Thanks to Linda Carmichael, Stephanie DerOhannessian, Dawn Marchadier, Susannah Elwin, Amrith Rodrigues and Teo Tram for keeping the lab running smoothly. Thanks to Debra Cromley for always running my plasma lipid test and FPLC and Linda Morell for isolating all the lipoprotein I ever needed. My biggest thanks go to the Animal Team, Aisha Wilson, Eduoard Edwige, and previously Maosen Sun for all their help with animal experiments, I could not have done it without you guys! Special thanks to Aish for always being so happy and bright and always being down for a coffee, I will greatly miss our chitchats! Thank you so much to other previous members of the lab that helped me on innumerable ways and always provided me with their support: Robert Bauer, Swapnil Shewale, Liya Yu, Andrea Berrido, Mikhaila Smith, Mayda Hernandez and many others.

Last, I want to acknowledge my family and friends. I want to thank my mom (Sarah Figueroa), my dad (Clemente Quiroz) and my brother (Angel D. Quiroz) for always being there for me, I would not be where I am without you! I would like to thank my best friend of 13 years Katherine Adams who my biggest fan and supporter. My fiancé and love of my life Christopher Parker-Rajewski. My PhD mates that have become my closest friends: Ryan Roark, Jennifer Aleman, Kelsey Kaeding, Antonia Bass and Priya Khurana! All of you have been my pillar throughout this time and I could never thank you enough for everything you have done for me.

ABSTRACT

FUNCTIONAL CHARACTERIZATION OF *TRIB1*, A GENE ASSOCIATED WITH MULTIPLE CARDIOMETABOLIC TRAITS

Katherine Quiroz-Figueroa

Daniel J. Rader

Genetic variants near the *TRIB1* gene are significantly associated with plasma lipid traits and coronary artery disease. While data suggest *TRIB1* is the causal gene for these traits, the mechanisms by which *TRIB1* affects plasma lipids are not fully understood. In these studies, I sought to elucidate the physiological and molecular mechanism by which *TRIB1* affects plasma lipids. Using a *Trib1* hepatocyte specific deletion mouse model (*Trib1^{Δhep}*), I demonstrated that *Trib1^{Δhep}* mice have significantly increased plasma total cholesterol, HDL cholesterol, non-HDL cholesterol, LDL cholesterol and apoB protein levels, as well as impaired postprandial triglyceride clearance. I also showed that *Trib1^{Δhep}* mice have markedly delayed catabolism of LDL-apoB and VLDL-apoB due to significantly decreased *Ldlr* mRNA and protein expression. Since *TRIB1*'s most studied molecular function is the COP1-mediated ubiquitination and proteasomal degradation the transcription factor CEBPa, I explored if this interaction is responsible for *TRIB1* effects on plasma lipids and LDLR. I demonstrated that hepatic deletion of *Cebpa* in *Trib1^{Δhep}* mice eliminated the effects on plasma lipids, apoB catabolism and hepatic LDLR regulation. Additionally, I identified the Activating Transcription Factor 3 (*Atf3*) as a possible novel mechanism linking *TRIB1* to the regulation of LDLR in a CEBPa dependent manner. We also discovered that *Trib1* whole body deletion (*Trib1* KO) on a pure C57BL/6 background leads to a highly penetrant neonatal lethal phenotype, with less than 5% of *Trib1* KO mice making to weaning stages. Our studies determined that *Trib1* KO perish between day 0

and day 1 after birth likely due to severely low blood glucose levels. I also determined that about adult *Trib1* KO mouse have decreased fasting glucose levels, and improved glucose and insulin tolerance. Overall, my studies establish *Trib1* and its regulation of CEBP α as critical factors in the regulation of multiple metabolic pathways affecting plasma lipids, as well as novel regulators of the LDLR and glucose metabolism.

TABLE OF CONTENTS

ACKNOWLEDGMENTS	iii
ABSTRACT	v
TABLE OF CONTENTS	vii
LIST OF TABLES	ix
LIST OF ILLUSTRATIONS	x
CHAPTER 1: INTRODUCTION	1
Plasma Lipids Regulation and Cardiometabolic Disease Association	1
VLDL, IDL and LDL Metabolism (Endogenous Lipoprotein Pathway)	2
Chylomicron metabolism (Exogenous lipoprotein pathway)	6
HDL metabolism (Reverse cholesterol transfer pathway).....	7
Human genome wide association studies (GWAS) are a helpful tool to identify novel genetic loci for cardiometabolic traits.	8
The TRIB1 Locus	13
<i>Tribbles</i> Discovery in <i>Drosophila Melanogaster</i>	13
Mammalian TRIB Family of Proteins Structure, Homology and Functions	14
Mammalian <i>TRIB1</i> , a GWAS hit for multiple cardiometabolic traits	17
Hepatic <i>TRIB1</i> in the regulation of plasma lipids metabolism	18
Goal of this Thesis	22
CHAPTER 2: METHODS	23
CHAPTER 3:	34
ABSTRACT	34
INTRODUCTION	35
RESULTS	36
DISCUSSION	43
FIGURES	48
CHAPTER 4:	68

Hepatic <i>TRIB1</i> regulates LDL metabolism through CEBPA-mediated regulation of the LDL receptor.	68
ABSTRACT	68
INTRODUCTION	69
RESULTS	71
DISCUSSION	79
FIGURES	85
CHAPTER 5:	106
Constitutive deletion of <i>Trib1</i> in mice leads to highly penetrant neonatal lethality due to impaired glucose metabolism.	106
ABSTRACT	106
INTRODUCTION	107
RESULTS	111
DISCUSSION	117
FIGURES	122
SUMMARY AND FUTURE DIRECTIONS	132
APPENDIX	141
Hepatocyte deletion of <i>Trib1</i> leads to the plasma secretion of an unidentified protein of approximately 20 kDa.	141
BIBLIOGRAPHY	146

LIST OF TABLES

Table 1. TaqMan Probes used for Gene Expression Analysis by qRT-PCR	33
Table 2. Motif enrichment analysis of CEPBA ChIP-seq in liver from Trib1 ^{Δhep} mice. ...	105
Table 3. Selected mass spectrometry results based on the size of the unidentified protein band and higher abundance on Trib1 ^{Δhep} vs control mice.....	144

LIST OF ILLUSTRATIONS

Chapter 3: Hepatic TRIB1 regulates plasma lipids by modulating the rates of lipoprotein clearance mediated by the LDL Receptor, as well as modulating the rates of lipoprotein secretion from the liver.

Figure 3. 1: Hepatic Trib1 mRNA levels in Trib1 ^{Δhep} mice relative to control mice.	48
Figure 3. 2: Hepatic Deletion of <i>Trib1</i> increases plasma cholesterol in male mice.	49
Figure 3. 3: Hepatic deletion of <i>Trib1</i> increases plasma cholesterol in female mice.	51
Figure 3. 4: Hepatic deletion of <i>Trib1</i> increases plasma ApoB protein levels in male mice.	53
Figure 3. 5: Hepatic deletion of <i>Trib1</i> increases plasma LDL lipoprotein fractions in male mice.	54
Figure 3. 6: Hepatic deletion of <i>Trib1</i> increases plasma LDL lipoprotein fractions in female mice.	55
Figure 3. 7: Hepatic deletion of <i>Trib1</i> protects against diet induced obesity and show indications of liver damage.	56
Figure 3. 8: Hepatic deletion of <i>Trib1</i> impairs post-prandial triglyceride clearance in male and female mice.	58
Figure 3. 9: Hepatic deletion of <i>Trib1</i> impairs LDL and VLDL apoB clearance in male mice.	59
Figure 3. 10: Hepatic deletion of <i>Trib1</i> impairs LDL apoB clearance in female mice.	61
Figure 3. 11: Hepatic deletion of <i>Trib1</i> reduces <i>Ldlr</i> mRNA and protein levels in male and female mice.	62
Figure 3. 12: Hepatic deletion of <i>Trib1</i> in the absence of <i>Ldlr</i> increases steady state plasma lipids.	63
Figure 3. 13: Hepatic deletion of <i>Trib1</i> in the absence of <i>Ldlr</i> increases steady state plasma lipids.	64
Figure 3. 14: Hepatic deletion of <i>Trib1</i> in the absence of <i>Ldlr</i> increases steady state plasma lipids due to increase in the hepatic secretion of ApoB.	65
Figure 3. 15: Role of Hepatic <i>Trib1</i> in the regulation of LDL-apoB.	67

Chapter 4: Hepatic TRIB1 regulates LDL metabolism through CEBPA-mediated regulation of the LDL receptor.

Figure 4. 1: *Cebpa*^{Δhep} model validation.85

Figure 4. 2: Hepatic deletion of *Trib1* in the absence of *Cebpa* decreases plasma cholesterol in chow and WTD feeding.....86

Figure 4. 3: Hepatic deletion of *Trib1* in the absence of *Cebpa* decreases LDL lipoprotein fractions in in chow and WTD feeding.....88

Figure 4. 4: Hepatic deletion of *Trib1* in the absence of *Cebpa* normalizes hepatic lipids, ALT and albumin levels.89

Figure 4. 5: Hepatic deletion of *Trib1* in the absence of *Cebpa* improves post-prandial triglyceride clearance in mice.90

Figure 4. 6: Hepatic deletion of *Trib1* in the absence of *Cebpa* normalizes LDL and VLDL apoB kinetics and LDLR expression.91

Figure 4. 7: Summary of differentially expressed genes between different groups from RNAseq dataset.93

Figure 4. 8: Zoomed in versions of selected volcano plots of differentially expressed genes in RNAseq dataset.94

Figure 4. 9: Ingenuity Pathway Analysis plots representing the changes in LDLR upstream regulators between different groups.....95

Figure 4. 10: Effects of hepatic deletion of *Trib1* and *Cebpa* on SREBP family members.96

Figure 4. 11: Hepatic deletion of *Trib1* increases *Atf3* mRNA and protein levels in a CEBPA dependent manner97

Figure 4. 12: Ingenuity pathways analysis plot of *Atf3* downstream regulated factors in RNAseq cohort samples98

Figure 4. 13: *Atf3* siRNA deletion efficiency99

Figure 4. 14: Downregulation of *Atf3* in *Trib1*^{Δhep} mice reduces total cholesterol and HDL-C 100

Figure 4. 15: Effects of downregulation of *Atf3* in *Trib1*^{Δhep} mice on lipoprotein distribution. 102

Figure 4. 16: Downregulation of *Atf3* in *Trib1^{Δhep}* mice increases LDLR protein levels. 103

Figure 4. 17: Proposed mechanistic model of how *Trib1* regulates the LDLR in a CEBPa dependent manner. 104

Chapter 5: Whole body deletion of *Trib1* in mice leads to highly penetrant neonatal lethality due to impairment in glucose metabolism

Figure 5. 1: Trib1 KO neonate mice have decreased plasma glucose levels. 122

Figure 5. 2: Trib1 KO mice have normal hepatic lipids and plasma ketones, but reduced plasma lactate and hepatic glycogen levels. 123

Figure 5. 3: Hepatic gene expression of lipogenic genes in neonate mice. 124

Figure 5. 4: Hepatic gene expression of glucogenic genes in neonate mice. 125

Figure 5. 5: Adult Trib1 KO mice have increased levels of plasma total cholesterol, non-HDL cholesterol and ALTS. 126

Figure 5. 6: Adult Trib1 KO mice have impaired postprandial triglyceride clearance. ... 127

Figure 5. 7: Adult Trib1 KO mice have decreased fasting glucose and increased fasting lactate, with normal ketone levels. 128

Figure 5. 8: Adult Trib1 KO mice have improved glucose and insulin tolerance. 129

Figure 5. 9: Hepatic deletion of *Trib1* improves glucose tolerance with no changes in insulin tolerance. 130

Figure 5. 10: Hepatic gene expression in adult Trib1 KO mice. 131

Appendix

Figure 6. 1. *Trib1^{Δhep}* mice secrete an unidentified protein of around 15-25 kDA. 143

CHAPTER 1: INTRODUCTION

Plasma Lipids Regulation and Cardiometabolic Disease Association

Lipids are a diverse group of organic compounds that are grouped together due to their insolubility in water, and include fats, oils, steroid hormones, and other cellular membrane components[1-4]. Lipids have an array of biological functions such as energy storage, phospholipid bi-layer formation, signaling, and transport, which makes them essential for life [1]. Additionally, cellular lipid composition and systemic lipids are highly influenced by dietary, environmental, and genetic factors. As lipids are insoluble in water, they are transported in the circulation in association with proteins in complexes called lipoproteins, which are complex particles containing cholesterol esters and triglycerides in their center and surrounded by phospholipids, free cholesterol and apolipoproteins [2, 5]. Lipoproteins are commonly divided into six classes which are based on size and lipid composition: chylomicrons, chylomicron remnants, very low-density lipoproteins (VLDL), intermediate density lipoproteins (IDL), low density lipoproteins (LDL) and high-density lipoproteins (HDL); organized from higher to lower triglyceride content [5, 6].

These lipoproteins are sub-divided in two additional categories based on the main apolipoprotein they contain. The first group contains apolipoprotein B (apoB) as their main protein, which includes chylomicrons, VLDL and their remnant particles, as well as LDL lipoproteins. The second group contains apolipoprotein A-I (apoA-I) as their key structural protein, which include HDL lipoproteins [6, 7]. The plasma concentrations of all these lipoproteins have been broadly studied for many decades and are related to risk or protection from coronary artery disease (CAD), the leading cause of death worldwide [8],

and other vascular diseases. CAD is a complex disease characterized by a buildup of plaque in the walls of coronary arteries which limits the flow of blood to the heart, a process called atherosclerosis [9]. Many risk factors have been associated with CAD development and some of the most studied ones include elevated levels of lipoproteins such LDL cholesterol (LDL-C) and triglyceride-rich lipoproteins (TRLs), which included VLDLs and Chylomicrons, as well as low levels of HDL-C [8]. Further details on the mechanisms by which these lipoproteins are produced and metabolized, as well as their associations with CAD and other metabolic diseases will be discussed below.

VLDL, IDL and LDL Metabolism (Endogenous Lipoprotein Pathway)

The endogenous lipoprotein pathway is activated in the absence of dietary fats in the liver. In the endoplasmic reticulum of hepatocytes, triglycerides and cholesterol esters are transferred to newly synthesized apoB-100 to form VLDL lipoprotein particles [10]. VLDL are triglyceride rich particles that contain apoB-100 as their core structural protein, and may contain a combination of other apolipoproteins [6]. The early transfer of triglyceride to apoB-100 is facilitated by the microsomal triglyceride transfer protein (MTP), then VLDL particles go through a second MTP-independent lipidation step that is necessary for their proper formation and subsequent secretion [11]. VLDL particles have been broadly recognized as biomarkers of risk as well as an independent predictors of CAD risk [12]. Apo B-100 and MTP proteins are highly important regulators of lipid metabolism, as mutations in both have been shown to fail to produce VLDL, which results in improper secretion and decreased levels of plasma triglycerides and total cholesterol [13, 14].

After VLDL particles are formed, they are secreted to peripheral tissues where they interact with lipoprotein lipase (LPL), which mediates the hydrolysis of triglycerides that are carried in the VLDL particles [15]. This hydrolysis process forms free fatty acids that provide energy or that can be stored by muscle cells and adipocytes [16]. LPL is synthesized in muscle and adipocytes and is activated by apo C-II and apo A-V apolipoproteins [17]. Loss-of-function mutations in LPL, apo C-II and apo A-V can impair the system's ability to hydrolyze triglycerides to free fatty acids and can result in marked hypertriglyceridemia, which is highly associated with CAD [18-20]. There are also known proteins to inhibit the activity of LPL such as Apo C-III, angiopoietin like protein 3 and 4 (ANGPTL3 and 4) [21-23] and loss-of-function mutations in these genes are associated increased LPL activity and decreased plasma triglyceride levels [24, 25].

The hydrolysis of triglycerides from VLDL forms intermediate density lipoproteins (IDL), also named VLDL remnants. VLDL remnants are enriched in cholesterol esters and acquire apoE from HDL particles, which is crucial for their clearance from the circulation by interacting with LDL receptors (LDLR) and LDLR related proteins (LRP) in the liver [6, 26, 27]. VLDL remnants can also be further hydrolyzed by LPL to form low density lipoprotein (LDL). LDL particles are further enriched in cholesterol esters and also contain apoB-100 as the main apolipoprotein and carry most of the cholesterol in the circulation, for which they are known to be the lipoproteins with most associated with the development of CAD and other vascular diseases [5, 28]. LDL consist of a heterogenous spectrum of particles that vary in size and density that go from large buoyant, intermediate, and small dense LDLs. It has been broadly demonstrated that small dense LDLs are highly atherogenic and are seen in association with an array of diseases phenotypes such as hypertriglyceridemia, obesity, type 2 diabetes and low HDL [29, 30]. Small dense LDLs

have lower affinity for the LDLR, resulting in their prolonged accumulation in the circulation [30]. Their size also facilitates the easy entry to the arterial wall and their strong binding to intra-arterial proteoglycans, which promotes their entrapment on the artery [31]. Their entrapment to the arterial wall makes them more prone to oxidation, which increases their affinity for macrophage uptake and foam cell formation, which and contributes to atherogenesis [31-33].

Plasma levels of LDL are determined by the rates of LDL production as well as the rates of LDL clearance, both of which are regulated by hepatocytes [3]. About 70% of plasma LDL is cleared by hepatocyte LDLR through receptor mediated endocytosis, and the remainder of LDL is taken up by other receptors such as LRP and extra-hepatic tissues [27]. Increased levels of LDLR in hepatocytes leads to the increased clearance of LDL particles from the circulation and decreased plasma LDL levels and conversely, decreased hepatic LDLR levels decreases LDL clearance and leads to increased plasma LDL levels along with increased risk of cardiovascular disease [34]. The original evidence for the LDLR mediating the clearance of LDL was provided by Drs. Michael Brown and Joseph Goldstein after studying families with extremely high cholesterol levels and myocardial infarction (MI) at an early age. They discovered the *LDLR* gene as the one that mediates the uptake of LDL particles by the liver, and they showed that these patients inherited loss-of-function mutations in the *LDLR* gene, which led to their high levels of plasma LDL cholesterol [4].

The expression levels of the *LDLR* in hepatocytes is highly regulated by cellular cholesterol content and by the regulation of the sterol regulatory element binding proteins (SREBPs) [35]. Low cholesterol levels in the cell signal SREBPs to be transported from the endoplasmic reticulum (ER) to the Golgi where proteases cleave the SREBPs into

active transcription factors [36]. Active SREBPs are then transported to the nucleus where they stimulate the transcription of the LDLR, to induce the uptake of cholesterol, and other genes such HMG-CoA reductase, which is the rate limiting enzyme in cholesterol synthesis pathway [36]. When the cellular cholesterol content is high, SREBP proteins remain inactive in the ER and the synthesis of LDLR is not stimulated. The LDLR is targeted for proteasomal degradation by E3 ubiquitin ligase inducible degrader of the low-density lipoprotein receptor (IDOL) protein [37]. This process happens when the cellular cholesterol content is too high, which leads to the oxidation of cholesterol. Oxidized sterols activate the liver X receptor (LXR), a nuclear hormone receptor which stimulates the transcription of *IDOL*, which in turns leads to the ubiquitination and degradation of the LDLR to prevent further cholesterol uptake [38]. Additionally, the LDLR is also regulated by the Proprotein convertase subtilisin/kexin type 9 serine protease (PCSK9). PCSK9 is a secreted protein that binds to the LDLR and enhances its degradation in the lysosomes [39]. PCSK9 loss of function mutations have been shown to increased LDLR activity and decreased LDL levels while gain of function mutations in PCSK9 decrease LDLR activity and elevate LDL levels [40].

One of the most broadly used methods to lower plasma LDL cholesterol in humans are statins, which are HMG-CoA reductase inhibitors. Statins block the active site of HMG-CoA reductase, the rate-limiting enzyme in the cholesterol synthesis pathway, which results in reduced hepatic cholesterol synthesis and leads to increased production of microsomal HMG-CoA reductase and increased cell surface LDLR expression in the liver [41-44]. The increase in LDLR levels promotes the clearance of LDL-C from the circulation and results in reduction in circulating LDL cholesterol levels. The use of statins has reduced morbidity and mortality associated with CAD by lowering circulating LDL levels;

however, many patients remain at high cardiovascular risk despite high dose statin therapy, and other patients are statin intolerant and cannot achieve normal LDL cholesterol levels [45-47]. For this reason, a better understanding of the genetic regulation of LDL and other factors such as triglycerides and how they promote CAD could lead to the development of novel, or improved treatments for CAD.

Chylomicron metabolism (Exogenous lipoprotein pathway)

The exogenous lipoprotein pathway is activated after food consumption. Postprandial triglycerides are emulsified by bile acids and then hydrolyzed by intestinal lipases, which leads to the formation of fatty acids and monoglycerides [48]. The absorbed fatty acids and monoglycerides are then transported to enterocytes, where they can be re-esterified to form triglycerides, which are package together with cholesterol esters into chylomicrons lipoproteins particles in the endoplasmic reticulum [49]. Chylomicrons are larger triglyceride rich lipoproteins compared to VLDL, and their size is dependent on the amount and the type of fat ingested and absorbed by the intestine [48]. Chylomicrons and VLDLs have similar functions, as they both transport dietary triglycerides and cholesterol to peripheral tissues and the liver. The core structural protein of chylomicrons is apoB 48, and it is required for their formation in the ER [49]. ApoB 48 is shorter form of ApoB100, which is incorporated into chylomicrons due to RNA editing that occurs in the enterocytes but not hepatocytes in certain organisms [50, 51]. In mice, both apoB 48 and apoB 100 are present in hepatocytes [50]. As in VLDL, MTP is also required for the proper lipidation of the chylomicron particle in the endoplasmic reticulum.

After chylomicrons are formed, they are secreted to the circulation where they interact with LPL, which results in a smaller lipoprotein particle named chylomicron remnants, which are further enriched in cholesterol esters and acquire apo E from HDL [5, 17, 49, 52]. Chylomicron remnants are cleared from the circulation by the liver, this is mediated by the binding of Apo E to the LDLR and other hepatic receptors such as LRP and syndecan-4 [5]. Apo E is crucial for the clearance of chylomicron remnants and mutations in this apolipoprotein can result in decreased chylomicron clearance and increased cholesterol and triglyceride plasma levels [53, 54].

HDL metabolism (Reverse cholesterol transfer pathway)

HDLs are formed through the secretion of apoA-I, the main structural protein in HDL particles, which is mainly secreted from the liver and small intestinal enterocytes [5]. After its secretion, lipid-poor apoA-I acquires phospholipids and free cholesterol from cells in a process that is facilitated by ATP-binding cassette transporter proteins (ABCA1) on the cell surface [55, 56]. This process allows the nascent apoA-I particles to mature into HDLs. ABCA1 mutations impair the process of lipid transfer to newly secreted apoA-I, which leads to the rapid catabolism of apoA-I and low levels of mature HDL lipoproteins [57]. HDLs can also acquire phospholipids and cholesterol from other tissues that express ABCA1 such as muscle cells and adipocytes, and from other lipoproteins such as chylomicrons and VLDL during the process of hydrolysis by LPL [55]. The transfer of phospholipids between lipoproteins is mediated by the phospholipid transfer protein (PLTP) [58].

To form mature HDL particles, the free cholesterol transferred from cells to the surface of the HDL need to be esterified to cholesterol ester, a process mediated by the lecithin:cholesterol acyltransferase (LCAT) enzyme [59]. Patients with LCAT deficiency present low HDL cholesterol and apo A-I levels and a high levels of small HDL particles in the circulation [60]. The cholesterol ester in the core of mature HDL particles can then be exchange for other lipids in a process mediated by the cholesteryl ester transfer protein (CETP) [61] . Humans with CETP deficiency show very high HDL cholesterol levels and large HDL particles [61]. HDL particles are susceptible to lipolysis by extracellular lipases which promote their catabolism and clearance to liver and other tissues via the scavenger receptor class BI (SR-BI) protein [62]. This process mediates the uptake of HDL cholesterol without inducing the degradation of the HDL apolipoprotein, apoA I, which is maintained in the circulation and can mature into large HDL through the subsequent accumulation of lipids [63]. In contrast to LDL, evidence suggests that high levels of HDL and the reverse cholesterol transport have an inverse relationship with CAD risk.

Human genome wide association studies (GWAS) are a helpful tool to identify novel genetic loci for cardiometabolic traits.

One of the main goals of human genetics is to understand and identify risk factors for rare and complex diseases in the population. Rare diseases follow Mendelian genetics and the concept of dominant and recessive traits and prior to GWAS it was thought that they were caused by mutations within one or a few genes; on the other hand, complex diseases and traits, have been known to be controlled by multiple genes and their inheritance does not follow mendelian genetics [64]. However, since GWAS came to light, we have discovered that many traits and diseases, rare and complex, are influenced by hundreds to thousands

genetic mutations and environmental risk factors [65]. Complex traits such as plasma lipids, blood pressure, height and body mass index are highly influenced by numerous environmental and genetic factors which contributes to their high rates of genetic variation and complicates the determination of the exact genetic contributors for a certain trait [66]. Given the fact that many of these traits highly contribute to disease, there is a lot of interest in identifying all the genetic contributors to these phenotypes and understanding their mechanism of action.

One of the most useful technologies used to determine the genetic contributors for common traits is genome wide association studies (GWAS). GWAS measures and analyzes DNA sequence variation across the human genome with the goal of identifying genetic risk factors for diseases that are common in the population [65, 67]. This is accomplished by using high-throughput technologies that search for millions of genetic variants across the genomes of thousands of individuals, called single nucleotide polymorphisms (SNPs), with the goal of identifying genotype to phenotype associations that occur more frequently in people with a particular disease or trait than in people without the disease [65, 67, 68]. The results from GWAS can ultimately lead to the prediction of who is at risk of disease, the discovery of novel genetic biology and the identification of new preventions and treatments for the specific disease.

In the last two decades, GWAS has identified many genetic factors associated with common traits and complex diseases and their modifiable causal factors in large populations, which has revolutionized the field of complex disease genetics. One of GWAS greatest strengths is that it has been able to confirm previously known genes associated with specific traits. For example, in the case of plasma lipid levels it was able to re-discovered *LDLR*, *HMG-CoA*, *LPL*, *ApoC*, *ApoB*, *Lp(a)* and others as mayor

regulators of plasma lipid levels, this showing that the experiment works as advertised [69]. GWAS findings also implicate genes of unknown function or genes without previously known relevance for a certain trait, however their results only present statistical associations between variants within a genetic loci and traits [68]. In the case of plasma lipids some novel genetic associations include *SORT1*, *TRIB1*, *ANGPTL3* and others [69]. For this reason, experimental validation of these loci is required to identify the specific candidate genes causing the phenotype, which could lead to the discovery of novel biological mechanisms underlying diseases [70]. For this purpose, genetically modified mouse models and cell-based assays are ideal systems for investigating the physiological functions of candidate genes identified by GWAS [68, 71].

Even though GWAS have helped identify a great number of genetic variants associated with common diseases and traits, this methodology possesses some limitations. GWAS variants only account for a modest proportion of the estimated heritability of most complex traits, for which reason they are unable to fully explain the genetic risk of common diseases [68]. GWAS is also unable to pinpoint the actual causal variants for the specific traits, this because of local correlation of multiple genetic variants by linkage disequilibrium, which makes it difficult to identify the specific causal variant [71]. Many GWAS signals map to non-coding regions of the genome, which complicates interpretation of the biological significance of the associations [68]. Additionally, GWAS functional validation of causal genes has been challenging, with only a handful of all GWAS hits being experimentally validated. Even with these challenges, recent technical advances in genome editing, stem cells, and high-throughput screening methods combined with rapidly growing genomic databases are anticipated to accelerate the functional validation of hits from GWAS studies.

Although the validation of GWAS hits has been a slow process, there has been several successes worth mentioning. One of the first successes of GWAS was the identification a major risk factor for age-related macular degeneration (AMD), the Complement Factor H gene [72]. They identified DNA sequence variations in this gene that led to its increased activity and that were associated with disease, additionally, the biological basis of these effects was validated using knockout mouse models [73, 74]. Another success of GWAS was the discovery of SNPs in the gene *ATG16L1* that pointed toward the role of autophagy in Crohn's disease [75]. These SNPs lead to missense mutations and diminished autophagy under cellular stress, which impaired intracellular bacterial clearance and increased inflammatory cytokine production, leading to a chronic inflammatory state [76]. Other GWAS studies implicated the gene loci *SLC16A11* with Type 2 diabetes (T2D) through its regulation of insulin secretion [77]. Additionally, GWAS studies for obesity, another common and complex trait have identified the genes Zinc Finger Protein 90 (*ZFP90*) and Complement C3a receptor 1 (*C3AR1*) to be implicated in regulating adiposity [78]. The association of both these genes with the regulation of adiposity has been validated using transgenic mice and knockout models [78]. These successes show that there are still a lot of opportunities to uncover and validate more GWAS genetic associations that could lead to a better understanding and possible therapeutic target for certain diseases.

Since the introduction of GWAS in the mid-2000s, plasma lipids have been some of the most studied complex traits, this because of their close association with the development of multiple cardiometabolic diseases. Some of the most studied lipid traits are the levels of high-density lipoprotein cholesterol (HDL-C), low-density lipoprotein cholesterol (LDL-C), total cholesterol and triglycerides. The first GWAS studies for lipid traits were published in

2008 and consistent of almost 9,000 participants [79, 80]. In these studies, the authors identified various genes with already known functions in the regulation of plasma lipids, however, they were also able to identify several novel genetic loci associated with the regulation of plasma lipid traits. For the regulation of LDL-C they identified 2 main gene loci: the *SORT1/CELSR2/PSRC1* gene locus as well as the *NCAN/CILP2/PBX4* gene locus. The *GALNT2* gene locus and *MVK/MMAB* gene locus were identified for the regulation of HDL-C; and the *TBL2*, *MLXIPL*, *TRIB1*, and *ANGPTL3* gene loci were identified for regulation of triglyceride levels [79, 80]. Since the original GWAS reports, several follow-up studies and meta-analyses have validated these original findings and have identified many new loci associated with at least one lipid trait [81-85]. Also, several groups have validated the association of some of these loci with plasma lipid metabolism using cell and mouse models.

Since the first lipid GWAS studies, follow up studies were able to increase the number of participants, which have allowed for the determination of more loci associated with lipid traits. In 2013, the Global Lipids Genetics Consortium (GLGC) reported a GWAS for all major lipid traits, which included total cholesterol, HDL-C, LDL-C and TG, as well as CAD incidence [69]. The GLGC studies were performed in about 196,000 participants and included individuals of European and non-European descent and identified 95 genetic loci associated with plasma lipid traits and CAD, of which 59 were novel associations with unknown roles in plasma lipid regulation [69]. Of the 95 genetic loci associated with plasma lipid traits, only 4 loci were associated with all major lipid trait as well as the incidence of CAD in different populations. These loci were within the associated interval of the *CETP*, *FADS1,2,3*, *APOA1* and *TRIB1* genes, with *TRIB1* being the only one with no previous

known association to plasma lipid metabolism and CAD [69]. These findings made *TRIB1* a very interesting candidate for novel studies regarding plasma lipid association and CAD.

More than 200 genetic loci have been associated with multiple lipid traits, which has provided with an array of targets for study lipid metabolism as well as possible therapeutics targets for cardiometabolic diseases [69, 80-86]. The last few years our laboratory has been interested in exploring the possible physiological and molecular mechanism by which several plasma lipid GWAS signals regulate blood lipids. My thesis project further contributes to this goal by characterizing the novel GWAS hit *TRIB1* and its effects on the regulation of lipid metabolism and cardiometabolic traits.

The *TRIB1* Locus

Tribbles Discovery in *Drosophila Melanogaster*

The Tribbles family of proteins was first identified in the fly species *Drosophila Melanogaster* as a regulator of cell division and morphogenesis. In the 2000's several studies described *Drosophila* Tribbles as a novel regulator of *String* in morphogenesis, is the fly orthologue of mammalian cdc 25, a phosphatase that regulates cell cycle progression [87]. Two independent studies identified *Tribbles* as a novel gene required for delayed mitosis during the formation of *Drosophila* ventral furrow, a key morphogenetic event that leads to the internalization of mesodermal precursors during gastrulation [88-90], however they both showed that tribbles expression alone is not enough to stop mitosis. Other studies went further and provided a molecular model for Tribbles function, demonstrating that slbo levels, a fly homologue of mammalian CCAAT/enhancer-binding

protein (CEBP) transcription factor, are regulated by *Tribbles* in a ubiquitin-dependent manner and that *Tribbles* has a regulatory role during oogenesis, affecting fly wing development [91]. Overall, *Tribbles* was shown to regulate embryonic development in *Drosophila* at several stages through its regulation of Cebp and Cdc25 protein levels by mediating their degradation.

Mammalian TRIB Family of Proteins Structure, Homology and Functions

Since *Tribbles* discovery in *Drosophila*, 3 mammalian homologs have been identified, named *TRIB1*, *2* and *3*. The human genes share high degrees of sequence similarity with each other, with *TRIB1/TRIB2* sharing 71.3%; *TRIB2/TRIB3* sharing 53.7%; and *TRIB1/TRIB3* sharing 53.3% of similarity [92]. Also, the TRIB family of proteins have been shown to be highly conserved among human and mouse, with sequence similarities of 97.5% for *TRIB1*, 99.2% for *TRIB2* and 81.2% [93]. for *TRIB3*. Despite being so highly conserved, each TRIB protein has been demonstrated to have different functional properties.

The TRIB family of proteins are ubiquitously expressed, and their structure is comprised of three regions: a N-terminal region, a central pseudokinase domain and a C-terminal region [92, 94]. The N-terminal region is a short, 60–80-amino acid region which highly enriched in proline and serine, named a PEST region, which is known to be present in proteins with short half-lives [95]. The central pseudokinase domain of the TRIB family is similar to a canonical kinase, however it lacks critical motifs and residues that are necessary for anchoring ATP and phosphate transfer, as well residues important for the catalysis and orientation of ATP, which makes them catalytically inactive [96, 97]. Even

though they do not have catalytic activity, pseudokinases have been proved vital in the regulation of many cellular processes and have been associated with key biological pathways dysregulated in disease. The C-terminal region of TRIB proteins contains two motifs: a constitutive photomorphogenic 1 (COP1) ubiquitin ligase binding motif and a MEK1 (MAPK (mitogen-activated protein kinase)/ERK (extracellular- signal-regulated kinase) kinase 1)-binding motif, both of which are highly conserved in mammalian TRIB homologues [98]. Both MEK1 and COP1 binding sites result in TRIB modulation of the MAPK/ERK signal transduction pathway via increased ERK phosphorylation, and proteasomal degradation of target protein by interaction with the COP1 E3 ubiquitin ligase, which is facilitated by the pseudokinase domain which anchors target proteins near the E3 ligase [99, 100]. This mechanism helps facilitate TRIB family pseudokinases best known function, which is COP1-dependent degradation of the transcription factors CEBPs [101-104].

CEBP proteins (CEBP α , β , γ , δ , ϵ , ζ), are members of the basic-leucine zipper class of transcription factors that act as homo or heterodimers [105]. TRIB protein family members have been broadly associated to interact and regulate the CEBP transcription factors, which has been shown to affect cell development and differentiation in different systems [101, 106-108]. CEBPs is an intron-less gene that is transcribed into a single mRNA, which is translated into two isoforms by alternative start codon usage; the full-length CEBPa (p42) and a shorter CEBPa (p30), which that lacks the full trans-activation potential of p42, which is crucial for cell differentiation [109, 110]. The ratio between the p30 and the p42 in cells is critical for the development of granulocytes, as the p30 protein fails to induce differentiation and increases cell proliferation of myeloid progenitors [111].

TRIB family members have been associated with the development or protection of certain cancers. In the hematopoietic system, TRIB1 and TRIB2 mediate degradation of the CEBP α p42, which results in an excess of the p30 isoform and impaired neutrophil differentiation and enhanced eosinophils, monocytes and macrophages differentiation in a mechanism that is similar to what occurs in acute myeloid leukemia (AML) patients with CEBPA mutations [112, 113]. TRIB1 is a biomarker of immune mediated chronic allograft failure associated with a poor prognosis in the setting of kidney disease transplantation [114]. TRIB2 was highlighted as a potential predictive biomarker for treatment response in blood cancer patients because it confers sensitivity to the novel treatment agent Venetoclax [115].

In addition to control of hematopoietic cell development, TRIB proteins have also been shown to be involved in the regulation of innate inflammation signaling, endoplasmic reticulum stress and adipocyte differentiation; this through protein interactions with NF- κ B, ATF4 and AKT, respectively [103, 116, 117]. Additional to cancer pathologies, links between the dysregulation of TRIB family of proteins and other diseases and traits have been described. Changes in expression TRIB3 have been associated with progression of Parkinson's disease as well as changes on inflammatory gene expression in diabetic kidney disease [118, 119]. Also, as mentioned before, multiple unbiased GWAS studies have indicated multiple associations between *TRIB1*, plasma lipid traits, and the development of CAD [120].

Mammalian *TRIB1*, a GWAS hit for multiple cardiometabolic traits

The focus of this dissertation is characterizing *TRIB1*, a genetic locus identified in multiple GWAS with multiple metabolic phenotypes. The locus 8q25, which contains the *TRIB1* gene, was first shown to be involved in plasma lipid metabolism by two papers that showed noncoding variants within in the *TRIB1* gene locus are associated with circulating triglyceride and LDL-C levels in humans [79, 80]. The GLGC then published meta-analyses comparing more than 190,000 individuals of diverse genetic background that further validated the relationship of *TRIB1* with lipid metabolism [69, 86]. The findings of these studies displayed *TRIB1* as the only novel locus from these studies to be associated with all 4 lipid traits (triglycerides, total cholesterol, HDL-C and LDL-C) as well as CAD. Further, it was the first time that *TRIB1* had been associated with the regulation of lipid metabolism, creating a lot of interest in determining the mechanisms contributing to these traits. Since its original GWAS discovery, many other studies have corroborated the importance of *TRIB1* in the regulation of plasma lipids. More recently in the Million Veteran Program GWAS of lipids in more 300,000 participants, the lead variant rs2001846 near *TRIB1* was associated with a significant increase in LDL-C ($p = 2.73E-82$) [81]. Additional GWAS studies have also associated variants within the *TRIB1* locus with the development of hepatic steatosis [121, 122], adiponectin levels [123] and levels of liver enzymes such as alanine transaminases (ALTs) [124], making this gene even more interesting to study.

The significantly associated SNPs in this locus fall around 40 kb upstream of the *TRIB1* gene, and it was annotated as the gene of interest due to its position as the nearest gene to the lead SNP. However, no direct expression quantitative trait loci (eQTLs) have yet been identified for *TRIB1*, which mean that no changes in *TRIB1* expression have been directly associated with the specific traits associated within this locus. Even though no

eQTLs have been found in humans, many studies have demonstrated the important role of *TRIB1* in the regulation of plasma lipids and other traits using cell and animal models and I will be discussing these findings in the next section.

Hepatic *TRIB1* in the regulation of plasma lipids metabolism

Since the *TRIB1* GWAS lipid associations were indicated, a lot of interest developed in determining how *TRIB1* affects plasma lipids and CAD. Using a model of AAV-mediated overexpression of *Trib1* in adult C57B/6 mice, Burkhardt et al. [125] demonstrated that increasing levels of hepatic *Trib1* decreased plasma total cholesterol, HDL-C, LDL-C, and triglycerides levels in a dose-dependent manner. Mice overexpressing *Trib1* also showed a decrease in triglyceride production and hepatic lipogenic gene expression. The authors repeated the *Trib1* overexpression in various mouse models of lipid metabolism, including the *Ldlr* KO hyperlipidemic model and the *Ldlr* KO /*Apobec1* KO/human apoB transgenic (LAhB) humanized mouse model, which have lipid profiles similar to humans. In all mouse models tested, *Trib1* overexpression resulted in significant reductions in plasma cholesterol and triglycerides. In the LAhB mice, *Trib1* overexpression also caused a significant reduction in plasma apoB protein. The authors also performed *in vitro* studies with HepG2 cells and *ex vivo* studies of primary hepatocytes and showed that these cells have reduced cellular triglyceride production and secretion, with HepG2 cells overexpressing *TRIB1* also showing a reduction in apoB protein. Furthermore, using a previously reported whole-body deletion model of *Trib1* on a mixed background, the investigators demonstrated that deletion of *Trib1* leads to increased plasma total cholesterol, VLDL, LDL, triglyceride secretion and hepatic lipogenesis. Based on their results, they concluded that *TRIB1* can modulate VLDL secretion from the liver by regulating the level of triglycerides available for VLDL assembly in hepatocytes [125].

In another publication, Bauer et al. [104] demonstrated that hepatic specific deletion of *Trib1* increases hepatic triglyceride content, lipogenic gene expression, and de novo lipogenesis in mice. These mice also had increased hepatic CEBPa protein, which was shown to be both necessary and sufficient to drive the hepatic lipogenic phenotypes in *Trib1* hepatic deleted mice [104]. The results from these studies established that *TRIB1* regulation of hepatic lipogenesis is mediated through CEBPa. Additionally, *Trib1* liver knockout mice had increased plasma lipids; however, the association of CEBPa regulation with this phenotype was not fully elucidated [104].

CEBPa is well known for its function as a regulator of myeloid cell development and hematopoiesis [126], however it is also known to be involved in the regulation of energy homeostasis [127]. CEBPa protein is highly expressed in adipose tissue and the liver in mouse and humans, and has been broadly described as regulator of adipogenesis, critical for glucose and lipid homeostasis and for the regulation of several metabolic genes in the liver [104, 128, 129]. CEBPa whole body knockout neonates have been reported to die postnatally due to lack of glycogen, severe hypoglycemia, and lack of lipid accumulation in their hepatocytes and adipocytes [127]. These results confirmed the importance of CEBPa for energy homeostasis, glucose metabolism and postnatal survival in mice. CEBPa has also been implicated the regulation of hepatic lipogenesis in mouse models of obesity. Hepatic deficiency of CEBPa in the leptin-deficient *ob/ob* mouse model of obesity and *db/db* mouse model of diabetes abrogated fatty liver caused by a high carbohydrate diet, decreased circulating triglycerides, lipogenic gene expression and the transcription of SREBP1 [130, 131]. These reports support a role for CEBPa in the regulation of lipid metabolism and go in line with the results from Bauer et al., [104] which elucidated the roles of *Trib1* and CEBPa in hepatic lipid metabolism.

Additional to CEBPa, other hepatic mechanisms have been proposed by which *TRIB1* regulates plasma lipids, although not fully explored. As mentioned before, The C-terminal region of TRIB proteins contain a MEK1 binding motif which has been shown to modulate MAP kinase signaling by promoting the phosphorylation of ERK1/2 [99]. Phosphorylation of ERK1/2 has previously been shown to down-regulate the expression of Stearoyl-CoA desaturase-1 (*SCD1*) in HepG2 cells, which encodes a protein (*SCD1*) that that catalyzes a rate-limiting step in the synthesis of unsaturated fatty acids [132]. *Scd1* has consistently been shown to be differentially expresses in mouse models of *Trib1* overexpression and hepatic deletion [104, 125]. Inhibition of MEK/ERK signaling using an ERK1/2 inhibitor was also shown to improve VLDL assembly in HepG2 cells and to increase apoB secretion from these cells [133]. These observations are in line with the observed lipid phenotypes of mice with hepatic overexpression and hepatic deletion of *Trib1*, thus implicating altered MAP kinase signaling as a potential mechanism of metabolic regulation by *TRIB1*. However, these findings have not been replicated on in vivo models of *TRIB1* metabolism and more research is needed to fully elucidate this mechanism.

TRIB1 has been reported to regulate hepatic lipogenesis via the carbohydrate response element binding protein (ChREBP) [134]. *In vitro* overexpression and mammalian yeast 2-hybrid assays showed that *TRIB1* interacts and regulates both the mRNA and the protein levels with the transcription factor *ChREBP*, this by promoting its ubiquitination and proteasomal degradation in a process similar to *TRIB1* and CEBPa relationship [134]. ChREBP is a glucose sensing transcription factor that is involved in the regulation of genes associated with hepatic lipogenesis [135]. Some of ChREBP targets are pyruvate kinase, liver and RBC (PKLR), Acetyl-CoA Carboxylase Alpha (ACACA), Fatty Acid Synthase (FASN) and ChREBP itself [135], some of which are differentially expressed in mouse

models of *Trib1* overexpression or down-regulation [104, 125]. These findings support the notion that *TRIB1* modulates ChREBP control of lipogenesis.

Another study also used a yeast-two-hybrid screen and found the Sin3A-associated protein of 18 kDa (SAP18) to be a novel binding partner of *TRIB1*, which demonstrated that knockdown of Sap18 in mouse liver decreased plasma lipid and increased hepatic lipid levels, while Sap18 overexpression had the opposite effects [136]. They also performed transcriptome analysis of the mouse liver revealed that changes in Sap18 expression inversely regulated MTP levels, which is crucial for the assembly of VLDL particles. ChIP analysis showed that SAP18, *TRIB1* and mSin3A bind together at the regulatory sequences of the MTP, an interaction that is crucial for MTP regulation [136]. The findings further support *TRIB1* involvement in the regulation of plasma and hepatic lipids. In support of this findings suggesting a possible effect of *TRIB1* on MTP, another group showed that knockdown of *TRIB1* in primary human hepatocytes leads to MTP mRNA and protein reduction, however, this was attributed to reduced levels of hepatocyte nuclear factor 4 alpha (HNF4a), a highly conserved member of the nuclear receptor family [137]. HNF4a is essential for triglycerides and cholesterol homeostasis and bile acid metabolism, and it also helps regulate the expression of several key lipoprotein regulators including APOC3 and MTP [138]. In several in vitro and ex vivo cell lines, *TRIB1* suppression resulted in decreased while *TRIB1* abundance increased HNF4A and they also demonstrated that *TRIB1* and HNF4A can form complexes in vivo [137]. The data presented in these last studies propose a model where *TRIB1* regulates MTP activity through its interaction with SAP18 and HNF4a. However, the results from these studies propose an opposite directionality of triglyceride levels as to what has been observed in

mouse models of Trib1 overexpression and knockout, which suggest these interactions need to be fully explored using *in vivo* models.

Overall, there are numerous possible physiological and molecular mechanisms by which hepatic *TRIB1* regulates plasma lipid metabolism that remain unclear. Most of the established mechanistic partners of *TRIB1* had been studied using *in vitro* models, which need to be investigated and confirmed in *in vivo* models. Further, the molecular and physiological mechanisms by which TRIB1-CEBPa interactions affect plasma lipids remains to be elucidated.

Goal of this Thesis

The main goal of this dissertation is to functionally characterize *TRIB1*, a gene associated with multiple cardiometabolic traits. My first aim is to determine the physiological mechanism by which murine hepatic *Trib1* deletion increases plasma lipids. I will explore how murine hepatic *Trib1* deletion affects the processes of liver lipoprotein production, secretion, and clearance. My second aim is to determine the molecular mechanism by which *Trib1* regulates plasma lipids in mice, with my main target being exploring if *Trib1* regulation of CEBPA is involved in the modulation of plasma lipid metabolism. My third aim is to explore the underlying mechanism of the highly penetrant neonatal lethality we observed in whole body *Trib1* knockout mice. Overall, the findings from my studies will expand the knowledge as to how murine *Trib1* regulates multiple cardiometabolic traits, which will shed light into similar mechanisms in humans.

CHAPTER 2: METHODS

Animals

Mice harboring a conditional allele of *Trib1* (C57BL/6-*Trib1*^{tm1.1mrl}/*Trib1*^{flox;flox}) were provided by Merck and were produced for Merck by contract with Taconic; details of the mice can be found at <http://www.taconic.com/10265>. *Trib1* constitutive knockout mice (C57BL/6-*Trib1*^{tm1.2mrl}/*Trib1* KO) were provided by Merck and were produced for Merck by contract with Taconic; details of the mice can be found at <https://www.taconic.com/10385>. Previously reported mice harboring a conditional allele of *Cebpa* (*Cebpa*^{tm1Dgt/J}/*Cebpa*^{flox;flox}) were obtained from the Jackson Laboratory (stock number 006447). C57BL/6J wild type mice (Controls) were obtained by the Jackson Laboratory (000664). *Ldlr* constitutive knockout (*Ldlr* KO) mice were obtained from Jackson Laboratory (stock Number 002207). All mice were maintained in a monitored small animal facility at the University of Pennsylvania under Institutional Animal Care and Use Committee -approved protocols. Mice were fed ad libitum with a standard chow or Western type diet (WTD) containing 40% kCal fat, 43% kCal carbohydrate and 17% kCal, protein from OpenSource Diets (D12079B, Research Diets) for the indicated periods of time. For experiments with WTD, mice were injected with adeno-associated virus (AAV), then plasma lipids were monitored for 5 weeks under chow feeding before switching to WTD. All mice were provided *ad libitum* access to water and were maintained on a 12/12 light cycle with lights off from 7:00 p.m. to 7:00 a.m. daily. For all studies, male mice aged 10–12 weeks were used; for some of the studies, female mice of similar age were also included. Five to ten mice per group were used for all studies.

Adeno-Associated Virus 8 (AAV-8) Viral Vector Preparation

AAV serotype 8 vectors containing an empty vector expression cassette (AAV8-Null) or encoding Cre recombinase (AAV8-CRE) were generated by the University of Pennsylvania Vector Core (Philadelphia, Pennsylvania, USA). The transgene in these vectors is selectively expressed in hepatocytes driven by the thyroxine-binding globulin (TBG/Serpina7) promoter [139]. For all experiments utilizing AAV-CRE or AAV-NULL, animals were injected with AAV vectors at a dose of 1.5×10^{11} genome copies via i.p. injection and examined at the indicated time points. Control mice refer to either *Trib1^{fl/fl}* mice receiving AAV-NULL or wild type mice receiving AAV-CRE. *Trib1^{Δhep}* mice refer to *Trib1^{fl/fl}* mice receiving AAV-CRE. *Cebpa^{Δhep}* mice refer to *Cebpa^{fl/fl}* mice receiving AAV-CRE. *Trib1^{Δhep}; Cebpa^{Δhep}* also named double knockout mice (DKO) refer to our crossed line between *Trib1^{fl/fl}* and *Cebpa^{fl/fl}* mice receiving AAV-CRE.

Atf3 and Luciferase Control siRNA injections

Atf3 and luciferase control siRNA were provided by Alnylam. Control and *Trib1^{Δhep}* mice were injected with *Atf3* or luciferase control siRNA at a dose of 10mg/kg and examined at the stated time points.

Plasma lipid phenotypic characterization

Blood samples were collected from mice after isoflurane anesthesia by retro-orbital bleeding using EDTA-coated glass tubes. Blood was centrifuged at 10,000 rpm for 7 min at 4°C and plasma was obtained. Plasma total cholesterol, HDL-C, triglyceride, phospholipids and ALTs levels were measured using an Axcel clinical autoanalyzer (Alfa Wassermann Diagnostic Technologies). Non-HDL-C was calculated as the difference between the TC and HDL-C measurements. All measurements were made from 4 hour-

fasted plasma samples unless stated otherwise. In addition, plasma samples were pooled by experimental group after collection and 150 μ l of plasma was separated by Fast Protein Liquid Chromatography (FPLC) on a Superose 6 gel-filtration column (GE Healthcare Life Sciences) into 0.5 ml fractions. Total cholesterol and triglycerides were measured from FPLC-separated fractions using Infinity Liquid Stable cholesterol and triglyceride reagents (Thermo Scientific) in 96-well microplates with a Synergy Multi-Mode Microplate Reader (BioTek).

Hepatic Lipid characterization

Hepatic triglycerides and total cholesterol were measured from animals sacrificed by isoflurane inhalation and cervical dislocation, flash frozen in liquid nitrogen and stored at -80°C until processed. Frozen liver ($\sim 100\text{mg}$) were weighed and homogenized in 1xPBS. Liver homogenates were diluted (1:10-1:20 dilutions) and then incubated with 1% deoxycholate (Acros Organics, Inc) for triglycerides and 0.25% deoxycholate for total cholesterol. Total cholesterol and triglycerides were measured using Infinity Liquid Stable cholesterol and triglyceride reagents (Thermo Scientific) for colorimetric assays.

Plasma Glucose characterization

Blood glucose, lactate and ketone bodies were measured using a One-Touch Ultra glucometer (Lifescan, Inc.), Lactate Plus lactate meter (Nova Biomedical) and Nova Max Plus Ketone meter respectively at indicated nutritional conditions.

Measurement of Tissue Glycogen Levels

Neonatal mice at postnatal day 1 were sacrificed by decapitation and liver tissue was flash frozen in liquid nitrogen. Frozen tissue samples ($\sim 10\mu\text{g}$) were homogenized in PBS.

Homogenates were quantified for protein by the BCA method (Thermo Scientific). Tissue samples were used for detection of glycogen levels by colorimetric assay protocol according to manufacturer's instructions (Biovision). Glycogen levels in samples were determined from a standard-curve method generated by the assay.

Oral fat tolerance test

Mice were fasted overnight 12-16 hours, then bled for baseline triglycerides levels. The mice were then gavaged with olive oil (20ul x BW (g).) and plasma was collected at 1, 3, 5 and 7 hours post-gavage. Triglyceride levels were measured using Infinity Liquid Stable triglyceride reagents (Thermo Scientific) in 96-well microplates with a Synergy Multi-Mode Microplate Reader (BioTek). Data was plotted as the change from baseline from for every timepoint and the resulting data was analyzed calculating the area under the curve.

Glucose tolerance test

Mice were fasted overnight for 14-16 hours. Mice were then injected with 10ul x BW (g) of glucose from a 20% w/v glucose solution, via intraperitoneal (I.P.) injection. Blood was collected by tail bleeding and was used to measure glucose concentrations using a One-Touch Ultra glucometer (Lifescan, Inc.) at 0, 15, 30, 60, 90 and 120 minutes after glucose administration.

Insulin tolerance test

Mice were fasted for 6 hours before I.P. injection of 0.75U/kg body weight of recombinant insulin (Novolin R; Novo Novodisk A/S). Blood glucose concentrations were measured using a One-Touch Ultra glucometer (Lifescan, Inc.) at 0, 15, 30, 60, 90 and 120 minutes after insulin administration.

LDL-ApoB Kinetic Experiments

LDL was isolated from human plasma by ultracentrifugation. LDL ApoB was iodinated with ¹²⁵I directly using the iodine mono-chloride method [140]. Approximately 2.0 ml of LDL in 10 mM ammonium bicarbonate buffer (0.2–0.4 mg/ml) was iodinated with 1 mCi of ¹²⁵I (PerkinElmer), 300 µl of 1 M glycine, and 150 µl of 1.84 M NaCl/2.84 µM ICl solution, vortexed, and applied to a PG-10 desalting column (Amersham Biosciences) that was pre-equilibrated with 0.15 M NaCl/1 mM EDTA solution. Iodinated proteins were eluted in a final volume of 2.5 ml in NaCl/EDTA solution and dialyzed against PBS before measurement of protein concentration by BCA assay, ¹²⁵I activity was confirmed by gamma counting and fractionated by FPLC to measure cholesterol and ¹²⁵I activity in the LDL fractions. For ¹²⁵I-LDL-ApoB clearance studies, iodinated LDL-ApoB specific activity was approximately 50-100 counts/ng protein. Mice were administered by intravenous tail vein injection with approximately 2 million counts ¹²⁵I-LDL in 100µl of plasma. Mice were bled 2 minutes after injection, then again at 1 , 2 , 3 , 4 , 6 , 12 , and 24 hours after radioisotope administration and sacrificed at 24 h. ¹²⁵I activity at each timepoint was measured from 5 µl of each plasma sample by counting on a Packard Cobra II Auto-Gamma counter. The relative activity at each time point was determined as the fraction of activity at 2 min for each mouse respectively.

VLDL-ApoB Kinetic Experiments

VLDL was isolated from human plasma by ultracentrifugation. VLDL ApoB was iodinated with ¹²⁵I directly using the iodine mono-chloride method using the same method described for LDL iodination [140]. Mice were bled at 1 min, 5 min, 15min, 30min, 1h, 3h, 6 h, and 24 h after radioisotope administration and sacrificed at 24 h. ¹²⁵I activity at each timepoint was measured from 5 µl of each plasma sample by counting on a Packard Cobra II Auto-

Gamma counter. To get VLDL-ApoB specific counts, plasma was subjected to isopropanol precipitation and the precipitate was measured for counts on the gamma counter. The relative activity at each time point was determined as the fraction of activity at 1 min for each mouse, respectively.

Triglyceride and apoB secretion Experiments

Mice were fasted for 4 hours and then injected intravenously with 0.67mg/g body weight Pluronic F127 NF Prill Poloxamer 407 (P407) (BASF, material 30085239) and 300-400 μ Ci Easytag EXPRES 35 S protein labeling mix (35 SMet/Cys) (Perkin Elmer NEG772). Blood samples were taken immediately prior to the P407/ 35 S Met/Cys injection and at 30, 60, 90, and 120 minutes post injection. Blood samples were kept on ice and centrifuged to collect plasma within 15 minutes of collection. Plasma triglycerides concentration was measured at all time points by colorimetric assay with the Infinity Liquid Stable triglyceride reagents (Thermo Scientific).

Newly synthesized and total secreted total plasma apoB100 was measured by the incorporation of 35 S Met/Cys into apoB100 that was secreted into the systemic circulation during the 2 hour experimental period. Total plasma was boiled in Laemli sample buffer and separated on a 3-8% Tris Acetate gel (Novex), the gel was dried onto filter paper under vacuum, and the labeled proteins visualized by autoradiography. The apoB100 bands were cut and analyzed for 35 S activity by liquid scintillation counting. To mitigate differences in total labeled hepatic protein synthesis, counts were adjusted based on the incorporation of 35 S methionine into all proteins in plasma trichloroacetic acid (TCA) precipitated protein counts. To determine TCA precipitated protein counts, 5 μ l of plasma was blotted onto a 1x1cm square of filter paper. Plasma proteins were precipitated by incubating the filter paper in 20% TCA on ice followed by 10% TCA heated to 100°C. The

filter paper was subsequently rinsed with 100% ethanol, dried, and ³⁵S activity calculated by liquid scintillation counter.

Sucrose Gradient Ultracentrifugation Experiment

Sucrose gradient ultracentrifugation of apoB-containing lipoproteins was conducted as previously described [141]. All solutions contained 0.1 mM leupeptin, 1 μM pepstatin A, 0.86 mM phenylmethylsulfonyl fluoride, 100 units/ml aprotinin, 5 μM ALLN, 5 μM EDTA, 150 mM NaCl, and 50 mM phosphate-buffered saline, pH 7.4. The sample layer was prepared by diluting 200 μl of pooled plasma from the 120 min post-injection time point from mice in the apoB secretion studies in 2.3 ml of PBS and adding 2.5 ml of 25% sucrose in PBS. The sucrose gradient was formed by layering from the bottom of the tube: 2 ml of 47% sucrose, 2 ml of 25% sucrose, 5 ml of sample in 12.5% sucrose, and 3 ml of phosphate-buffered saline. The gradients were spun at 35,000 rpm in a Beckman SW41 rotor for 65 h at 12 °C, and then 12 fractions were removed from the top to the bottom and subjected to immunoprecipitation for apoB.

Western blot analysis

Protein extracts were prepared from ~100mg of liver tissue homogenized in Lysis Buffer (25mM Tris-HCL, 10mM Na₄P₂O₇, 1% NP40, 10mM NaF, 1mM EGTA, 1mM EDTA, 1mM PMSF, 5ug/ul Leupeptin, 5ug/ul 10nM okadaic acid, Protease Inhibitor tablet (Roche), Phospho tablet (Roche)). Samples were homogenized, shaken for an hour at 4 degrees and centrifuged at 12,000g for 10 min. Protein was separated by SDS-PAGE using the NuPage system (Invitrogen). ApoB Antibody was acquired from Abcam (ab31992), LDLR antibody was acquired from Abcam (ab52818), monoclonal anti B-Actin antibody- clone AC-15 was acquired from Sigma Aldrich (A5441), CEBPα antibody was obtained from Cell

Signaling (D56F10) and pEIF2a was obtained from Enzo Life Sciences (BML-SA405). For ATF3, SREBP1 and SREBP2 a nuclear enriched isolation protocol was used. Protein extracts were prepared from ~100mg of liver tissue homogenized in Lysis Buffer (50mM HEPES, 10mM Na₄P₂O₇, 1% NP40, 300mM NaCl, 0.2mM EGTA, 10mM EDTA, 1mM MgCl₂, 1mM CaCl₂, 1mM PMSF, 5ug/ul Leupeptin, 5ug/ul 10nM okadaic acid, Protease Inhibitor tablet (Roche) and 20% glycerol. Samples were homogenized, shaken for an hour at 4 degrees, centrifuged at 15,000g for 30 min and then the supernatant was sonicated. Protein was separated by SDS-PAGE using the NuPage system (Invitrogen). ATF3 antibody was obtained from Novus Biologicals (NBP1-85816), SREBP1 antibody (2A4- SC 13551) and SREBP2 antibody (NB100-74543). ECL HRP-conjugated secondary antibodies were from GE Healthcare Life Sciences and the Crescendo ECL reagent (Millipore) was used for protein development.

Albumin protein levels

Circulating Albumin levels were determined in plasma collected after 4-hour fasting using the Mouse Albumin ELISA Kit, E99-134 according to manufacturer's instructions (Bethyl Laboratories).

RNA Isolation and Quantitative RT-PCR

RNA was collected from approximately 100 mg flash-frozen liver tissue using the mirVana Kit (Invitrogen) following the manufacturer's protocol. cDNA was produced from 1 µg of total RNA with the High Capacity cDNA Reverse Transcription Kit (Applied Biosystems) following the manufacturer's instructions. Quantitative reverse transcription PCR (qRT-PCR) analysis was performed using standard TaqMan Gene Expression probes (Invitrogen) on a QuantStudio RT-PCR machine. The relative quantity of each mRNA was

calculated using the $\Delta\Delta C_t$ method and normalized to the combined mean C_t of Mr1p19, Ywhaz, and Ipo8 housekeeping genes. Table 1 contains the sequences for all probes used for qRT-PCR.

Statistics

All data are reported as the mean \pm SEM. Statistical comparisons between groups were performed using a two-tailed Student's t-test, one-way ANOVA, or two-way ANOVA as appropriate and when assumptions of distribution of the data were valid. Statistical significance was defined as $p < 0.05$.

Gene-expression profiling (RNA Seq) and Ingenuity Pathway Analysis

RNA was collected from approximately 100 mg flash-frozen liver tissue using the mirVana Kit (Invitrogen) following the manufacturer's protocol. Total RNA was analyzed using the Agilent RNA 600 Nano Kit following the manufacturer's protocol. Whole Transcriptome, High-throughput library was prepared using Illumina truSeq stranded mRNA kit. Sequencing was performed on a HiSeq4000 (100 bp, single end reads), to get approximately 312 million reads. RNA-Seq and data analysis were performed by the Penn Functional Genomics Core (Philadelphia, Pennsylvania, USA). Raw sequence files (fastq) for 27 samples were mapped to the transcriptome using Salmon [142] against the mouse transcripts described in genecode (version M22, built on the mouse genome GRCm38.p6) [143]. Transcript counts were summarized to the gene level using tximport [144], and normalized and tested for differential expression using DESeq2 [145]. Differential expression was determined using a False Discovery Rate cutoff of 10%.

Mass spectrometry analysis

Samples were prepared and ran as described in the Western blot methods section. Gels were stained with Coomassie blue staining, and the bands of interest were submitted for analysis at the Quantitative Proteomics Resource Core at the School of Medicine at the University of Pennsylvania. Peptides were analyzed on a an Orbitrap Fusion (Thermo Scientific) attached to an UltiMate™ 3000 RSLCnano System (Thermo Scientific) at 400 nL/min. Proteome Discoverer (Thermo Fisher Scientific, version 2.3) was used to process the raw spectra. The uniprot Mus musculus database was used for database searching. For label-free quantitation, All the chromatographic data were aligned and normalized the peptide groups and protein abundances, impute missing values and scale them. Here, it was applied the normalization of the total abundance values for each channel across all files, equalizing the total abundance between different runs.

Table 1. TaqMan Probes used for Gene Expression Analysis by qRT-PCR

Gene Symbol	TaqMan Code
<i>Trib1</i>	Mm00454875_m1
<i>Cebpa</i>	Mm00514283_s1
<i>Ldlr</i>	Mm01177349_m1
<i>Atf3</i>	Mm01177349_m1
<i>Srebpf1</i>	Mm00550338_m1
<i>Srebpf2</i>	Mm01306292_m1
<i>Fasn</i>	Mm00662319_m1
<i>Acaca</i>	Mm01304257_m1
<i>Pepck</i>	Mm01247058_m1
<i>G6pc</i>	Mm00839363_m1
<i>Gys1</i>	Mm01962575_s1

CHAPTER 3:

***Trib1* regulates plasma lipids by modulating both the rates of hepatic lipoprotein secretion and LDLR-mediated clearance**

ABSTRACT

Genetic variants near the *TRIB1* gene are significantly associated with plasma lipid traits and coronary artery disease. While data suggest *TRIB1* is the causal gene for these traits, the physiological mechanisms by which its protein product TRIB1 affects plasma lipids are not fully understood. Plasma lipid levels are directly impacted by the rates of secretion from the liver and intestines in the form of triglyceride rich lipoproteins (VLDL and chylomicrons), as well as by the rates of plasma clearance by either LPL-mediated triglyceride hydrolysis or LDLR-mediated clearance by the liver. In these studies, I sought to elucidate how *TRIB1* affects plasma lipids by investigating each of these possible mechanisms. Using a *Trib1* hepatocyte specific deletion mouse model (*Trib1*^{Δ*hep*}), I demonstrated that *Trib1*^{Δ*hep*} mice have significantly increased plasma total cholesterol, HDL cholesterol, non-HDL cholesterol, LDL cholesterol and apoB protein levels, as well as impaired postprandial triglyceride clearance. I also showed that *Trib1*^{Δ*hep*} mice have markedly delayed catabolism of LDL-apoB and VLDL-apoB due to significantly decreased *Ldlr* mRNA and protein expression. In the absence of the *Ldlr*, deletion of *Trib1* did not further impair LDL-apoB or VLDL-apoB catabolism, suggesting that the apoB clearance phenotypes are due to the *Trib1*-mediated decrease in *Ldlr*. I also demonstrated that *Trib1*^{Δ*hep*} mice have increased secretion of apoB containing lipoproteins, which was replicated in the absence of *Ldlr*. These findings establish hepatic *Trib1* as a critical

regulator of multiple metabolic pathways affecting plasma lipids, and as a novel regulator of the LDLR.

INTRODUCTION

The *TRIB1* gene, which encodes Tribbles homolog 1 protein (TRIB1), has been suggested as the causal gene for the highly robust GWAS signals at human chromosomal locus 8q24 for a remarkable number of cardiometabolic traits, including plasma lipids and lipoproteins, hepatic steatosis, adiponectin levels, and coronary artery disease [69, 79, 124, 146]. The *tribbles* gene was first identified in *Drosophila* as a regulator of cell division and morphogenesis and was shown to regulate the proteins encoded by *string* and *slbo*, the *Drosophila* homologs of the dual phosphatase CDC25A, and CEBPa respectively [88, 89, 91]. In humans, *TRIB1* encodes a highly conserved pseudokinase that functions as a signal transduction pathway modulator and scaffolding protein, including interacting with the E3 ubiquitin ligase COP1 to target the transcription factors CEBPa and CEBPb for ubiquitination and proteasomal degradation, a process that has been broadly explored in myeloid cell differentiation [100].

Since the establishment of a genetic link between *TRIB1* and cardiometabolic traits, limited investigation of its role in the liver has been performed. Our laboratory previously reported that *Trib1* overexpression in mouse liver decreased plasma lipids, hepatic *de novo* lipogenesis, and very low-density lipoprotein (VLDL) production [125]. We also demonstrated that *Trib1* hepatic deletion in mice increases plasma lipids, hepatic fat and *de novo* lipogenesis [104]. Furthermore, *Trib1* deletion significantly increased hepatic levels of CEBPa protein, which helped explain the increased *de novo* lipogenesis and

hepatic lipid phenotypes [104]. However, questions regarding the physiological mechanism by which *TRIB1* specifically regulates plasma lipids and LDL-C metabolism remained unanswered.

Even though *TRIB1* is ubiquitously expressed, in these studies I focused in understanding how hepatic *Trib1* regulates plasma lipid metabolism in mice. The liver is one of the most important tissues for lipid homeostasis, and therefore understanding the effects of hepatic *Trib1* expression is critical to elucidate its role in lipid metabolism. Further, constitutive *Trib1* deletion on a C57BL/6 background presents a highly penetrant neonatal lethality (discussed in chapter 5). In this chapter, I functionally characterize a *Trib1* hepatocyte knockout (*Trib1^{Δhep}*) mouse model and determine the effects on multiple pathways that regulate plasma lipids. I demonstrated that in addition to the previously reported *Trib1* effects on hepatic lipogenesis, VLDL secretion and lipid levels, hepatic *Trib1* is involved in the regulation of post prandial triglycerides clearance, the catabolism of VLDL and LDL apoB lipoprotein particles through its regulation of LDLR, and the secretion of small apoB particles from the liver. Our findings establish hepatic *Trib1* as a player of multiple physiological pathways that regulate plasma lipid metabolism as well as a novel regulator of the LDLR.

RESULTS

Generation of hepatocyte-specific *Trib1* knockout mouse line (*Trib1^{Δhep}*)

To assess the effects of hepatic *Trib1* deletion on plasma lipids, we acquired C57BL/6 mice with loxP sites flanking the second exon of *Trib1* (*Trib1^{fllox/fllox}*). Mice were

administered AAV-Cre to induce *Trib1* hepatocyte-specific deletion. The results from these mice were compared to control mice, which were wild type C57BL/6 mice receiving an AAV-CRE injection. Male *Trib1^{Δhep}* mice had greater than 95% reduction in liver *Trib1* mRNA expression eight weeks after AAV-CRE injection (Figure 3.1A). Mice were fed a western type diet (WTD) for 22 weeks to represent the caloric intake of the typical North America diet. Male *Trib1^{Δhep}* mice on WTD similarly had a significant reduction in hepatic *Trib1* mRNA expression (Figure 3.1B). Female mice also showed >95% percent deletion in *Trib1* mRNA expression at similar time-points both on chow and WTD (Figure 3.1C, D). The residual expression of *Trib1* is likely attributable to its expression in other cells in the liver. These results demonstrate efficient and stable hepatocyte *Trib1* deletion using our approach.

***Trib1^{Δhep}* mice have increased plasma lipids and apoB protein levels.**

We then went on to confirm hepatic *Trib1* effects on plasma lipids. Male *Trib1^{Δhep}* mice had no change in triglyceride levels (Figure 3.2A) but had significantly increased total cholesterol (Figure 3.2B), HDL-C (Figure 3.2C) and non-HDL-C levels (Figure 3.2D), measured four weeks post-deletion in chow diet. After challenge with WTD feeding, male *Trib1^{Δhep}* mice still had no difference in triglyceride levels compared with WT controls (Figure 3.2E), whereas the differences in total cholesterol (Figure 3.2F), HDL-C (Figure 3.2G) and non-HDL-C (Figure 3.2H) were substantially enhanced over time. *Trib1^{Δhep}* female mice had a similar, but more modest plasma lipid phenotype on both chow and WTD (Figure 3.3). Since apoB is the major lipoprotein component of non-HDL-C, we also examined plasma for changes in apoB protein abundance and found that *Trib1^{Δhep}* male

mice have increased plasma apoB in both chow (Figure 3.4A) and WTD (Figure 3.4B) conditions.

***Trib1*^{Δhep} mice have increased LDL triglyceride and cholesterol lipoprotein particles**

To determine which specific lipoproteins were increased in the plasma of *Trib1*^{Δhep} mice, pooled plasma from mice was fractionated by FPLC. On chow, male *Trib1*^{Δhep} mice had a modest increase in triglyceride and total cholesterol in the LDL lipoprotein fractions compared with control mice (Figure 3.5 A-B). However, after being fed a WTD the increase of triglyceride and total cholesterol on the LDL lipoprotein fractions was further amplified in male *Trib1*^{Δhep} mice (Figure 3.5 C-D). Female *Trib1*^{Δhep} mice showed a similar but more modest pattern of increased LDL triglycerides and cholesterol increase on chow (Figure 3.6 A-B) but had a more robust response after WTD feeding (Figure 3.6 C-D). These results indicate that *Trib1*^{Δhep} mice accumulation of plasma lipids is primarily due to LDL particles, contributing to the increase in total cholesterol and apoB.

***Trib1*^{Δhep} mice have increased liver lipid accumulation and indications of liver damage but are resistant to diet induced obesity.**

On chow diet, *Trib1*^{Δhep} male mice had no difference in body weight to control mice (Figure 3.7A). However, after WTD feeding, their body weight was significantly lower than control mice (Figure 3.7A), even though their plasma lipid levels were significantly increased. These results suggest that *Trib1*^{Δhep} mice are resistant to diet induced obesity. Even though their body weight was not changed or decreased compared to control mice, *Trib1*^{Δhep} mice had significantly increased liver to body weight ratio (Figure 73.B), that was associated with an increased in hepatic triglycerides (Figure 3.7C) and cholesterol (Figure

3.7D) levels. *Trib1*^{Δhep} mice also had significantly increased plasma levels of ALTs over time in chow and WTD (Figure 3.7E), and decreased levels of circulating albumin protein (Figure 3.7F), both measures that are associated with impaired liver health.

***Trib1* LSKO mice have impaired plasma triglyceride clearance.**

Although steady state plasma triglycerides did not show significant changes in *Trib1*^{Δhep} mice (Figure 3.2 A,E; Figure 3.3A, E), the FPLC results clearly showed that *Trib1*^{Δhep} mice accumulate triglycerides in the LDL lipoprotein fractions (Figure 3.5A, C, Figure 3.6A,C). These results suggest that there might be an impairment in the clearance of plasma triglycerides in *Trib1*^{Δhep} mice. To test if plasma triglyceride accumulation is due to its improper clearance, we performed oral fat tolerance tests (OFTT), which measures the rates of postprandial lipemia. Upon challenge with an oral fat load, male *Trib1*^{Δhep} mice, both on chow and WTD fed conditions, showed significantly impaired TG clearance compared to control mice (Figure 3.8 A-B), which was confirmed by an increased area under the curve (Figure 3.8C). Female *Trib1*^{Δhep} mice also had a similar defect in triglyceride clearance on both diets (Figure 3.8D-F). These results indicate that deletion of *Trib1* in hepatocytes markedly impairs the ability of mice to clear triglyceride rich lipoproteins, thus leading to the increase in plasma triglycerides in FPLC fractions in the LDL range.

***Trib1*^{Δhep} mice have impaired LDL and VLDL apoB lipoprotein clearance.**

We then tested if the increased cholesterol in the LDL fractions was due to impaired apoB catabolism. *Trib1*^{Δhep} and control mice were injected with ¹²⁵I labeled human LDL and the decay of plasma ¹²⁵I was determined over 24 hours. Male *Trib1*^{Δhep} mice exhibited

markedly slower LDL catabolism, both on chow (Figure 3.9 A-B) and on WTD (Figure 3.9 C-D). Similar reductions in LDL catabolism were noted in female *Trib1^{Δhep}* mice, though not to the same degree as in male mice (Figure 3.10 A-D). We also examined whether VLDL-apoB catabolism was delayed. *Trib1^{Δhep}* and control mice were injected with ¹²⁵I-VLDL and the decay of plasma ¹²⁵I was determined over 24 hours. *Trib1^{Δhep}* mice had a significant reduction in the rate of VLDL-apoB catabolism compared with control mice (Figure 3.9 E-F). Thus, *Trib1^{Δhep}* mice have substantially slower turnover of both LDL-apoB and VLDL-apoB compared with control mice, both contributing to the accumulation of plasma apoB-containing lipoproteins.

Trib1^{Δhep} mice have significantly decreased hepatic Ldlr mRNA and protein.

Given the substantial defect in clearance of apoB-containing lipoproteins in *Trib1^{Δhep}* mice, we measured hepatic *Ldlr* mRNA and protein abundance. The LDLR is a key regulator of hepatic apoB catabolism and genetic variants that reduce *LDLR* expression or function in humans leads to elevated plasma LDL cholesterol levels [3]. Both male and female *Trib1^{Δhep}* mice on chow diets had significantly reduced hepatic expression of *Ldlr* mRNA compared with control mice (Figure 3.11 A, C), as well as reduced levels of LDLR protein (Figure 3.11 B, D). Thus, deletion of *Trib1* in mouse hepatocytes resulted in substantial downregulation of the LDLR, providing a molecular basis for the impaired clearance of apoB containing lipoproteins.

Hepatic deletion of *Trib1* in the absence of *Ldlr* has increased lipids, but no effect on LDL-apoB or VLDL-ApoB clearance.

To determine whether the effects of *Trib1* deletion on the clearance of apoB-containing lipoproteins were mediated solely by downregulation of the *Ldlr*, we generated a *Trib1*^{flox/flox}; *Ldlr* KO mice and injected them with AAV8-CRE or AAV8-NULL, permitting the comparison of *Trib1*^{Δhep} to *Trib1* WT mice on the background of *Ldlr* deficiency. Hepatic *Trib1* mRNA levels showed the expected >95% reductions of *Trib1* in *Trib1*^{Δhep}; *Ldlr* KO mice and *Ldlr* mRNA and protein levels were undetectable in both groups compared to controls (Figure 3.12 A-B). We measured plasma lipids and found that deletion of *Trib1* in hepatocytes in the absence of *Ldlr* further increased plasma triglycerides, total cholesterol, HDL cholesterol and non-HDL cholesterol (Figure 3.12 C-F). Fractionation of plasma by FPLC revealed that triglycerides and total cholesterol were increased in the VLDL and LDL fractions (Figure 3.12 G-H).

We also performed LDL-apoB and VLDL-apoB kinetic studies in the three groups of mice. As expected, the turnover of both LDL-apoB and VLDL-apoB was markedly slower in *Trib1* WT; *Ldlr* KO mice compared with control mice (Figure 3.13). However, deletion of hepatic *Trib1* in the absence of the LDLR had no further effect on clearance of LDL-apoB and VLDL-apoB (Figure 3.13). These data indicate that the effect of *Trib1* deletion on apoB-containing lipoprotein clearance is dependent on *Ldlr*. However, these results also indicate that *Trib1* deletion increases steady state plasma lipids in a mechanism that is independent of its regulation of apoB clearance.

***Trib1*^{Δ_{hep}} mice have increased secretion of triglyceride-poor apoB containing lipoproteins from the liver and increased hepatic endoplasmic reticulum (ER) stress.**

The previous results suggested that hepatic *Trib1* modulates apoB clearance through its regulation of *Ldlr*, but that steady state lipids are regulated through an independent mechanism. Previous studies have suggested that *Trib1* regulates the levels of VLDL secretion from the liver and we decided to test this in our model. We performed newly synthesized apoB secretion studies by administration of pluronic to inhibit lipoprotein lipolysis and found that *Trib1*^{Δ_{hep}} mice have significantly increased apoB secretion despite having no difference in triglyceride secretion (Figure 3.14 A-B). We also measured apoB secretion in the context of the *Ldlr* KO background and observed the same results (Figure 3.14 C-D). The increase in apoB secretion without an increase in triglyceride secretion suggested that a relatively triglyceride-poor apoB-containing lipoprotein is being secreted by the *Trib1*^{Δ_{hep}} hepatocytes. To test this, we pooled post-pluronic plasma from the newly synthesized apoB secretion experiments and performed sucrose density ultracentrifugation to separate the lipoproteins based on their density. This experiment showed a shift of the newly synthesized apoB in the *Trib1*^{Δ_{hep}} mice toward the LDL density fractions compared with control mice (Figure 3.14E), consistent with the secretion of more dense apoB-containing lipoproteins. Because changes on ER stress are known to affect the secretion of apoB lipoprotein particles [147], we assessed pEIF2a, a known marker of ER stress, and found it to be markedly increased in *Trib1*^{Δ_{hep}} mice independent of *Ldlr* genotype (Figure 3.14 F-G). We conclude that hepatocyte-specific *Trib1* deletion results in increased secretion of apoB as more dense particles, exacerbating the increase in

plasma LDL cholesterol and apoB levels beyond the contribution of delayed LDL-apoB clearance.

DISCUSSION

In the last decade, GWAS have served as a strong method to identify new genetic targets for cardiometabolic diseases. The 8q24 locus, near the *TRIB1* gene, was one of the first and most strongly associated loci for all 4 major plasma lipids traits and well as CAD [69]. Additionally, this locus has also been associated with levels of ALTs and the development of hepatic steatosis [124, 146, 148]. Since all these associations came to light, *TRIB1* has been the target of multiple studies with the goal of investigating its direct association with plasma lipid traits as well as the possible mechanisms of action. Our group was the first one to show direct association of *Trib1* with plasma lipid regulation *in vivo* using mouse models. Using an AAV-mediated *Trib1* hepatic overexpressing system, mice had a decrease in plasma lipids and hepatic lipogenesis [125]. We also demonstrated that *Trib1* liver specific deletion in mice leads to increases in plasma lipids, hepatic lipogenic gene expression and de novo lipogenesis, which lead to hepatic steatosis development [104]. However, more questions regarding *TRIB1* effect on other lipoprotein metabolism pathways remain unanswered.

In this study, I confirmed that hepatic deletion of *Trib1* in mice increases plasma levels of total cholesterol, HDL cholesterol and non-HDL cholesterol in a chow diet. Additionally, I showed that this accumulation of lipids is specifically in the LDL triglyceride and cholesterol fractions and that *Trib1*^{Δ*hep*} mice have an increased accumulation of apoB proteins, the main apolipoprotein in LDL. The results from these experiments were confirmed in male and female mice as well as in a WTD which is designed to approximate

the "typical" human diet of North America, which makes our results biologically relevant to human populations. We also discovered that even though *Trib1*^{Δ_{hep}} mice have increased plasma lipids, they are resistant to diet induced obesity, however the molecular mechanism by which hepatic *Trib1* might be regulating this phenotype has not been elucidated. Previous research has suggested that in white adipose tissue (WAT), *Trib1* expression is upregulated during acute and chronic inflammation in *db/db* mice, and *Trib1* heterozygous knockout mice have impaired cytokine gene expression mediated by NF-κB interaction in WAT, which protects them from weight gain and adiposity when fed a high fat diet [149]. It would be interesting to study the effects of *Trib1* hepatic deletion on cytokine gene expression and to determine if a similar mechanism is responsible for the protection against obesity in the liver. It is also possible that hepatic deletion of *Trib1* might have secondary effects on other tissues such as WAT, and that might be mediating this phenotype.

Variants within the *TRIB1* locus have been repeatedly associated with the develop of hepatic steatosis in humans [146, 148]. Consistent with this association, *Trib1*^{Δ_{hep}} mice showcase an increased liver to body weight ratio that is characterized by increased hepatic triglyceride and cholesterol compared to control mice. *Trib1*^{Δ_{hep}} mice also presented strikingly high levels of plasma ALTs, which is an enzyme that is produced by the liver and its levels can increase when liver cells are damaged, so its levels can be used to evaluate the condition of the liver [150]. Additionally, *Trib1*^{Δ_{hep}} mice had significantly low levels of plasma albumin. Albumin is a protein that is produced by the liver and serves as a transport protein to helps carry vitamins, enzymes, and other important substances in the circulation, and it is also used to determine liver health [151]. Certain liver diseases, such as cirrhosis, are characterized by decreased albumin levels,

as well as impaired albumin function [151]. Overall, *Trib1*^{Δ_{hep}} mice have increased hepatic lipids and dysregulated markers of liver health, which align with the GWAS associations with the development of hepatic steatosis.

We demonstrated that hepatic deletion of *Trib1* in mice impairs postprandial lipemia, which leads to accumulation of triglycerides in the LDL lipoprotein fractions. We also demonstrated that accumulation of total cholesterol in the LDL lipoprotein fractions *Trib1*^{Δ_{hep}} mice is due to the improper catabolism of LDL and VLDL lipoproteins and most importantly, we demonstrated that the improper catabolism of these lipoproteins is due to a decrease of the *Ldlr* mRNA and protein levels. As mentioned before, the LDLR is the main receptor that mediates the clearance of plasma LDL-C from the circulation to the liver, and it is well known that mutations that interfere with LDLR function lead to elevated plasma LDL-C levels which are associated with increased risk of cardiovascular disease.

Prior to my investigation, hepatic *TRIB1* had not been directly associated with the regulation of the LDLR, but some studies suggested a possible interaction. One group discovered that the small molecule compound BRD0418 upregulates *TRIB1* expression in HepG2 cells [152]. BRD0418 was able to suppress triglyceride synthesis and apoB secretion, in addition to downregulating the expression of MTP and APOC3, both key components of the lipoprotein assembly pathway, as well as it was shown to modulate cholesterol metabolism in hepatic cells by elevating the expression of the *LDLR* transcript and protein [152]. These phenotypes were phenocopied by *TRIB1* cDNA overexpression, however, the effects of BRD0418 persisted in *TRIB1*-null cells, indicating that *TRIB1* is sufficient but not necessary to transmit the effects of the drug [152]. Another group discovered that the compound Berberine, which is a natural lipid lowering drug that reduces plasma LDL cholesterol, total cholesterol and triglycerides in hyperlipidemic

patients and in mice by mechanisms involving upregulation of *LDLR*, is able to upregulate the levels of *Trib1* mRNA [153]. The increase in *Trib1* mRNA expression was associated with reduced expression of lipogenic genes including *Cebpa*, *Acc1* and *Scd1*. However, Berberine treatment was able to reduce plasma lipids in mice in a wild type background as well as in a hypercholesterolemic *Ldlr* deficient mice, suggesting that the role of *Trib1* in the Berberine mediated triglyceride lowering is independent of LDLR regulation [153]. Furthermore, a group that studies circadian regulation of lipid associated genes demonstrate that ablation of the liver clock in mice perturbs diurnal regulation of lipid-associated genes in the liver and markedly reduced the expression of the gene *Trib1*, and that *Trib1* rescue experiments lowered PCSK9 levels, increased LDLR protein expression and restored plasma cholesterol homeostasis in mice lacking a functional liver clock [154]. Their results illustrated a mechanism by which the biological clock regulates cholesterol metabolism and the expression of the *Ldlr* by regulating non-clock genes such as hepatic *Trib1*.

My studies show that hepatic *Trib1* can regulate plasma lipid metabolism both independently and by its regulation of the LDLR (Figure 3.15). I demonstrated that hepatic *Trib1* is able to regulate the clearance of apoB containing lipoproteins through its regulation of LDLR, but that steady state plasma lipids are regulated independently of the LDLR. As *Trib1* expression has been previously associate with the regulation of triglyceride production and VLDL secretion from the liver, we decided to explore if this is the mechanism by which *Trib1* is regulating steady state plasma lipids independently of LDLR regulation. Indeed, we demonstrated that in the absence of the *Ldlr*, *Trib1* deletion is able to further increase the secretion of apoB lipoproteins from the liver, a phenotype that was also observed in *Trib1* hepatic deleted mice in a wild type background.

Surprisingly, the increased in apoB secretion was not accompanied by an increase in triglyceride secretion from the liver, which suggest that hepatic deletion of *Trib1* leads to the secretion of triglyceride depleted apoB containing lipoproteins. This was a striking finding considering that *Trib1*^{Δ*hep*} mice have increased levels of triglycerides in their hepatocytes, however this triglyceride is not being incorporated into the newly formed VLDL particles. This finding was also surprising because the secretion of VLDL-apoB is a tightly regulated process by the Endoplasmic-reticulum-associated protein degradation (ERAD) complex, which targets improperly folded or improperly lipidated apoB proteins for ubiquitination and proteasomal degradation [147, 155]. In our studies we showed that hepatic deletion of *Trib1* results in increased ER stress in hepatocytes, which has been previously associated with increased apoB secretion from hepatocytes. However, more questions regarding the mechanism by which *Trib1* hepatic deletion results in the secretion of smaller VLDL particles as well as the molecular mechanism by which hepatic

FIGURES

Figure 3. 1: Hepatic *Trib1* mRNA levels in *Trib1*^{Δhep} mice relative to control mice.

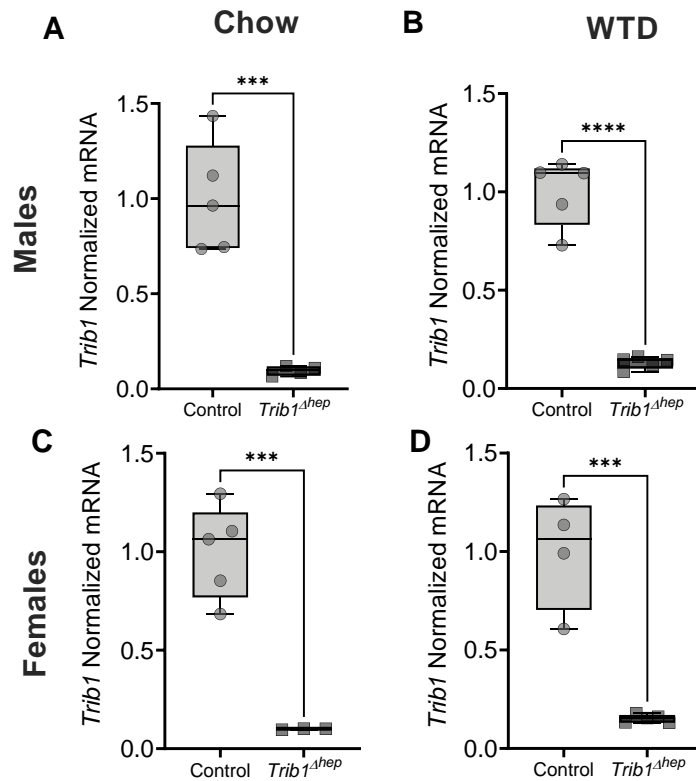


Figure 3.1: A-D. Hepatic transcript levels of *Trib1* in chow-fed male mice (n=5) 8 weeks after injection (A), 22 weeks post deletion (following 17 weeks on WTD) (B), in chow-fed female mice (n=5) 4 weeks after injection (C) and female mice (n=5), 22 weeks post injection and following 17 weeks of WTD feeding. Box plots indicate median, 25th and 75th percentiles with whiskers extending to minimum and maximum values. Symbols indicate single values. Significance was determined by two-tailed, unpaired Student's t test (**p ≤ 0.01; ***p ≤ 0.001; ****p ≤ 0.0001).

Figure 3. 2: Hepatic Deletion of *Trib1* increases plasma cholesterol in male mice.

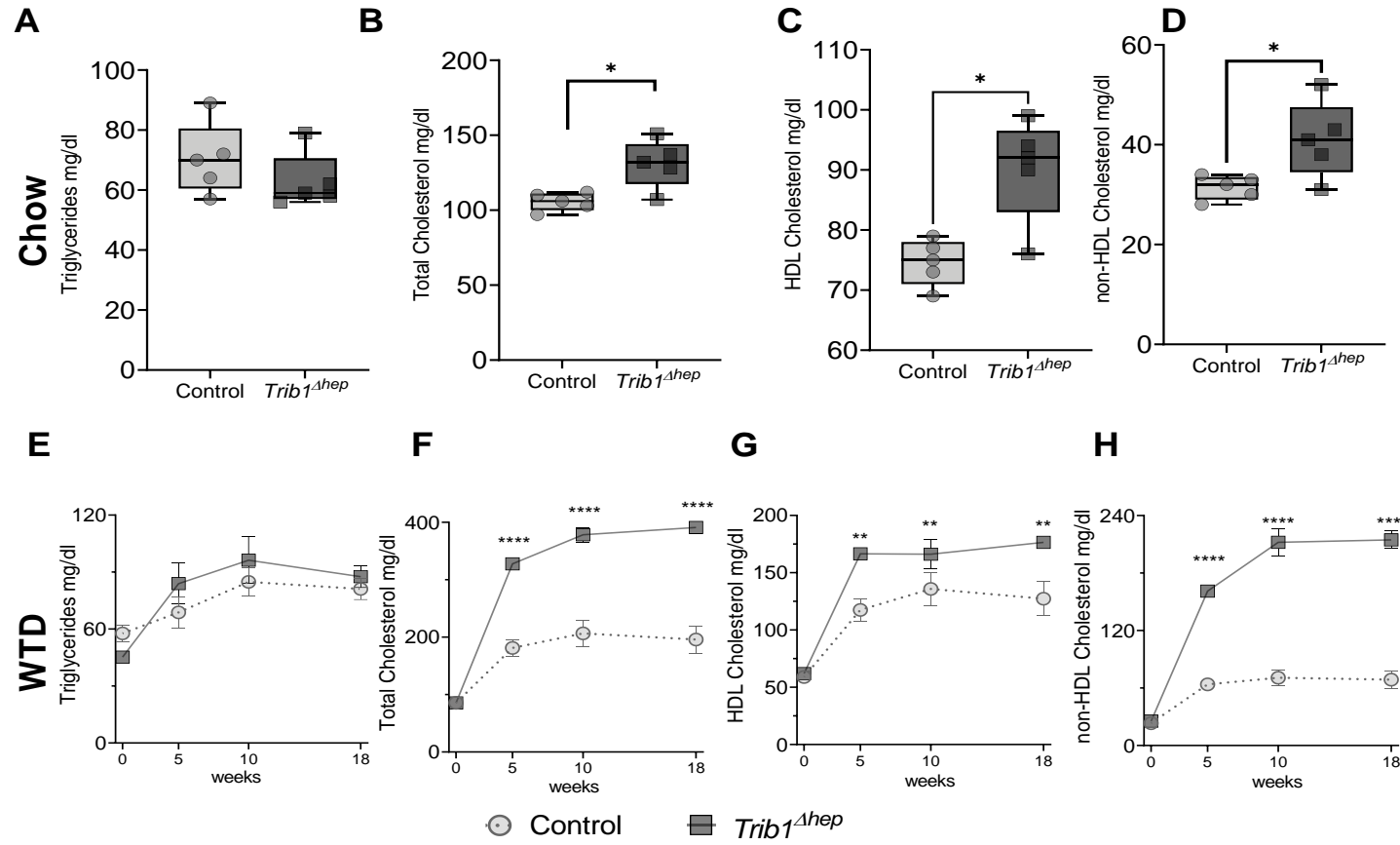


Figure 3.2: A- D. Plasma triglycerides, total cholesterol, HDL-cholesterol and non-HDL cholesterol levels in chow-fed *Trib1^{Δhep}* male mice 4 weeks post-deletion, (n=5). Box plots indicate median, 25th and 75th percentiles with whiskers extending to minimum and maximum values. Symbols indicate single values. Significance was determined using two-tailed, unpaired Student's t-test (*p≤0.05). **E-H.** Plasma triglycerides, total cholesterol, HDL-cholesterol and non-HDL cholesterol levels at indicated timepoints over 18 weeks of WTD-feeding (n=8). Data are expressed as mean ± s.e.m for the experimental group. Significance was determined using 2-way ANOVA with Tukey's multiple comparisons test (****p≤0.0001).

Figure 3. 3: Hepatic deletion of *Trib1* increases plasma cholesterol in female mice.

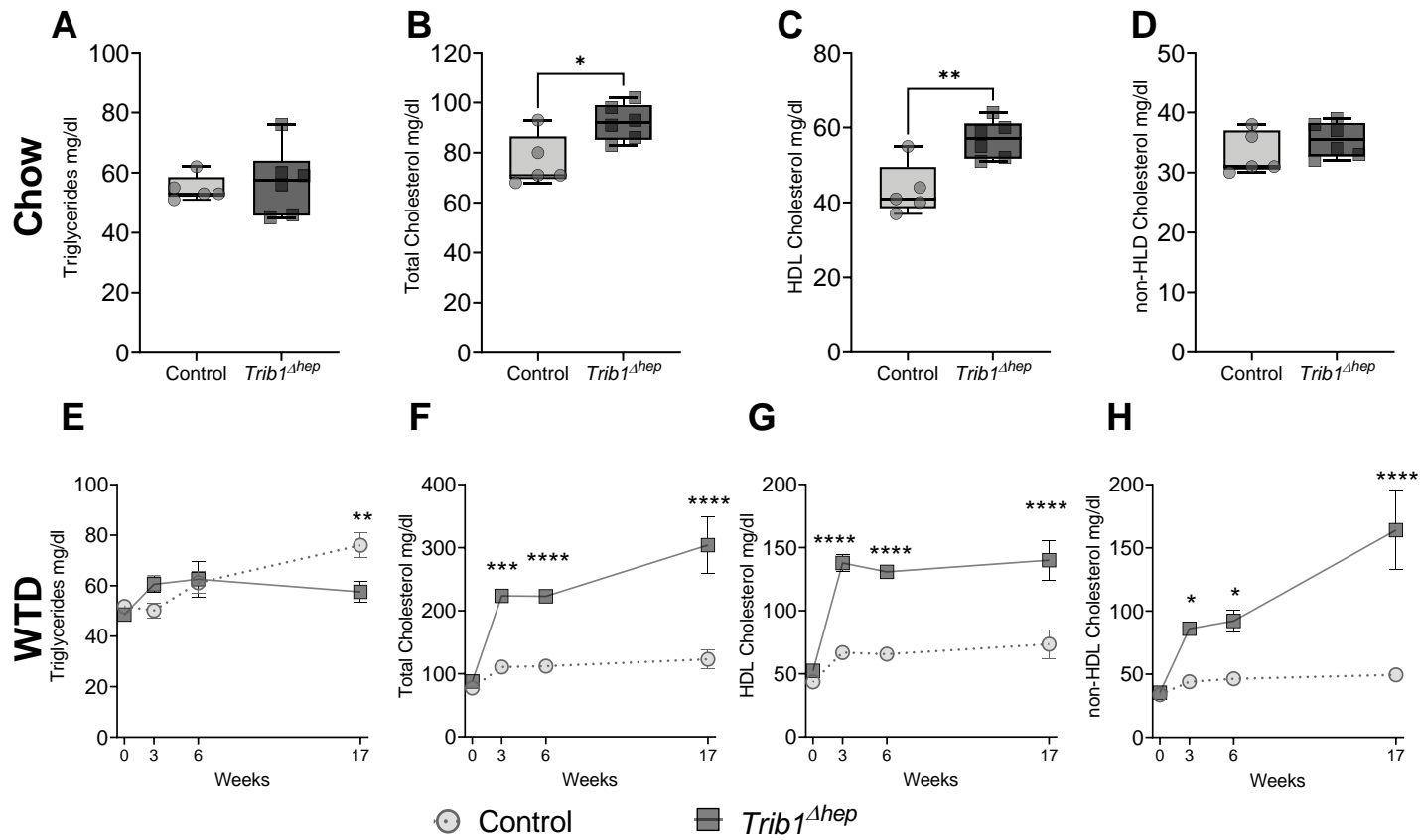


Figure 3.3: A-D. Plasma triglycerides, total cholesterol, HDL-Cholesterol and non-HDL cholesterol levels 2 weeks post-deletion on chow diet mice (n=5). Box plots indicate median, 25th and 75th percentiles with whiskers extending to minimum and maximum values. Symbols indicate single values. Significance was determined using two-tailed, unpaired Student's t-test (*p≤0.05, **p≤0.01). **E-H.** Plasma triglycerides, total cholesterol, HDL-cholesterol and non-HDL cholesterol levels at selected timepoints over 17 weeks on WTD, (n=5). Data are expressed as mean ± s.e.m for the experimental group. Significance was determined by one-way ANOVA with Tukey's multiple correction test (*p ≤ 0.05; **p ≤ 0.01, ***p ≤ 0.001; ****p ≤ 0.0001).

Figure 3. 4: Hepatic deletion of *Trib1* increases plasma ApoB protein levels in male mice.

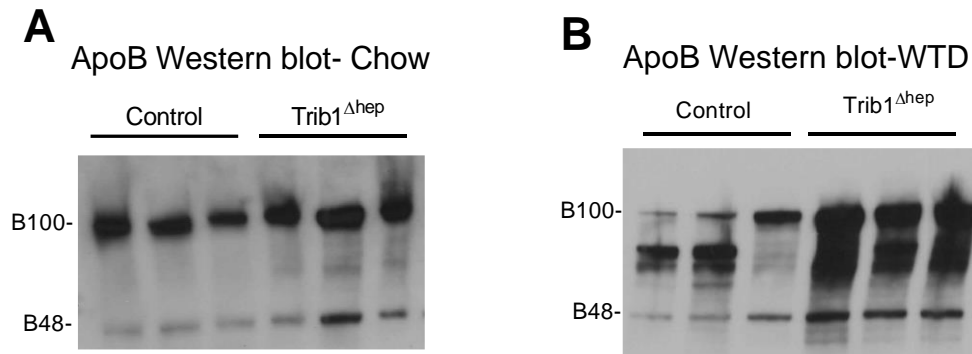


Figure 3.4: A-B. Immunoblots of ApoB protein in plasma from chow-fed mice 4 weeks post deletion (**A**), and mice fed WTD for 11 weeks. (**B**). Equal volumes of plasma were loaded in each well and gel was run for 3hrs at 90volts to properly separate apoB 100 from apoB 48.

Figure 3. 5: Hepatic deletion of *Trib1* increases plasma LDL lipoprotein fractions in male mice.

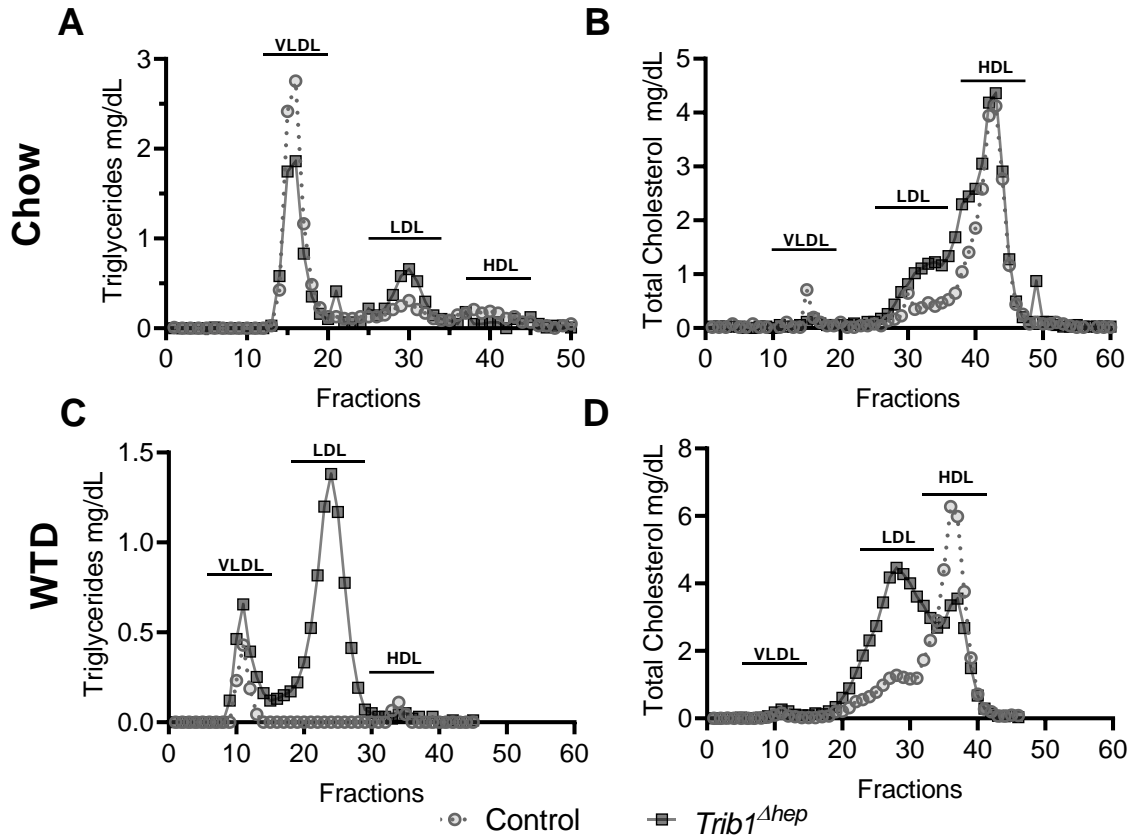


Figure 3.5: A-B. FPLC was performed on pooled plasma from male mice fed chow for 6 weeks and **C-D.** mice fed WTD for 12 weeks to separate lipoproteins based on their size. Triglycerides (**A, C**) and total cholesterol (**B, D**) concentrations were measured in all fractions.

Figure 3. 6: Hepatic deletion of *Trib1* increases plasma LDL lipoprotein fractions in female mice.

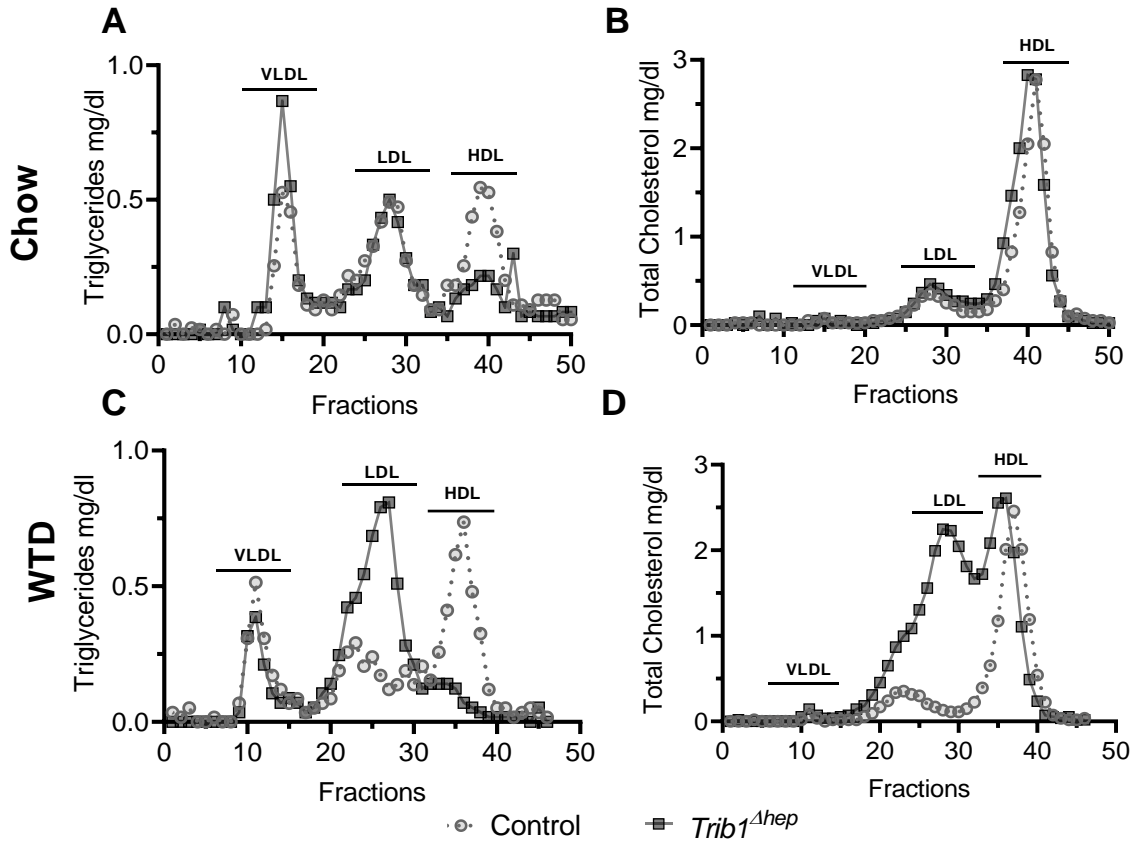


Figure 3.6: A-B. FPLC was performed on pooled plasma from female mice fed chow for 8 weeks and **C-D.** mice fed WTD for 12 weeks to separate lipoproteins based on their size. Triglycerides (**A, C**) and total cholesterol (**B, D**) concentrations were measured in all fractions.

Figure 3. 7: Hepatic deletion of *Trib1* protects against diet induced obesity and show indications of liver damage.

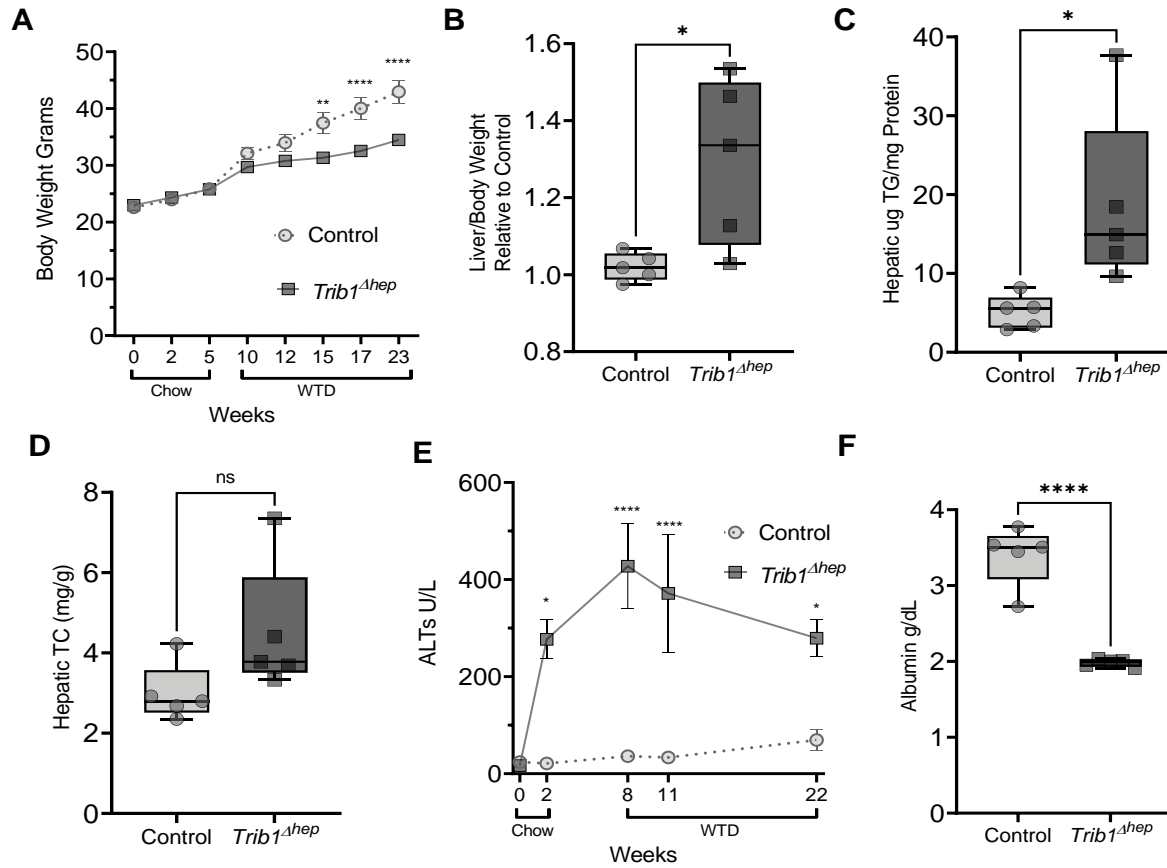


Figure 3.7: A. Changes in body weight during chow (weeks 0-5) and WTD (weeks 6-23) feeding (n=8). **B.** Liver to body weight ratio in chow fed mice 8 weeks post deletion (n=5). Hepatic triglyceride (**C.**) and total cholesterol (**D.**) levels in chow fed mice 8 weeks post deletion (n=5). **E.** Plasma ALT levels at indicated timepoints over 22 weeks of chow and WTD-feeding (n=8). **F.** Plasma Albumin levels in chow fed mice 4 weeks post deletion (n=5). **A,E.** Data are expressed as mean \pm s.e.m for the experimental group. Significance was determined using 2-way ANOVA with Tukey's multiple comparisons test. **B,C,D,F.** Box plots indicate median, 25th and 75th percentiles with whiskers extending to minimum and maximum values. Symbols indicate single values. Significance was determined using two-tailed, unpaired Student's t-test. For all the results: * $p \leq 0.05$, ** $p \leq 0.01$, **** $p \leq 0.0001$.

Figure 3. 8: Hepatic deletion of *Trib1* impairs post-prandial triglyceride clearance in male and female mice.

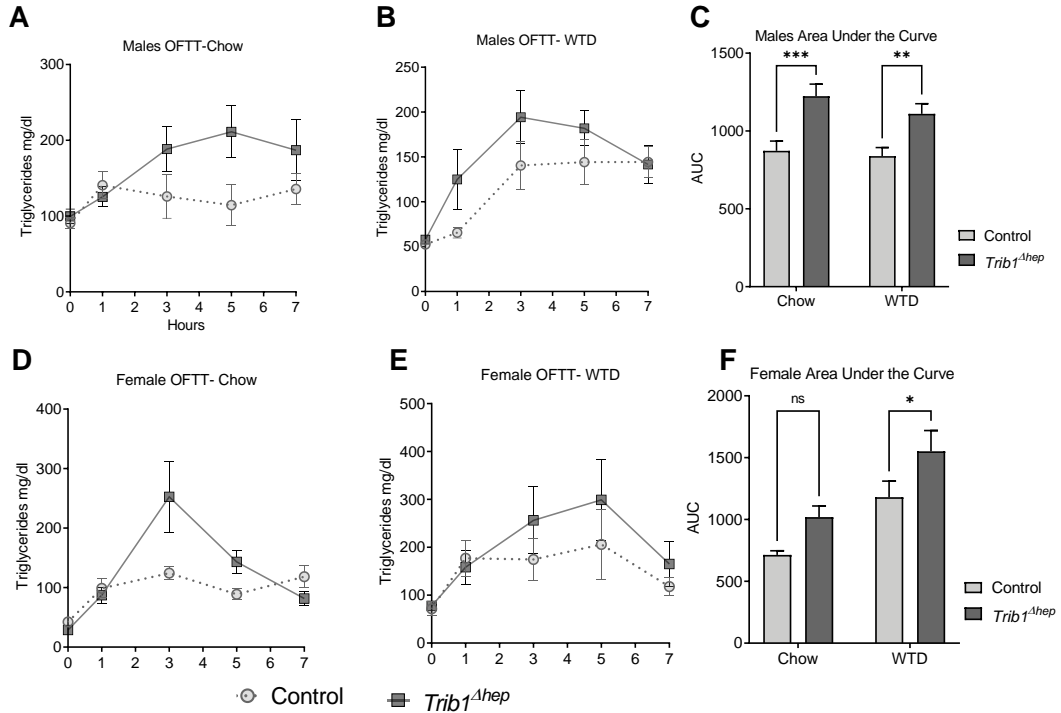


Figure 3.8: A-B. OFTT in male mice after 5 weeks on chow (A) and 5 weeks on WTD (B). **C.** AUC calculation for A and B. **D-E.** OFTT in female mice after 5 weeks on chow (D) and 6 weeks on WTD (E). **F.** AUC calculation for D and E. Data are expressed as mean ± s.e.m for the experimental group. Significance was determined using 2-way ANOVA with Tukey's multiple comparisons test (*p≤0.05, **p≤0.01, ***p≤0.001).

Figure 3. 9: Hepatic deletion of *Trib1* impairs LDL and VLDL apoB clearance in male mice.

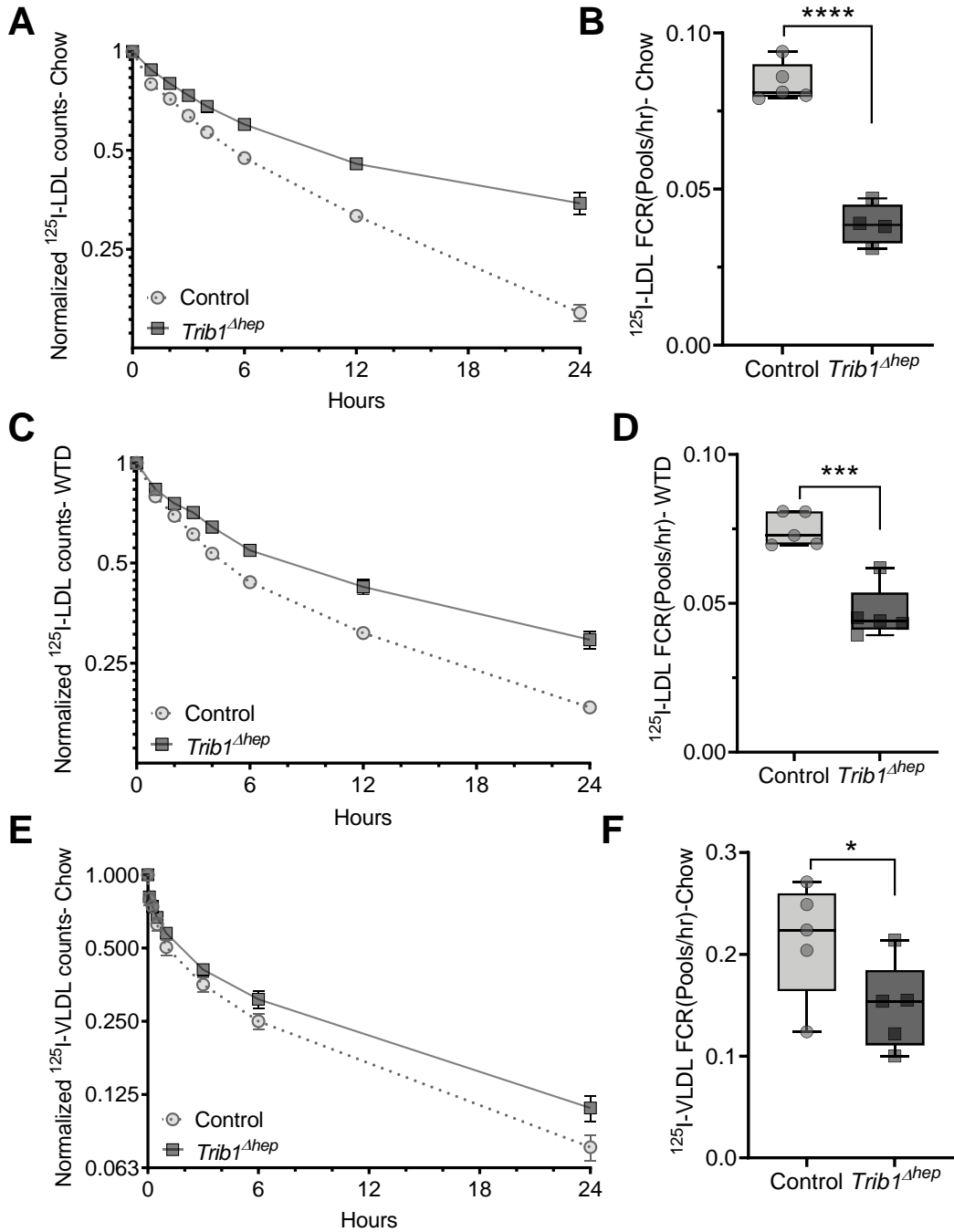


Figure 3. 9: A-B. LDL clearance in chow-fed mice 8 weeks after AAV injection (n=5) and **C-D.** WTD-fed mice for 19 weeks (24 weeks post AAV injection). **A-D.** Mice were injected with ¹²⁵I-radiolabeled LDL isolated from human plasma. Clearance of ¹²⁵I-LDL was determined by measuring residual ¹²⁵I-activity at different time-points after injection (2 min-24 hour); residual ¹²⁵I-activity is expressed as fraction of the total ¹²⁵I-activity, 2 min after injection. **B, D.** Fractional catabolic rate (FCR) of LDL from A and C, this is calculated from the reciprocal of the area under a fitted biexponential curve; and represents fraction of LDL cleared per hour. Results were confirmed in an independent cohort in chow fed mice and 2 independent cohorts in WTD fed mice. **E.** VLDL clearance in chow-fed male mice 8 weeks after AAV injection. Mice were injected with ¹²⁵I-radiolabeled human VLDL. Plasma was sampled at intervals over a period of 24 hours and the total remaining counts were normalized to the injected dose at 1 minute post injection of ¹²⁵I- VLDL. **F.** FCR of ¹²⁵I-VLDL. **A, C, D.** Data are expressed as mean ± s.e.m for the experimental group. **B, D, F.** Box plots indicate median, 25th and 75th percentiles with whiskers extending to minimum and maximum values. Symbols indicate single values. Significance was determined using two-tailed, unpaired Student's t-test (*p≤0.05, ***p≤0.001, ****p≤0.0001).

Figure 3. 10: Hepatic deletion of *Trib1* impairs LDL apoB clearance in female mice.

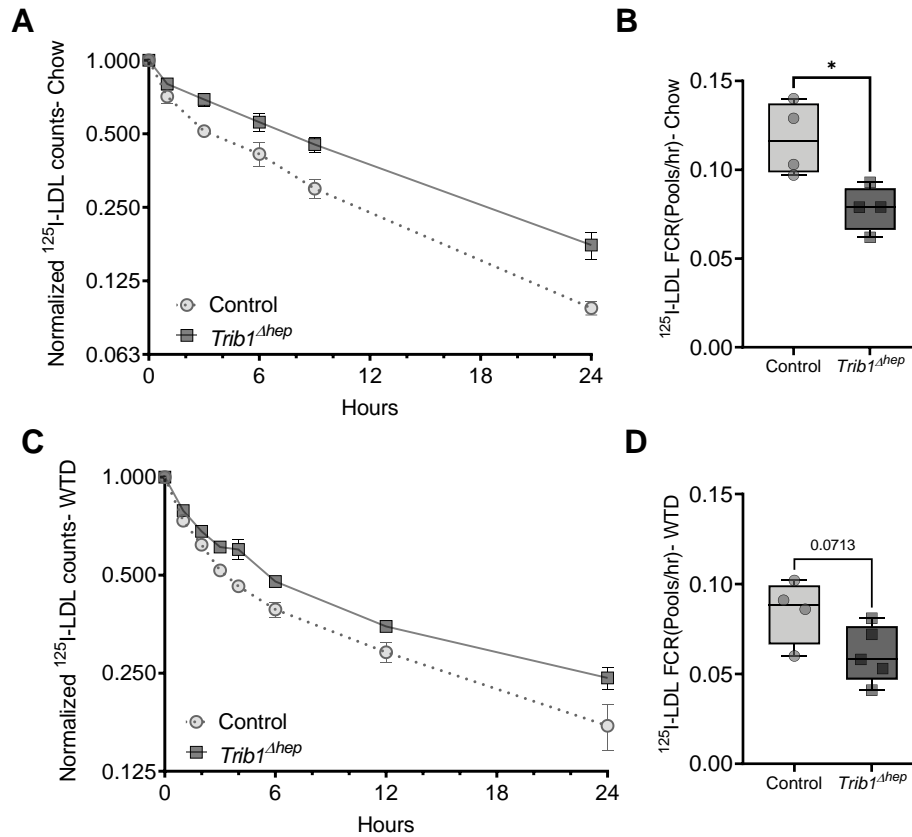


Figure 3.10: A-B. LDL clearance in chow-fed mice 10 weeks after AAV injection (n=5) and **C-D.** WTD-fed mice for 19 weeks (24 weeks post AAV injection). **B, D.** FCR of LDL from A and C is calculated from the reciprocal of the area under a fitted biexponential curve and represents fraction of LDL cleared per hour. **A, C.** Data are expressed as mean \pm s.e.m for the experimental group. **B, D.** Box plots indicate median, 25th and 75th percentiles with whiskers extending to minimum and maximum values. Symbols indicate single values. Significance was determined using two-tailed, unpaired Student's t-test (*p \leq 0.05).

Figure 3. 11: Hepatic deletion of *Trib1* reduces *Ldlr* mRNA and protein levels in male and female mice.

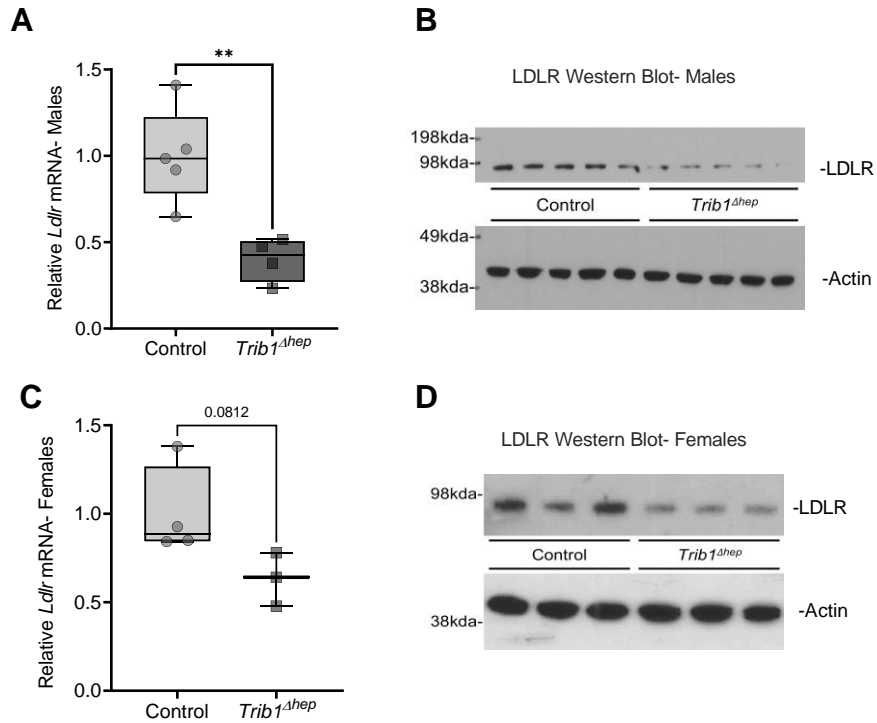


Figure 3.11. A. Hepatic transcript levels of *Ldlr* in chow fed male *Trib1*^{Δhep} mice relative to control mice 8 weeks after AAV injection (n=5). **B.** Hepatic protein levels of LDLR and β-actin in control and *Trib1*^{Δhep} mice (n=5) from mice in A. **C.** Hepatic transcript levels of *Ldlr* in female *Trib1*^{Δhep} mice relative to control mice 8 weeks after AAV injection (n=3 and 4). **D.** Hepatic protein levels of LDLR and β-actin in control and *Trib1*^{Δhep} mice (n=5) from mice in C. Box plots indicate median, 25th and 75th percentiles with whiskers extending to minimum and maximum values. Symbols indicate single values. Significance was determined using two-tailed, unpaired Student's t-test (**p≤0.01).

Figure 3. 12: Hepatic deletion of *Trib1* in the absence of *Ldlr* increases steady state plasma lipids.

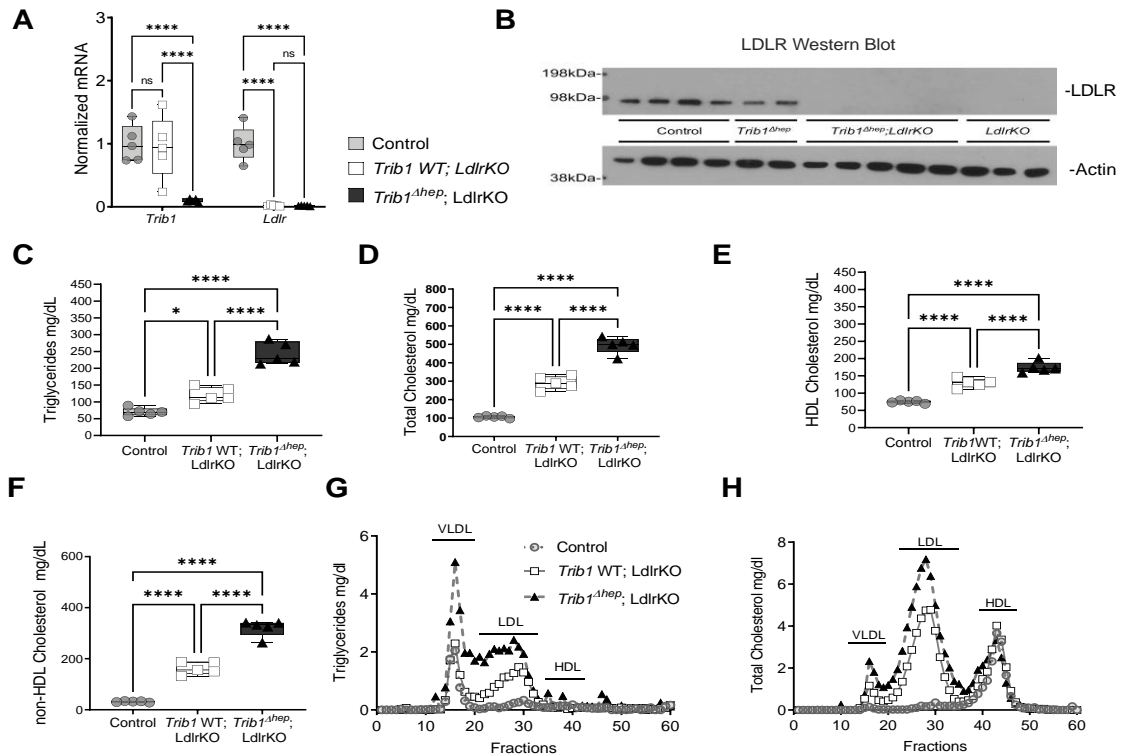


Figure 3.12: A. Hepatic mRNA levels of *Trib1* and *Ldlr* in male mice (n=5) 8 weeks post deletion. **B.** Hepatic LDLR and Actin protein levels in male mice 8 weeks post deletion. **C-F.** Plasma triglycerides, total cholesterol, HDL Cholesterol and non-HDL cholesterol levels in chow-fed male mice 4 weeks post-deletion. **G-H.** FPLC of triglyceride and total cholesterol performed on pooled plasma from chow fed mice for 6 weeks after AAV-CRE injection. Box plots indicate median, 25th and 75th percentiles with whiskers extending to minimum and maximum values. Symbols indicate single values. Significance was determined using ordinary One-way ANOVA with multiple comparisons test (*p<0.05, ****p<0.0001).

Figure 3. 13: Hepatic deletion of *Trib1* in the absence of *Ldlr* increases steady state plasma lipids.

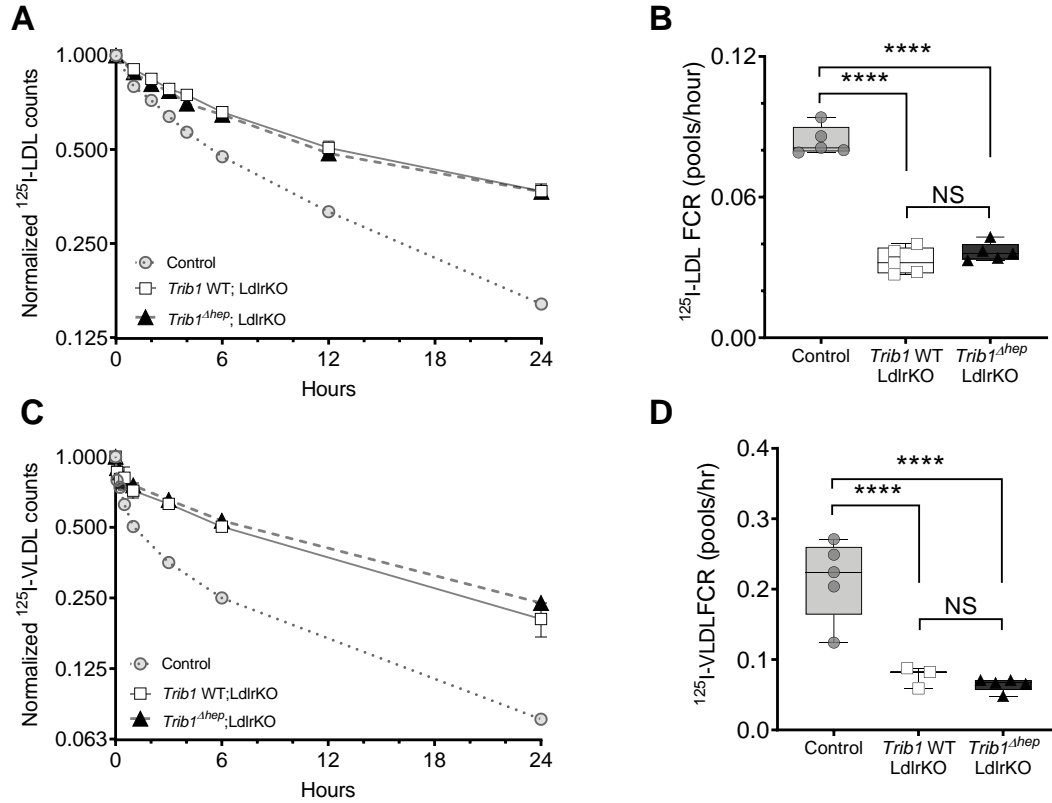


Figure 3.13: A. ¹²⁵I-LDL clearance in chow-fed male mice 8 weeks after AAV injection (n=5). **B.** FCR from panel A. **C.** ¹²⁵I-VLDL clearance in chow-fed male mice 8 weeks after AAV injection. **D.** FCR from panel C. **A, C.** Data are expressed as mean ± s.e.m for the experimental group. **B, D.** Box plots indicate median, 25th and 75th percentiles with whiskers extending to minimum and maximum values. Symbols indicate single values. Significance was determined using ordinary One-way ANOVA with multiple comparisons test (****p≤0.0001).

Figure 3. 14: Hepatic deletion of *Trib1* in the absence of *Ldlr* increases steady state plasma lipids due to increase in the hepatic secretion of ApoB

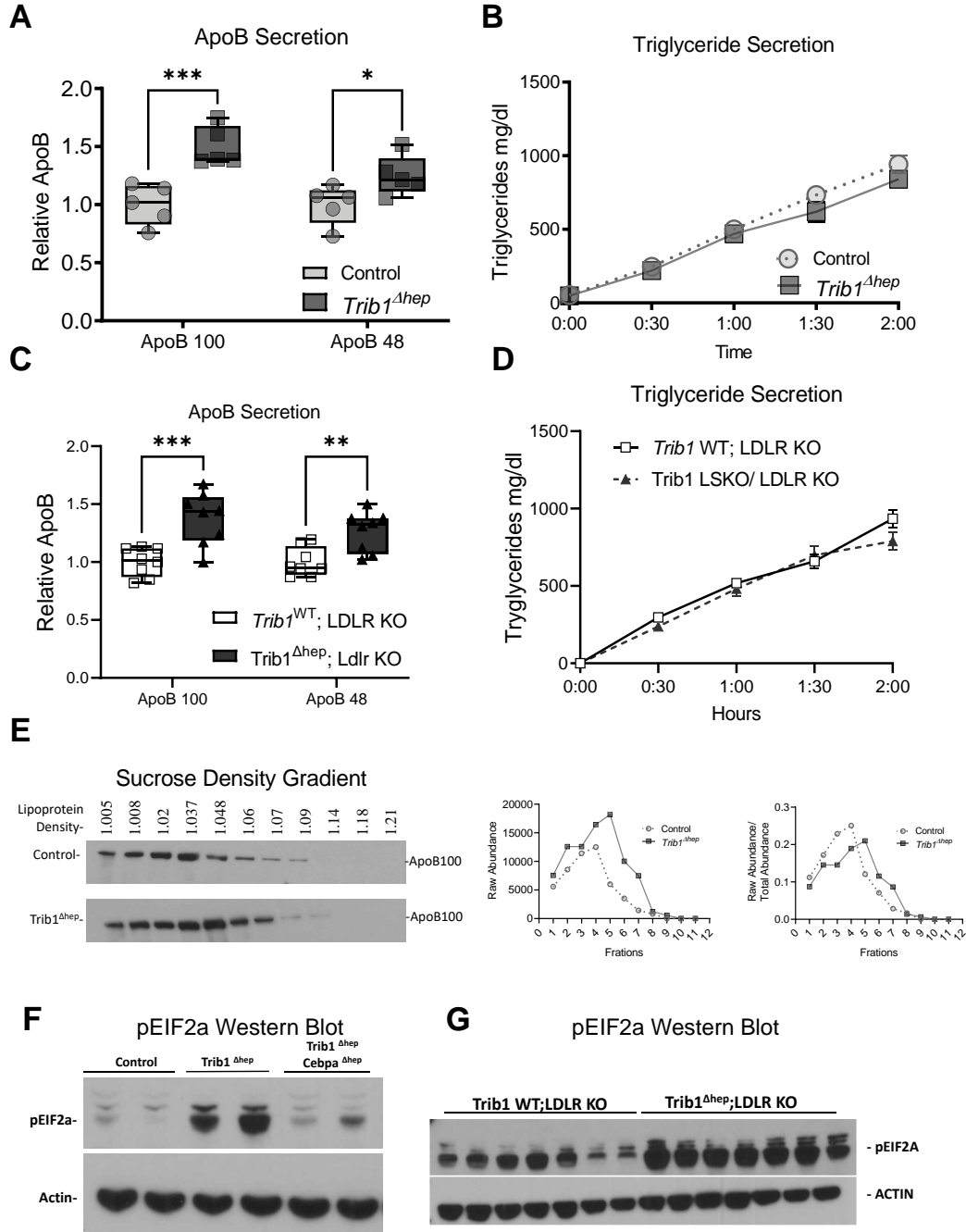


Figure 3.14: A, C. Quantification of apoB levels in plasma collected at 1.5 hours after injection with P407 and 200 μCi of ^{35}S methionine-cysteine. Box plots indicate median, 25th and 75th percentiles with whiskers extending to minimum and maximum values. Symbols indicate single values. **B, D.** Triglyceride production over time after injection with P407 and 200 μCi of ^{35}S methionine-cysteine. Data are expressed as mean \pm s.e.m for the experimental group. Significance was determined by one-way ANOVA with Tukey's multiple correction test (* $p \leq 0.05$, ** $p \leq 0.01$, *** $p \leq 0.001$). **E.** ApoB 100 protein from pooled plasma samples separated by sucrose density gradient after injection with P407 and 200 μCi of ^{35}S methionine-cysteine, raw quantification of ApoB100 levels and fractional distribution of ApoB100 across the gradient. **F.** Hepatic pEIF2a and Actin protein levels in male mice 4 weeks post deletion. **G.** Hepatic pEIF2a and Actin protein levels in male mice 8 weeks post deletion.

Figure 3. 15: Role of Hepatic *Trib1* in the regulation of LDL-apoB.

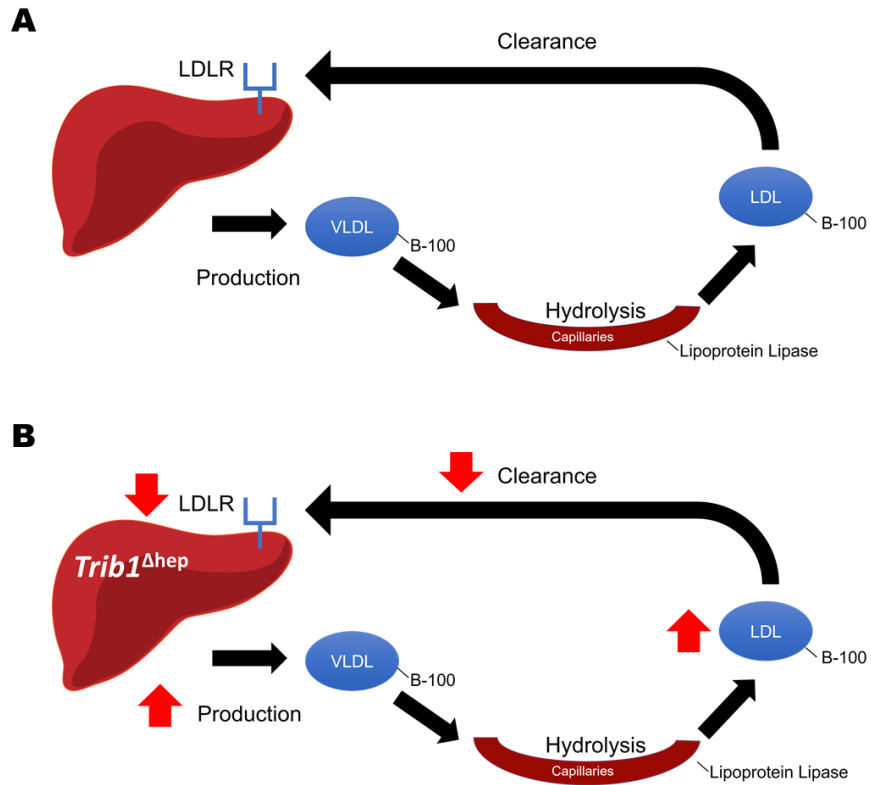


Figure 3.15: A. Simplified diagram of the endogenous lipoprotein metabolism pathway. Circulating lipids are highly regulated by the rates of production and secretion from the liver in the form VLDL. VLDL is then hydrolyzed in the capillaries mediated by LDL which converts them into LDL lipoproteins. LDL particles are then cleared to the liver mediated by the LDLR and other related receptors. **B.** *Trib1* hepatic deletion increases LDL-apoB levels by increasing the rates of ApoB production independently of the LDLR-mediated clearance of LDL-apoB.

CHAPTER 4:

Hepatic *TRIB1* regulates LDL metabolism through CEBPA-mediated regulation of the LDL receptor.

ABSTRACT

The *TRIB1* gene, a GWAS signal for plasma lipids and CAD, has been broadly demonstrated to regulate plasma lipids in cell and animal models. In the previous chapter I demonstrated that murine hepatic *Trib1* regulates the rates of lipoprotein secretion from the liver as well as the rate of apoB containing lipoprotein clearance mediated by the LDLR in hepatocytes. Since *TRIB1*'s most studied molecular function is the interaction with the E3 ubiquitin ligase COP1 to target the transcription factor CEBPA for ubiquitination and proteasomal degradation, we decided to explore if this interaction is responsible for *TRIB1* effects on the LDLR. The results from my studies showed that simultaneous deletion of *Cebpa* in *Trib1*^{Δhep} mice (*Trib1*^{Δhep};*Cebpa*^{Δhep}/ DKO mice), eliminated the effects of hepatic deletion of *Trib1* on plasma lipids, hepatic lipids, ALTs, apoB catabolism and hepatic LDLR regulation. We used RNA sequencing analysis to explore the mechanism by which hepatic *Trib1* regulates the *Ldlr* in a CEBPA-dependent manner and found that Activating Transcription Factor 3 (*Atf3*) was highly upregulated in the livers of *Trib1*^{Δhep} but not DKO mice. ATF3 is a stress-inducible transcriptional repressor that interacts with the promoter region of *LDLR* and represses its expression; furthermore, ATF3 directly binds to the CEBPA protein. We also demonstrated that downregulating *Atf3* in *Trib1*^{Δhep} mice reduced the plasma levels of total cholesterol, HDL- cholesterol and LDL-cholesterol, and partially attenuated the effects on the LDLR. Based on these data, we conclude that hepatic

deletion of *Trib1* leads to a post-translational increase in CEBPA, which drives *Atf3* expression, leading to the downregulation of the *Ldlr* and increased plasma LDL cholesterol. Our studies address a new regulatory interplay between TRIB1 and CEBPA in liver and the mechanisms by which TRIB1 regulates LDL cholesterol and lipoprotein metabolism.

INTRODUCTION

The *tribbles* gene was first identified in *Drosophila* as a regulator of cell division and morphogenesis and was shown to regulate the proteins encoded by the *string* and *slbo* genes, the *Drosophila* homologs of the dual phosphatase CDC25A, and CEBPA respectively [88, 89, 91]. Since its discovery, 3 homologs have been identified in humans (*TRIB 1-3*). The *TRIB* family of genes encode pseudokinase proteins that are highly conserved through different species [93]. These proteins are highly homologous to serine/threonine kinases yet lack residues that make them catalytically inactive [92-94]. *TRIB* family members instead can serve as a signal transducer modulator or scaffolding protein for important cellular processes. Some of these processes include the interaction with mitogen- activated protein kinase kinase (MAPKK) and further phosphorylation of ERK1/2 targets and the interaction with the ubiquitin ligase COP1 protein to target the transcription factors CCAAT enhancer- binding proteins alpha and beta (CEBP α/β) for proteasomal degradation [92-94]. *TRIB1*, the main gene studied in this dissertation, has been proposed to interact and regulate a variety of protein targets, including SAP18- Sin3A, HNF4A and ChREBP [134, 136, 137], however, regulation of the COP1-CEBPA axis remains the most fully described function of *TRIB1* [102, 112].

CEBPA is well known for its function as a regulator of myeloid cell development and hematopoiesis, however is also highly expressed in adipose tissue and the liver in mouse and humans, and has been broadly described as regulator of adipogenesis, critical for glucose and lipid homeostasis and for the regulation of several metabolic genes in the liver [106, 109, 110, 128, 156]. Bauer et al. [104] demonstrated that hepatic deletion of *Trib1* in mice results in increased hepatic triglyceride content, lipogenic gene expression, de novo lipogenesis and increased plasma lipids. These mice also displayed an increased in hepatic CEBPa protein, which was shown to be both necessary and sufficient to drive the lipogenic phenotype in *Trib1* hepatic deleted mice, establishing CEBPa as the mechanistic link between *TRIB1* and hepatic lipogenesis regulation [104]. However, the association of CEBPa and its possible involvement in the regulation of plasma lipids in this model was not fully elucidated. The main goal of these studies was to elucidate if *Trib1* regulation of CEBPa protein is involved in the regulation of plasma lipids, ALTs, apoB catabolism and LDLR regulation in mice.

I demonstrated that deletion of *Cebpa* in *Trib1^{Δhep}* mice eliminated the effects of hepatic deletion of *Trib1* on plasma lipids, hepatic lipids, ALTs, apoB catabolism and hepatic LDLR regulation. Also, through RNA sequencing analysis, we uncovered a novel binding factor mediating *TRIB1* regulation of the *LDLR* in a CEBPA-dependent manner, the Activating Transcription Factor 3 (*ATF3*), which was highly upregulated in the livers of *Trib1^{Δhep}* but not in DKO mice. *ATF3* is a stress-inducible gene that encodes a member of the ATF/CREB family of transcription factors, which share a basic-region leucine zipper (bZip) DNA binding domain [157-159]. *ATF3* expression is low in cells under steady-state conditions and is induced by a variety of extracellular stimuli, such as proinflammatory cytokines, nitric oxide, high concentrations of glucose and palmitate, and endoplasmic

reticulum (ER) stress [160-163]. A previous study using human liver Sk-Hep1 cells provided evidence that increased ER stress response or disturbance of mitochondrial function leads to the activation of *ATF3*, which causes a reduction on *LDLR* expression [164]. We also demonstrated that downregulating *Atf3* in *Trib1^{Δhep}* mice reduced the levels of total cholesterol, HDL- cholesterol and LDL-cholesterol, and partially attenuated the effects on the LDLR. Based on our results and previous literature findings we conclude that increased *Atf3* expression in the livers of *Trib1^{Δhep}* mice is leading to the down regulation of the LDLR expression in a sterol-independent mechanism.

RESULTS

Efficient hepatocyte-specific deletion of *Trib1* and *Cebpa* in *Trib1^{Δhep}*, *Cebpa^{Δhep}* and DKO mice.

It has been previously shown that hepatic deletion of *Trib1* in mice leads to increased hepatic CEBPA protein levels, and that this increase in CEBPA was sufficient to induce increased de novo lipogenesis and hepatic steatosis in mice. However, the association of *TRIB1* and CEBPA and their regulation of plasma lipids has not been fully elucidated. In order to determine if increased CEBPA protein is necessary for the effects of hepatic *Trib1* deletion on plasma lipids, apoB kinetics and LDLR regulation, we turned to a different model. For this, we crossed our *Trib1^{flox/flox}* mice to a *Cebpa^{flox/flox}* mice line with the goal of creating a DKO model. In these studies, we compared C57BL/6J wild type (control) mice to *Trib1^{Δhep}*, *Cebpa^{Δhep}* and DKO mice, all groups were injected with AAV-CRE. As

expected, liver *Trib1* and *Cebpa* mRNA levels showed the expected >95% reductions of *Trib1* in *Trib1^{Δhep}* mice and *Cebpa* in *Cebpa^{Δhep}* mice (Figure 4.1A). We also observed a 70% reduction of *Trib1* mRNA in *Cebpa^{Δhep}* mice and a 65% reduction of *Cebpa* mRNA in *Trib1^{Δhep}* mice (Figure 4.1A). In contrast to the reduction in *Cebpa* mRNA, the *Trib1^{Δhep}* mice had a substantial increase in CEBPa protein, particularly the p30 isoform (the isoform which is highly expressed certain patients with AML), whereas *Cebpa^{Δhep}* and DKO mice completely lacked CEBPa protein, as expected (Figure 4.1B). These findings are consistent with a post-translational effect of TRIB1 on CEBPA in promoting its degradation, as well as that TRIB1 and CEBPA participate in a tight feedback loop, where more CEBPA protein leads to increased *TRIB1* transcription and TRIB1 targets CEBPA for degradation.

Hepatic deletion of *Cebpa* in *Trib1^{Δhep}* mice decreases plasma cholesterol and LDL lipoprotein fractions levels.

We then went on to explore the effects of *Cebpa* deletion by itself as well as in the absence of hepatic *Trib1* on plasma lipids. As shown in my previous studies *Trib1^{Δhep}* mice had increased plasma total cholesterol, HDL-C and non-HDL-C, both on chow and WTD (Figure 4.2). *Cebpa^{Δhep}* mice had normal to decreased levels of triglycerides, total cholesterol, HDL-C and non-HDL-C in both chow (Figure 4.2 A-D) and WTD (Figure 4.2 E-H) as well as triglycerides and total cholesterol in the LDL fractions on chow and WTD feeding (Figure 4.3) when compared to control mice, further corroborating CEBPa involvement in the regulation of plasma lipids. Most interestingly, deletion of *Cebpa* in *Trib1^{Δhep}* mice eliminated the increase in total cholesterol, HDL cholesterol and non-HDL

cholesterol on both chow (Figure 4.2 A-D) and WTD (Figure 4.2 E-H). Deletion of *Cebpa* in male *Trib1^{Δhep}* mice also completely eliminated the increase in triglycerides and total cholesterol in the LDL fractions in a chow diet (Figure 4.3 A-B), and these effects were further amplified when the mice were challenged with a WTD (Figure 4.3 C-D) to levels similar to control mice or lower. These data prove that hepatic CEBPA protein itself is important for the regulation of plasma lipids, and that hepatic CEBPA protein is required for the phenotypic effect of hepatic *Trib1* deletion causing increased plasma lipids.

Hepatic deletion of *Cebpa* in *Trib1^{Δhep}* mice normalizes liver lipids, ALTs and Albumin levels.

My previous studies revealed that *Trib1^{Δhep}* mice have increased hepatic triglycerides and total cholesterol, increased ALTs and decreased Albumin protein levels (Figure 4.4). I demonstrated that *Cebpa^{Δhep}* mice had normal levels of hepatic lipids, ALTs and increased albumin levels, and that hepatic deletion of *Cebpa* in *Trib1^{Δhep}* mice eliminated the increased levels of hepatic lipids and circulating ALTs, and increased albumin levels back to control mice levels (Figure 4.4). These data prove that increased hepatic CEBPa protein is required for the phenotypic effect of *Trib1^{Δhep}* causing increased liver lipids, increased ALTs and decreased albumin levels, all of which are markers of impaired liver health.

Hepatic deletion of *Cebpa* in *Trib1^{Δhep}* mice improves the clearance of postprandial plasma triglycerides

As shown in my previous studies, even though *Trib1^{Δhep}* mice have no changes in steady state plasma triglycerides, they accumulate triglycerides on the LDL lipoprotein fractions, indicated by improper postprandial lipemia measured by OFTT. To test if *Trib1* regulation of CEBPa protein mediates this effect in postprandial lipemia, we performed OFTT studies in these cohorts. Here, I confirmed that *Trib1^{Δhep}* mice have impaired triglyceride clearance after challenge with an oral fat load (Figure 4.5). I also showed that *Cebpa^{Δhep}* mice have improved triglyceride clearance compared to control mice, and that hepatic deletion of *Cebpa* in *Trib1^{Δhep}* mice eliminated the impairment of triglyceride clearance compared to *Trib1^{Δhep}* mice and resulted in improved clearance compared to control mice, which was confirmed by a decreased area under the curve (Figure 4.5). Thus, increased CEBPa protein is necessary for the postprandial lipemia phenotype we previously observed in *Trib1^{Δhep}* mice.

Hepatic deletion of *Cebpa* in *Trib1^{Δhep}* mice improves the clearance of LDL- apoB and VLDL-apoB and normalizes the levels of the LDL-Receptor.

We then tested if *Trib1* effects on apoB catabolism was mediated through its regulation of CEBPa by injecting mice with ¹²⁵I labeled human isolated LDL or VLDL. As I showed before, *Trib1^{Δhep}* mice exhibited markedly slower LDL and VLDL catabolism calculated by its fractional catabolic Rate (Figure 4.6 A-D). *Cebpa^{Δhep}* mice had normal LDL and VLDL apoB catabolism, and what was more interesting is that DKO mice also had normal LDL and VLDL catabolism (Figure 4.6 A-D), suggesting that increased CEBPa protein is also

necessary for the *Trib1* deletion effect on apoB catabolism. As this defect in apoB catabolism was mediated by the LDLR in *Trib1*^{Δhep} mice, we assessed changes in the *Ldlr* mRNA and protein levels in the *Cebpa*^{Δhep} cohorts. *Trib1*^{Δhep} mice recapitulated the decrease in *Ldlr* mRNA and protein levels (Figure 4.6 E-F). Even though *Cebpa*^{Δhep} mice had decreased *Ldlr* mRNA, their LDLR protein levels were comparable to control mice (Figure 4.6 E-F) and more interesting deleting *Cebpa* in the absence of *Trib1* was not able to decrease the levels of *Ldlr* mRNA and protein levels (Figure 4.6 E-F). These data support that hepatic CEBPa protein is required for the phenotypic effect of hepatic *Trib1* deletion causing reduced *Ldlr* expression and impaired apoB-lipoprotein catabolism, leading to hypercholesterolemia. Thus, the increased CEBPa protein in hepatocytes due to loss of *Trib1* likely leads to reduced *Ldlr* expression.

Numerous *Trib1* genetics effects are mediated through its regulation of *Cebpa*

The abundance of hepatic LDLR protein is tightly regulated to ensure normal cellular function, at both the transcriptional and post-transcriptional levels. To gain further insight about the molecular mechanism by which *TRIB1* regulation of CEBPA leads to changes in the LDLR expression, we performed whole transcriptome RNA sequencing in livers from chow-fed control, *Trib1*^{Δhep}, *Cebpa*^{Δhep} and DKO mice. Volcano plot summaries of changes in gene expression between all groups can be found in Figure 4.7- 4.8. A total of 14,937 transcripts were differentially expressed between all groups, excluding transcripts with missing values. Out of these, 7,458 were upregulated (a positive Fold-Change relative to WT log₂FC), and 7,479 were downregulated (negative log₂FC) in *Trib1*^{Δhep} mice compared with control mice. Out of these, 916 transcripts (464 up, 452 down) were altered

by more than 1.5-fold between *Trib1*^{Δhep} and control mice (absolute log₂FC>0.6, adjusted p-value <0.00001) (Figure 4.7A, Figure 4.8A). Of the 916 differentially expressed transcripts, only 75 met the same adjusted p-value (<0.00001) cut-off in DKO mouse liver mRNA (Figure 4.7B, Figure 4.8B), indicating that the vast majority (91.8%) of the significant gene expression changes in *Trib1*^{Δhep} mouse liver were attributable to dysregulation of CEBPA levels. DKO mouse livers were much more similar to control mice (Figure 4.7B) and the comparison between *Cebpa*^{flox/flox} and DKO showed the fewest changes (Figure 4.7D), consistent with the critical role of elevated CEBPA protein in mediating the effects of *Trib1* deletion in liver on gene expression.

Trib1's CEBPa dependent regulation of the LDLR is mediated independently of SREBPs canonical pathways

We mined the RNA-seq data for transcriptional regulators upstream of *Ldlr* that were significantly altered by *Trib1* deletion that were dependent on CEBPa. We noted only modest changes in the expression of the genes encoding the SREBP1 and 2 proteins and noted that these were not dependent on CEBPa (Figure 4.9). *Srebf1* mRNA levels were unchanged when comparing all groups (Figure 4.10 A), and SREBP1 protein levels were modestly increased in *Trib1*^{Δhep}, which is the opposite directionality expected for the observed effect on LDLR (Figure 4.10B). *Srebf2* mRNA were decreased in *Trib1*^{Δhep} as well as in DKO mice (Figure 4.10C). However, levels of mature SREBP2 did not differ between the *Trib1*^{Δhep} and control mice (Figure 4.10D). Interestingly, the DKO livers had almost complete loss of mature SREBP2, which may account for the fact that their plasma

cholesterol levels are lower than controls. These results suggest that the canonical SREBP pathway has a relatively minor impact on LDLR in hepatocytes of lacking *Trib1*.

Trib1's CEBPA dependent regulation of the LDLR is mediated by ATF3.

After mining the RNA-seq data for transcriptional regulators upstream of *Ldlr* significantly altered by *Trib1* deletion that were dependent on CEBPA, we identified a potential target that could explain the effects of *Trib1* on the LDLR in a CEBPa dependent manner, the Activating Transcription Factor 3 (*ATF3*). *ATF3* is a stress-inducible transcriptional repressor that belongs to the ATF/cAMP-response element-binding protein family of transcription factors [165]. *ATF3* has been previously described to interact with the promoter region of LDLR and repress its expression [164]. Additionally, *ATF3* has also been described to physically interact with the transcription factor CEBPA [166, 167]. *Atf3* was one of the most highly upregulated genes in *Trib1*^{Δhep} liver (Figure 4.9A, 49.3 fold increase, adjusted p-val = 6.33E-46) and this was dependent on CEBPa, as *Atf3* expression did not differ between control and DKO livers (Figure 4.9B, 1.5 fold increase, adjusted p-value = 0.57). We confirmed these results by qPCR, finding that relative to control, *Atf3* mRNA was increased >25-fold in *Trib1*^{Δhep} liver but not in DKO liver (Figure 4.11A), which was also confirmed by western blot (Figure 4.11B), indicating that increased CEBPa is required for the upregulation of *Atf3* in *Trib1*^{Δhep} mice.

Additionally, through gene set enrichment we identified 54 *ATF3* downstream target genes that were differentially expressed in the *Trib1*^{Δhep} mouse liver and found that these were similarly CEBPa dependent (Figure 4.12 A-B). Pathway analysis of *ATF3* interacting genes in other datasets is shown in Figure 4.12 C-E. Furthermore, analysis of ChIP-seq

for differential CEBPa binding sites in *Trib1*^{Δhep} mouse livers confirmed that there is an enrichment in binding motifs for ATF family members, including ATF3 and its upstream regulator ATF4 in CEBPa bound regions (Table 2). Other factors with enriched binding motifs included CEBPA, NFIL3, CHOP, ATF1, and ATF7 (Table 2). These results are consistent with a model in which the deletion of *Trib1* allows CEBPa protein to escape targeted proteolysis resulting in increased CEBPa protein. The increased CEBPa protein directly interacts with the *Atf3* promoter and leads to its transcriptional upregulation, which then binds the *Ldlr* promoter and represses its activity thereby resulting in the downregulation of *Ldlr* mRNA and protein levels.

Knockdown of *Atf3* in *Trib1*^{Δhep} mice decreases total cholesterol and HDL cholesterol and increased LDLR protein.

To test the model that *Trib1* regulation of the LDL receptor is mediated by CEBPa and its effects on *Atf3* expression and function, we acquired an siRNA directed against mouse *Atf3* and a non-targeting control siRNA (directed against firefly luciferase), and injected *Trib1*^{Δhep} mice with siRNAs targeted to *Atf3* or luciferase and control mice with siRNA to luciferase. Our hypothesis was that preventing *Atf3* upregulation in *Trib1*^{Δhep} mice would impact LDLR protein and plasma cholesterol levels. *Trib1* mRNA levels were efficiently deleted in *Trib1*^{Δhep} mice (Figure 4.13A). The mRNA abundance of *Atf3* was substantially increased in the *Trib1*^{Δhep} mice receiving the control siRNA, but in the *Trib1*^{Δhep} mice receiving the *Atf3* siRNA this *Atf3* mRNA expression was mildly attenuated, but not significantly (Figure 4.13B). The protein abundance of ATF3 substantially increased in the *Trib1*^{Δhep} mice receiving the control siRNA and surprisingly, in *Trib1*^{Δhep} mice receiving the

Atf3 siRNA this was attenuated to levels comparable to control mice (Figure 4.13C), even though there was no reduction in mRNA levels. *Trib1^{Δhep}* mice receiving the *Atf3* siRNA had a significant reduction in the levels of total cholesterol (Figure 4.14 A-D) and HDL cholesterol (Figure 4.14 E-H), but no significant changes in non-HDL cholesterol or triglycerides (Figure 4.14 I-P), compared to *Trib1^{Δhep}* mice receiving the control siRNA. *Trib1^{Δhep}* mice receiving the *Atf3* siRNA also had a mild reduction in the levels of LDL cholesterol when compared to *Trib1^{Δhep}* mice receiving the control siRNA (Figure 4.15 A-C). The decrease in ATF3 protein did not affect the *Ldlr* mRNA levels (Figure 4.16 A) but was surprisingly associated with modestly increased levels of LDLR protein compared to mice injected with control siRNA (Figure 4.16B). This result supports the model that ATF3 contributes to the downregulation of LDLR in *Trib1^{Δhep}* mice.

In summary, our experiments show that deletion of hepatic *Trib1* increases plasma LDL cholesterol levels by resulting in downregulation of the expression of the LDLR leading to reduced LDL-apoB clearance and that this effect of TRIB1 is dependent on CEBPa. We also identified ATF3 as at least one mediator of the effects of TRIB1 and CEBPa regulation of LDLR expression. This study provides new functional insight into the strong genetic association between *TRIB1* and the regulation of plasma lipid levels in humans.

DISCUSSION

These studies were designed to elucidate the molecular mechanism by which murine hepatic *Trib1* regulates plasma lipids and the expression of the *Ldlr*. I demonstrated that increased CEBPa protein is required for the effects of *Trib1* hepatic deletion on plasma

lipids, hepatic lipids, ALTs, albumin levels, apoB-lipoprotein clearance and *Ldlr* regulation. As neither *Trib1* nor *Cebpa* had previously been associated with the regulation of *Ldlr*, we used RNA sequencing to identify possible interacting partners that might explain this regulation. We observed that hepatic deletion of *Trib1* led to a CEBPa-dependent increase in expression of the transcription factor ATF3, which has been shown to directly interact with CEBPa and to independently target the promoter region of the *LDLR* gene and repress its transcription (Figure 4.17). Our data reveal a novel mechanism regulating *Ldlr* expression and plasma LDL-C levels, namely that reduction in hepatic *Trib1* leads to increased CEBPa protein, which results in increased mRNA and protein levels of ATF3, which in turn leads to the downregulation of *Ldlr* mRNA and protein.

The LDLR is the main receptor that mediates the clearance of plasma LDL cholesterol to the liver [3, 4]. It is well known that mutations that abrogate or cause reduction on LDLR level or function lead to elevated plasma LDL-C levels which are associated with an increased risk of cardiovascular disease [3, 4, 168]. Because of this, the expression of *LDLR* is tightly regulated at multiple levels to ensure normal cellular function. At the transcriptional level, it is well known that the expression of *LDLR* gene is mainly regulated by sterol regulatory element-binding proteins 1 and 2 (SREBP-1, SREBP-2), this in response to intracellular cholesterol levels [35, 36]. At the post-translational level, regulation of LDLR is primarily governed by PCSK9 that upon binding to cell-surface LDLR, mediates its degradation [34, 39, 40, 169]. Other non-canonical mechanism for the LDLR regulation have been proposed, but not fully explained. RNA sequencing in the livers of the mice in all our cohorts didn't show major changes on the SREBP canonical pathways that regulate the LDLR expression, confirmed by qPCR and western blots for both SREBP-1 and SREBP-2. These results suggest that the SREBP pathways were not

contributing to the LDLR phenotype in *Trib1*^{Δhep} mice. The results from the RNA sequencing experiments led us to explore other non-canonical pathways that had been recently published as regulators of LDLR expression and we focused on finding transcription factors that changed significantly in *Trib1*^{Δhep} livers but were normalized in DKO livers.

Ingenuity pathway analysis of the RNA sequencing data led to identification of Atf3, which was substantially increased in *Trib1*^{Δhep} mouse livers but unchanged in DKO livers, indicating that its regulation by *Trib1* is CEBPa dependent. ATF3 is a stress-inducible gene that encodes a member of the ATF/CREB family of transcription factors, which share a basic-region leucine zipper (bZip) DNA binding domain [160, 165]. *ATF3* expression is low in cells under steady-state and is induced by a variety of extracellular stimuli, such as proinflammatory cytokines, nitric oxide, high concentrations of glucose and palmitate, and endoplasmic reticulum stress [160, 161, 170, 171]. ATF3 has been shown to regulate proliferation and apoptosis under stress conditions, this by forming dimers to activate or repress the expression of related genes [160, 165, 172, 173]. Further, ATF3 has been associated with the modulation of the immune response, atherogenesis, cell cycle, obesity and glucose homeostasis [170, 172, 174-177]. However, more studies are needed to determine the tissue specific roles of ATF3 in metabolic regulation. The effects of this gene have many similarities with the observed phenotypes of hepatic *Trib1* deletion, which makes it an interesting target for future investigation.

More interestingly, a previous study using human liver Sk-Hep1 cells provided evidence that increased endoplasmic reticulum (ER) stress response or disturbance of mitochondrial function leads to the activation of ATF3, which causes a reduction on *LDLR*

expression [164]. They demonstrated the region between -8 and -3 of the *LDLR* proximal promoter region as a putative binding site for ATF3 and confirmed their interaction by chromatin immunoprecipitation in a stress-dependent manner [164]. Our results also suggest that *Atf3* induction and possible function in *Trib1^{Δhep}* mice is mediated by the increased in CEBPa protein, which we believe is the connecting link in the downstream regulation of the LDLR. Previous studies focused on studying the bZIP protein-protein interaction networks demonstrated that ATF3 physically interacts with CEBPa, and this was demonstrated using electrophoretic mobility shift assay (EMSA), and fluorescence resonance energy transfer (FRET) [166]. Another group used EMSA as well as CHIP assays to demonstrate that ATF3 directly binds to the mouse CEBPa promoter, supporting the notion of mutual regulation of CEBPa and ATF3 [167]. Additionally, we identified 54 ATF3 downstream target genes that were differentially expressed in the *Trib1^{Δhep}* mouse liver and found that these were similarly CEBPa-dependent. Furthermore, analysis of CHIP-seq for differential CEBPa binding sites in *Trib1^{Δhep}* mouse livers confirmed that there is an enrichment in binding motifs for ATF family members, including ATF3 and its upstream regulator ATF4 in CEBPa bound regions. These results are consistent with a model in which the deletion of *Trib1* allows CEBPa protein to escape targeted proteolysis (via COP1) resulting in increased CEBPa protein. The increased CEBPa protein directly interacts with the *Atf3* promoter and leads to its transcriptional upregulation. The ATF3 protein (which CEBPa also binds directly) binds the *Ldlr* promoter and represses its activity thereby resulting in the downregulation of LDLR mRNA and protein.

A recent publication by Xu et al. [175] investigated the effects of hepatocyte *ATF3* in the regulation of bile acids, HDL metabolism and atherosclerosis, and demonstrated that

hepatocyte *ATF3* enhances HDL uptake, inhibits intestinal fat and cholesterol absorption and promotes macrophage reverse cholesterol transport. Consistent with earlier studies, they found that the mechanism by which *ATF3* regulates these is by inducing scavenger receptor group B type 1 (SR-BI) and repressing cholesterol 12 α -hydroxylase (CYP8B1) in the liver through its interaction with p53 and HNF4A [175]. Additionally they explored the effects of hepatic *Atf3* on the *Ldlr* and showed that that ATF3 upregulates hepatic expression and protein levels of LDLR in mice [175]. Strikingly, the direction of effect of ATF3 on LDLR in Xu et al. is opposite to the previously published results by Lim et al [164], from which we based our hypothesis. We speculate that this may be because in our *Trib1^{Δhep}* mice, levels of both ATF3 and CEBP α are elevated and that the concomitant elevation of CEBP α may change the nature of the effects of ATF3 on *Ldlr* transcription.

To further test our model, we acquired an siRNA directed against mouse *Atf3* and a non-targeting control siRNA with the hypothesis that preventing ATF3 upregulation in *Trib1^{Δhep}* mice would impact LDLR protein and plasma cholesterol levels. We injected *Trib1^{Δhep}* mice with siRNAs to *Atf3* or luciferase and control mice with siRNA to luciferase. Using this method, we were able to attenuate ATF3 protein levels in mice receiving *Atf3* siRNA to levels comparable to control mice. This normalization of ATF3 was associated with a significant reduction in plasma levels of total cholesterol and in HDL cholesterol, but had no effects on triglycerides and non-HDL cholesterol. The decrease in ATF3 protein was also associated with modestly increased levels of LDLR protein compared to mice injected with control siRNA. This result supports the model that ATF3 contributes to the down-regulation of LDLR in *Trib1^{Δhep}* mice. Based on these results and our current findings we conclude that increased *Atf3* expression in the livers of *Trib1^{Δhep}* mice is leading to the partial down regulation of the *Ldlr* expression in a sterol-independent mechanism.

However, it is important to note that the decrease in lipids and increase in LDLR protein in *Trib1*^{Δ_{hep}} mice treated with Atf3 siRNA were only partially attenuated, suggesting that ATF3 is not the only partner contributing to *Trib1* and CEBPa effects on lipids. It is very likely that other factors are also involved in this regulation.

In summary, our experiments show that deletion of hepatic *Trib1* regulates plasma LDL-C levels by resulting in downregulation of the expression of the *Ldlr* and consequently the rate of LDL-apoB clearance. *Trib1* mediates these effects through its post-translational regulation of CEBPa protein degradation. We also identified *atf3* as at least one mechanism by which *Trib1* and CEBPa regulate *Ldlr* expression. This study provides new functional insight into the strong genetic association between *TRIB1* and LDL-C levels.

FIGURES

Figure 4. 1: Cebpa^{Δhep} model validation.

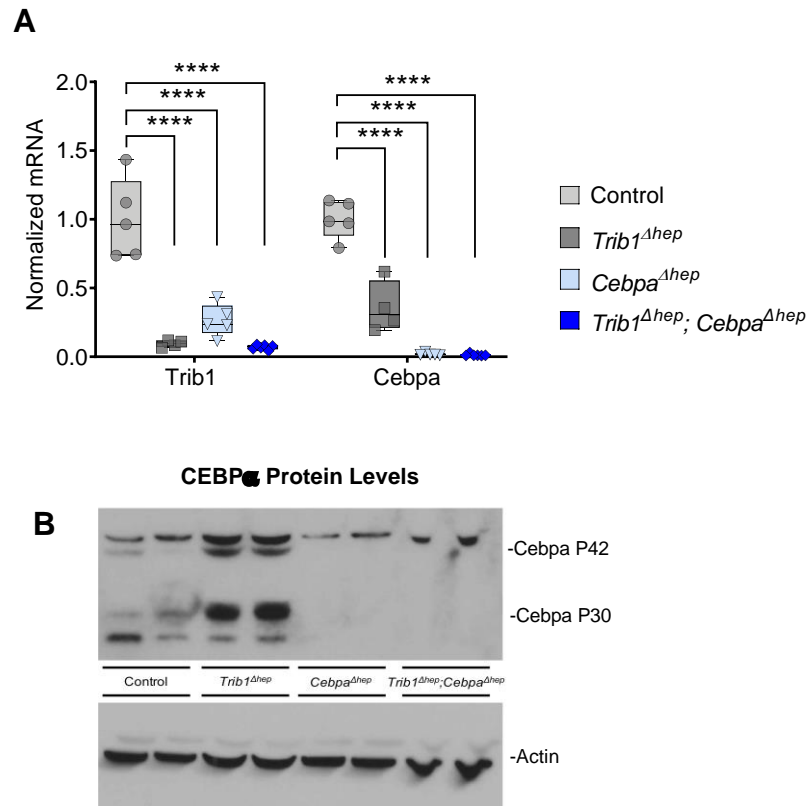


Figure 4.1: A. Hepatic transcript levels of *Trib1* and *Cebpa* in chow-fed mice ($n=5$) 10 weeks after AAV-Cre injection. Box plots indicate median, 25th and 75th percentiles with whiskers extending to minimum and maximum values. Symbols indicate single values. Significance was determined by Two-way ANOVA with Tukey's multiple correction test ($****p \leq 0.0001$). **B.** Hepatic protein levels of CEBP α and Actin in mice ($n=2$ per group), from A.

Figure 4. 2: Hepatic deletion of *Trib1* in the absence of *Cebpa* decreases plasma cholesterol in chow and WTD feeding.

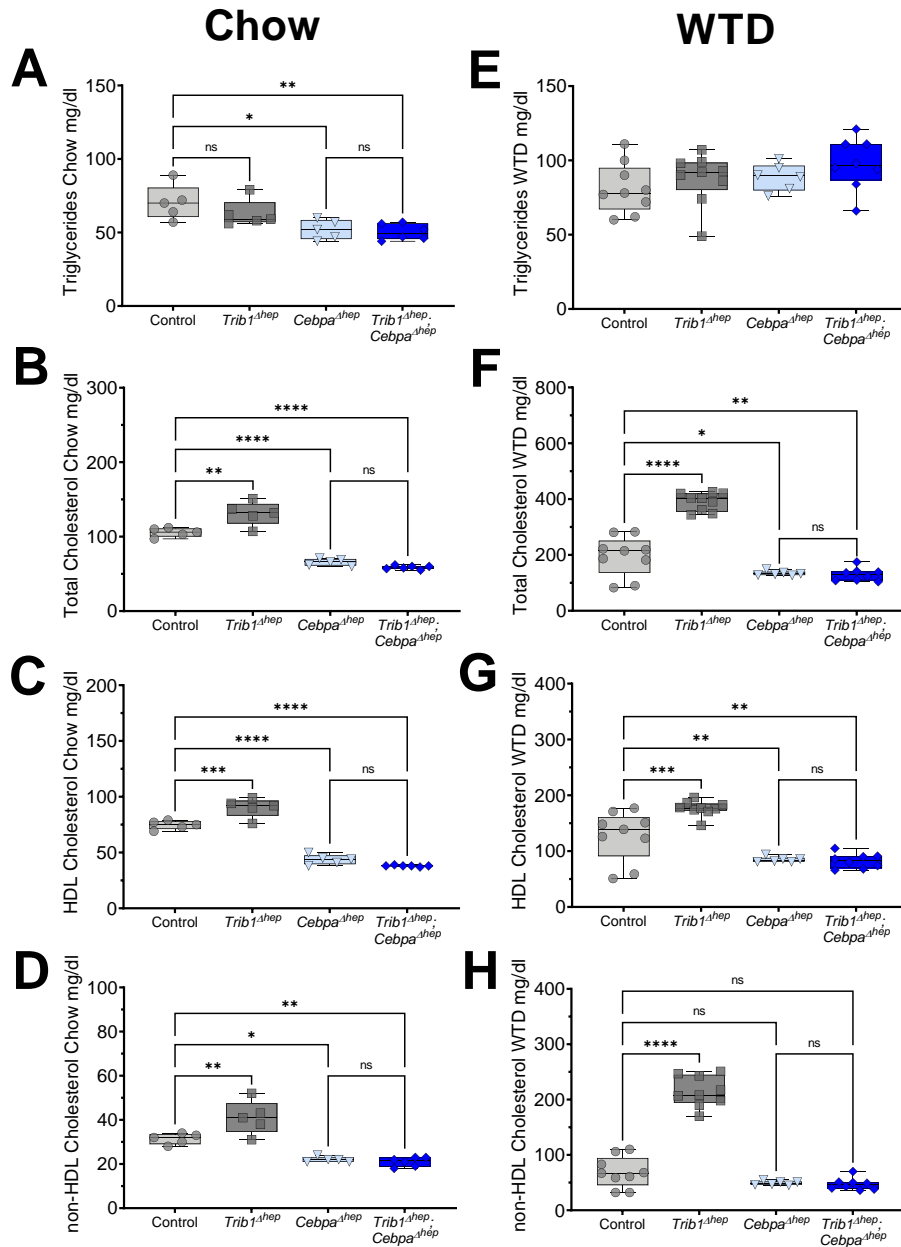


Figure 4.2: A-D. Plasma levels of triglycerides, total cholesterol, HDL cholesterol and non-HDL cholesterol in chow-fed male mice 4 weeks after AAV injection (n=5-6). **E-H.** Plasma levels of triglycerides, total cholesterol, HDL cholesterol and non-HDL cholesterol in WTD feed mice for 6 weeks (n=8-9). Box plots indicate median, 25th and 75th percentiles with whiskers extending to minimum and maximum values. Symbols indicate single values. Significance was determined by One-way ANOVA with Tukey's multiple correction test (*p ≤ 0.05, **p ≤ 0.01, ***p ≤ 0.001, ****p ≤ 0.0001).

Figure 4. 3: Hepatic deletion of *Trib1* in the absence of *Cebpa* decreases LDL lipoprotein fractions in in chow and WTD feeding.

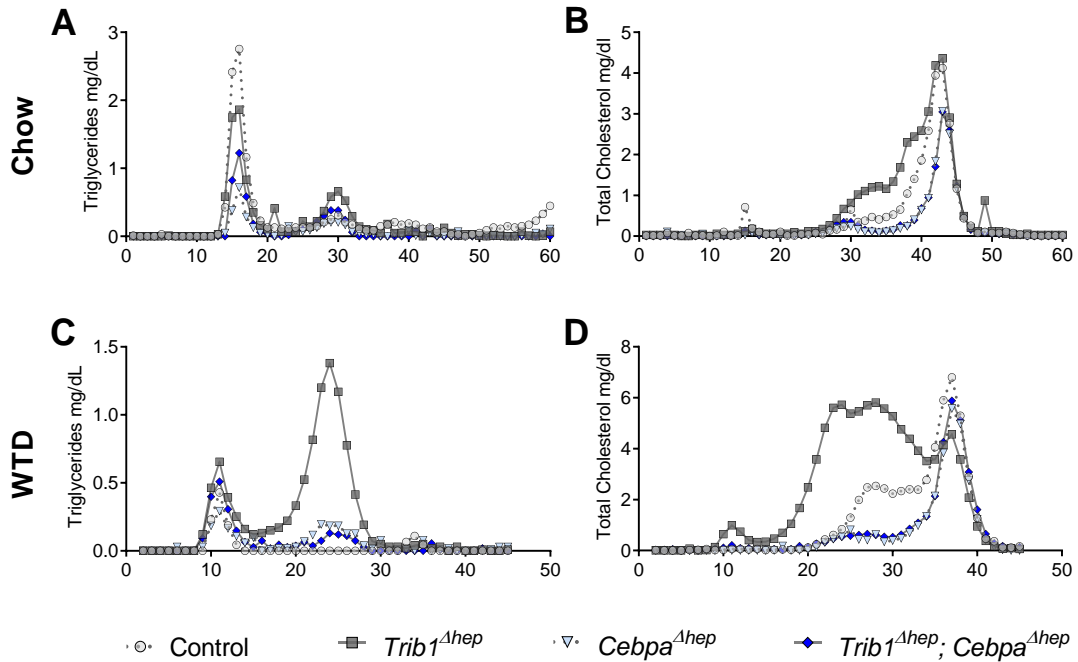


Figure 4.3: A-B. Fast Protein Liquid Chromatography (FPLC) was performed on pooled plasma from chow fed mice for 6 weeks and **C-D.** WTD fed mice for 14 weeks to separate lipoproteins based on their size. Triglycerides (**A, C**) and total cholesterol (**B, D**) concentrations were measured in all fractions.

Figure 4. 4: Hepatic deletion of *Trib1* in the absence of *Cebpa* normalizes hepatic lipids, ALT and albumin levels.

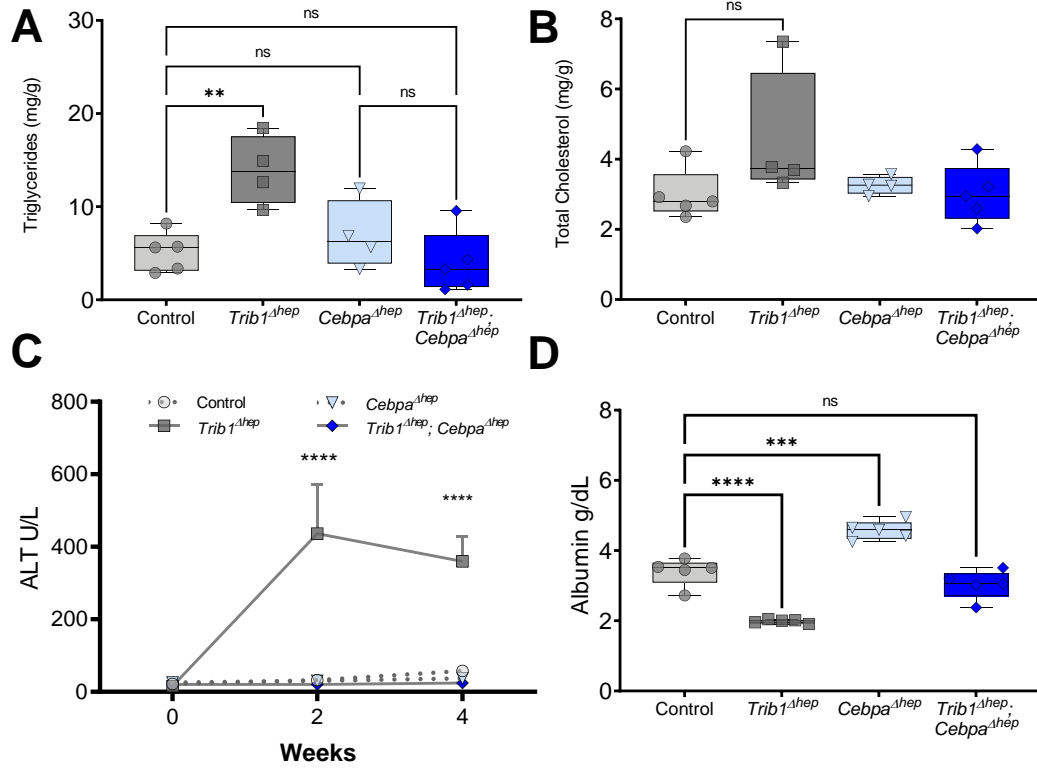


Figure 4.4: A-B. Hepatic triglyceride and total cholesterol levels in chow fed mice 8 weeks post deletion (n=5). **C.** ALT levels at indicated timepoints over 4 weeks of chow feeding (n=5). **D.** Plasma Albumin levels in chow fed mice 4 weeks post deletion (n=5). A, B, D. Box plots indicate median, 25th and 75th percentiles with whiskers extending to minimum and maximum values. Symbols indicate single values. Significance was determined by One-way ANOVA with Tukey's multiple correction test. C. Data are expressed as mean \pm s.e.m for the experimental group. Significance was determined by Two-way ANOVA with Tukey's multiple correction test (* $p \leq 0.05$, ** $p \leq 0.01$, *** $p \leq 0.001$, **** $p \leq 0.0001$).

Figure 4. 5: Hepatic deletion of *Trib1* in the absence of *Cebpa* improves post-prandial triglyceride clearance in mice.

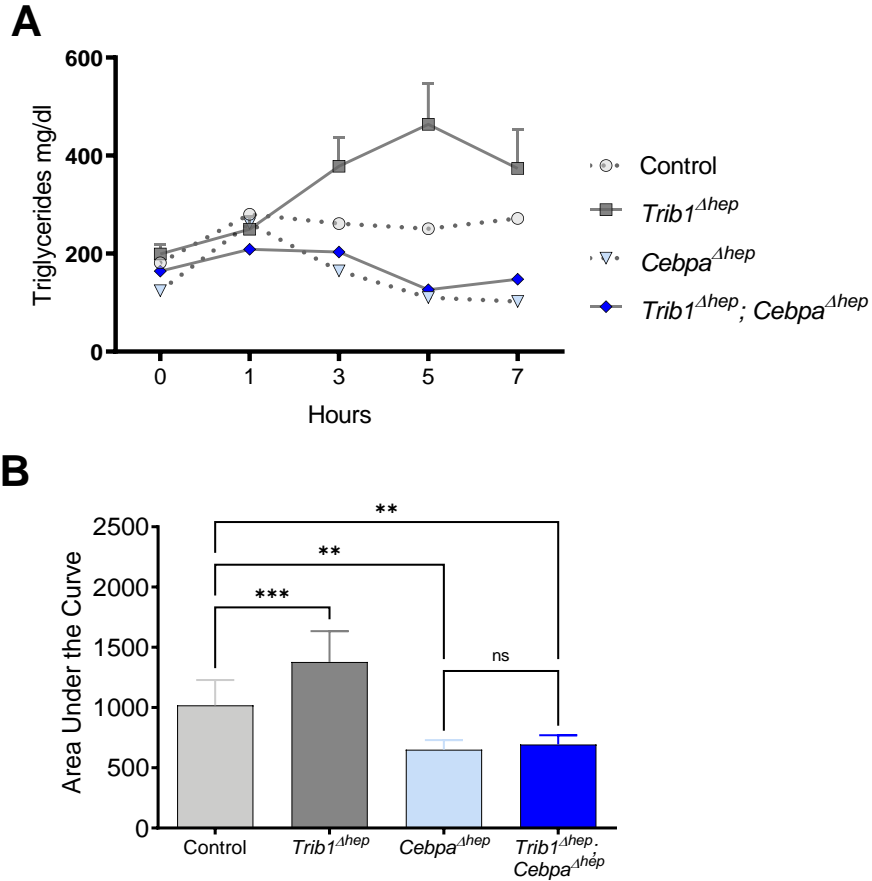


Figure 4.5: A. Oral fat tolerance test (OFTT) in male mice at 5 in chow diet. Data are expressed as mean \pm s.e.m for the experimental group. **B.** Area under the curve calculation for **A**. Data are expressed as mean \pm s.e.m for the experimental group. Significance was determined using one-way ANOVA with Tukey's multiple comparisons test (** $p \leq 0.01$, *** $p \leq 0.001$)

Figure 4. 6: Hepatic deletion of *Trib1* in the absence of *Cebpa* normalizes LDL and VLDL apoB kinetics and LDLR expression.

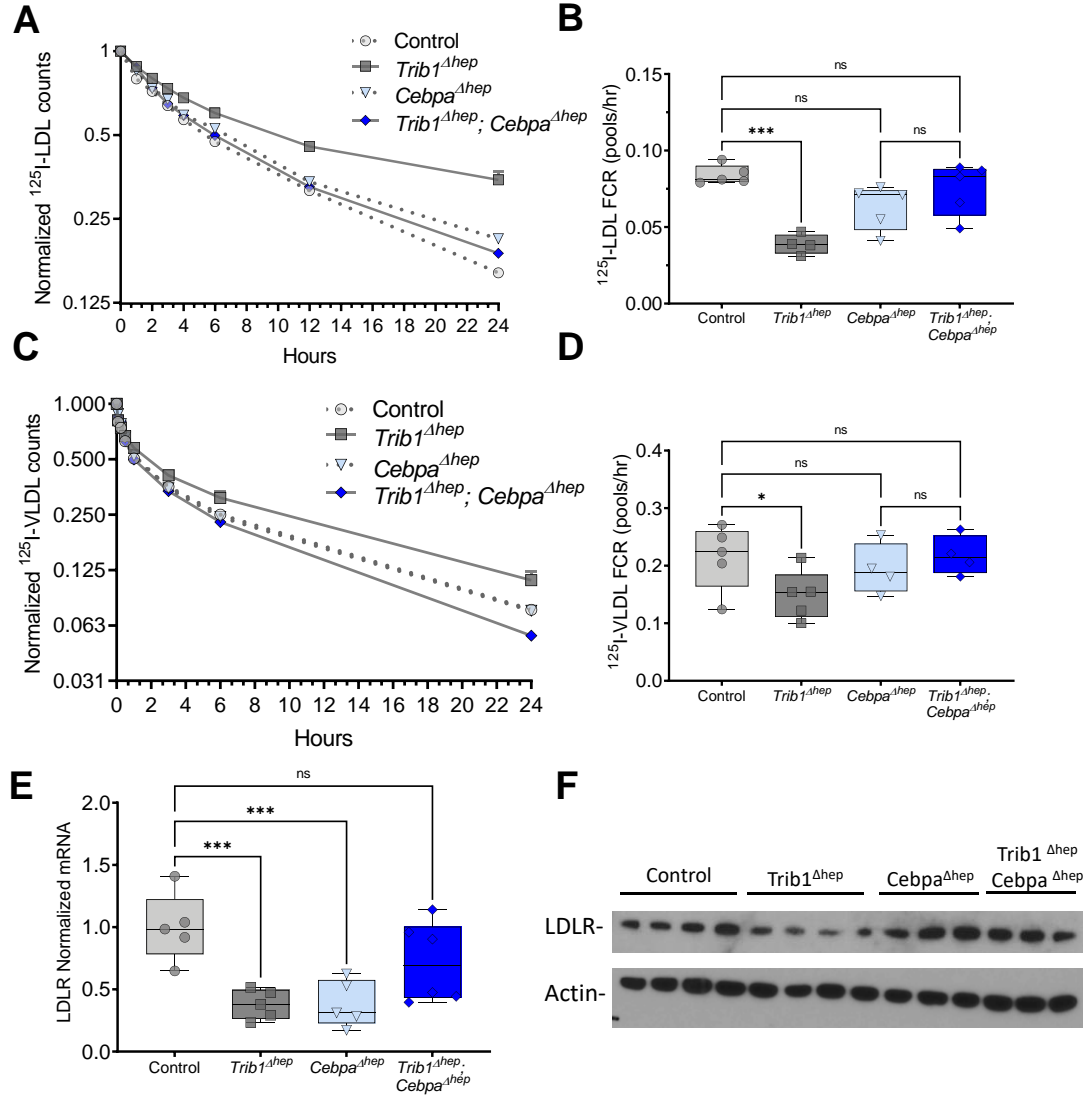


Figure 4.6: A-B. ^{125}I -LDL-apoB clearance and FCR in chow-fed male mice 8 weeks after AAV injection (n=5). **C-D.** ^{125}I -VLDL-apoB clearance and FCR in chow-fed male mice 8 weeks after AAV injection. **E.** Hepatic transcript levels of Ldlr in mice 8 weeks after AAV injection (n=5), **F.** Representative immunoblot of hepatic LDLR and β -actin from samples in E. A, C. Data are expressed as mean \pm s.e.m for the experimental group. B, D, E. Box plots indicate median, 25th and 75th percentiles with whiskers extending to minimum and maximum values. Symbols indicate single values. Significance was determined by one-way ANOVA with Tukey's multiple comparison test (* $p \leq 0.05$; ** $p \leq 0.01$; *** $p \leq 0.001$, **** $p \leq 0.0001$).

Figure 4. 7: Summary of differentially expressed genes between different groups from RNAseq dataset.

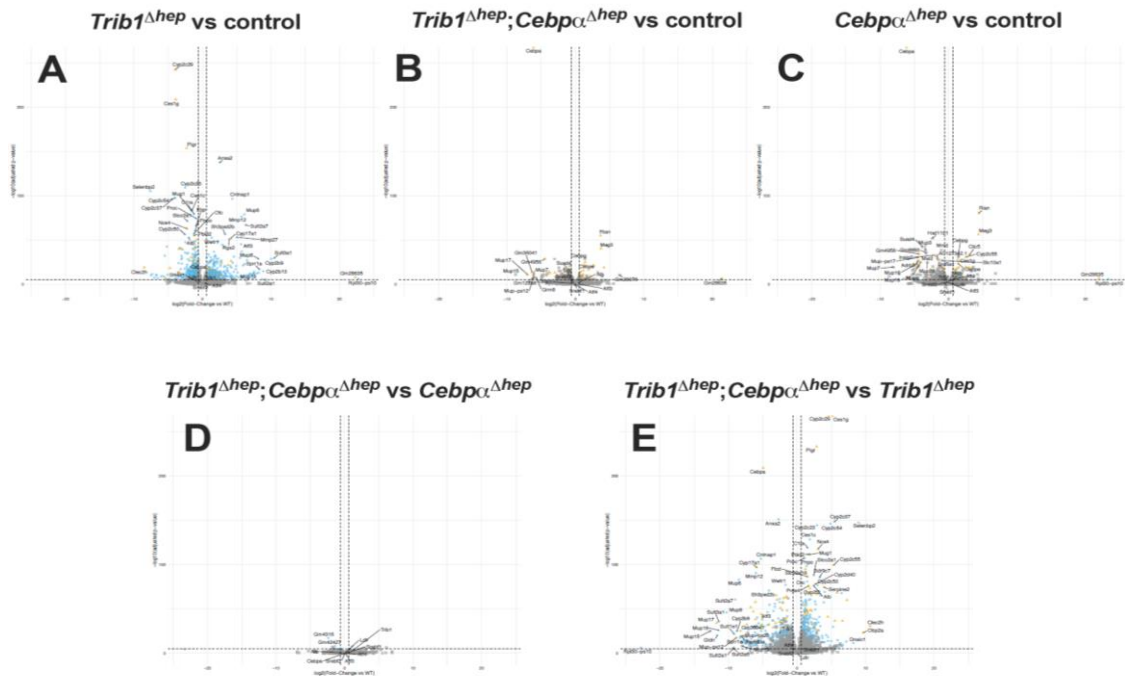


Figure 4.7: Volcano plots representing the totality of differentially expressed genes in $Trib1^{\Delta hep}$ compared to control mice (**A**), in $Trib1^{\Delta hep};Cebpa^{\Delta hep}$ compared to control mice (**B**), in $Trib1^{\Delta hep};Cebpa^{\Delta hep}$ compared to $Trib1^{\Delta hep}$ mice (**C**), in $Cebpa^{\Delta hep}$ as compared to control mice (**D**) and in $Trib1^{\Delta hep};Cebpa^{\Delta hep}$ compared to $Cebpa^{\Delta hep}$ mice (**E**). Analysis was performed in chow fed mice 4 weeks after AAV-CRE injection (n=6). Dashed horizontal line $-\log_{10}(\text{adjusted } p\text{-value} = 0.00001)$, dashed vertical lines indicate absolute \log_2 fold-change relative to control = 0.6 (equivalent to $\pm 1.5x$). Grey squares, non-significant; blue circles, significant for comparison between $Trib1^{\Delta hep}$ and control; orange triangles, significant for comparison between $Trib1^{\Delta hep}$ and control, but not for $Trib1^{\Delta hep};Cebpa^{\Delta hep}$ compared to control.

Figure 4. 8: Zoomed in versions of selected volcano plots of differentially expressed genes in RNAseq dataset.

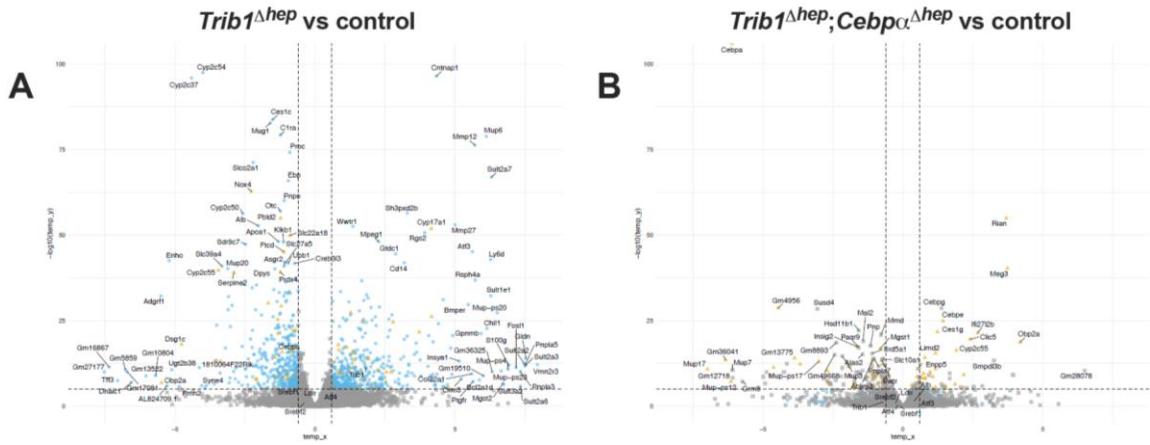


Figure 4.8: A. Cropped volcano plot of differentially expressed genes in $Trib1^{\Delta hep}$ compared to control mice. **B.** Cropped volcano plot of differentially expressed genes in $Trib1^{\Delta hep};Cebpa^{\Delta hep}$ compared to control mice. Analysis was performed in chow fed mice 4 weeks after AAV-CRE injection (n=6). These plots represent the same data as that in Fig. S10A and B, zoomed in for additional detail. Dashed horizontal line $-\log_{10}(\text{adjusted } p\text{-value} = 0.00001)$, dashed vertical lines indicate absolute \log_2 fold-change relative to control = 0.6 (equivalent to $\pm 1.5x$). Grey squares, non-significant; blue circles, significant for comparison between $Trib1^{\Delta hep}$ and control; orange triangles, significant for comparison between $Trib1^{\Delta hep}$ and control, but not for $Trib1^{\Delta hep};Cebpa^{\Delta hep}$ compared to control.

Figure 4. 9: Ingenuity Pathway Analysis plots representing the changes in LDLR upstream regulators between different groups

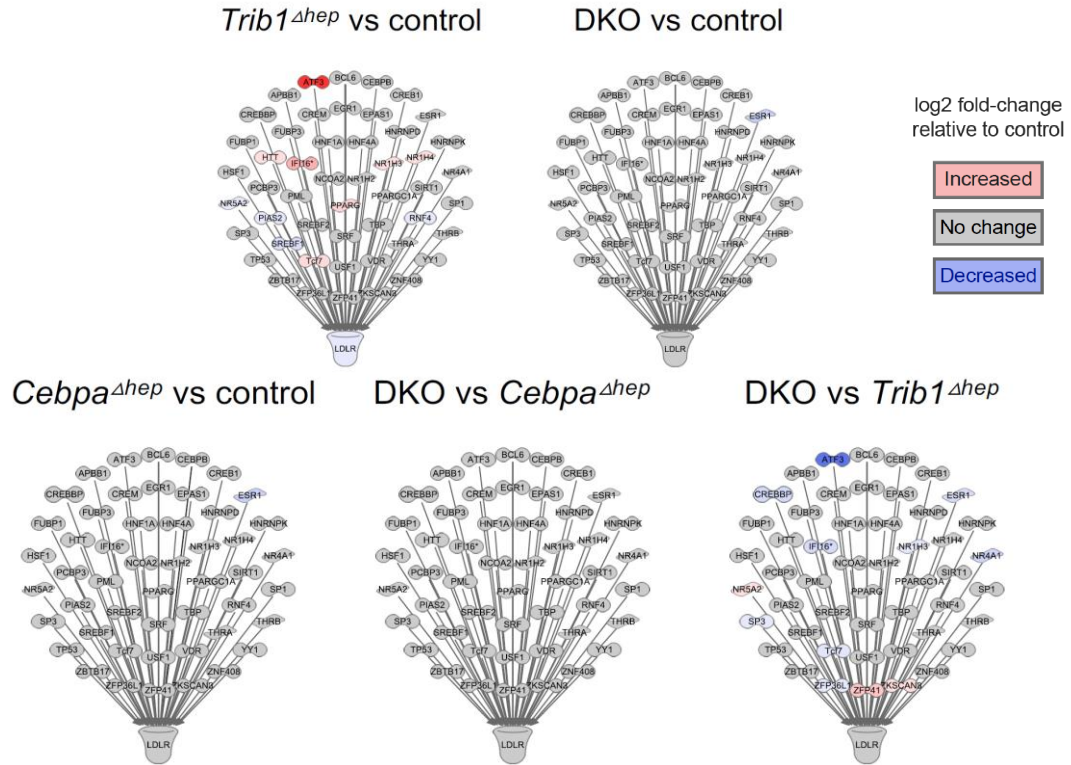


Figure 4.9: Ingenuity pathway analysis of all predicted liver-expressed ligand-dependent nuclear receptors, transcription factors, and transcriptional regulators upstream of *Ldlr* (based on IPA knowledge base) overlaid with color-coded mouse liver RNAseq from the comparisons listed above each plot. Analysis was performed in chow fed mice 4 weeks after AAV-CRE injection (n=6). DKO=*Trib1*^{Δhep};*Cebpa*^{Δhep}. Red= upregulated genes, Blue= downregulated genes.

Figure 4. 10: Effects of hepatic deletion of *Trib1* and *Cebpa* on SREBP family members.

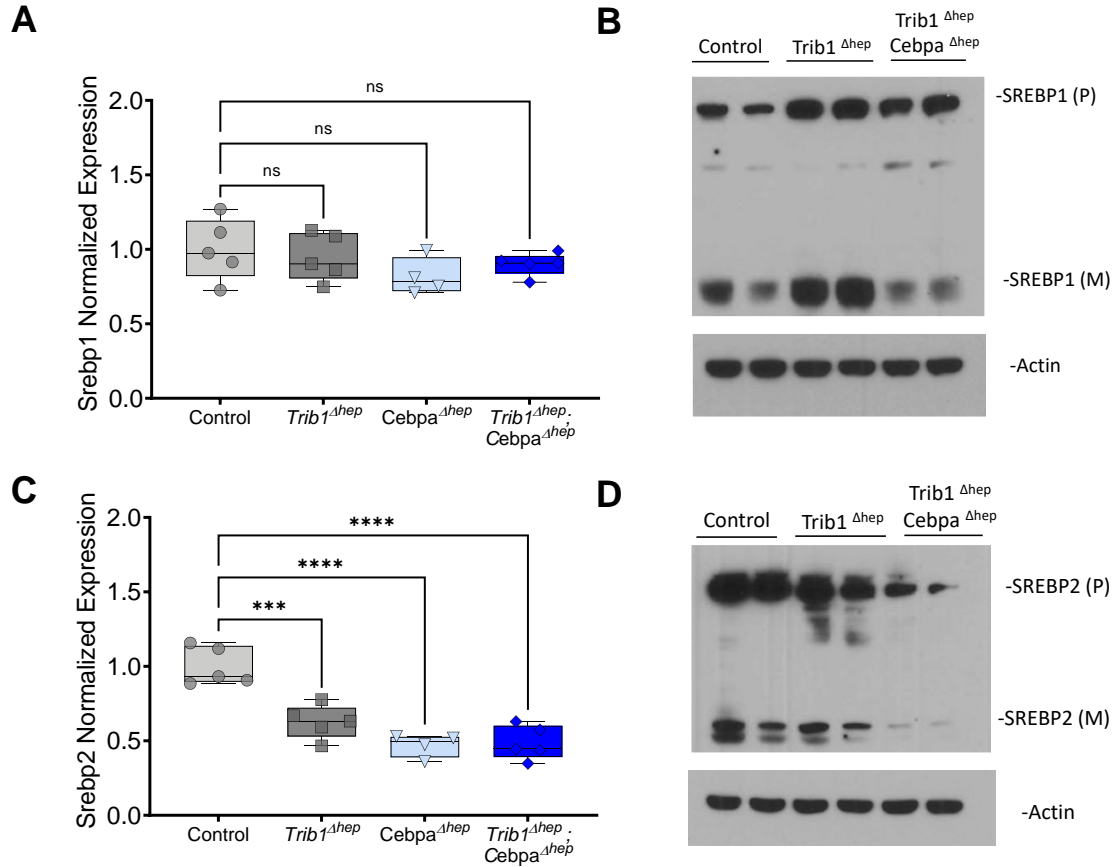


Figure 4.10: A-B. Hepatic *Srebf1* mRNA and SREBP1 protein levels in chow fed mice 4 weeks after AAV8-CRE injection. **C-D.** Hepatic *Srebf2* mRNA and SREBP2 protein levels in chow fed mice 4 weeks after AAV8-CRE injection. P, preprotein; M, mature protein. Box plots indicate median, 25th and 75th percentiles with whiskers extending to minimum and maximum values. Symbols indicate single values. Significance was determined by one-way ANOVA with Tukey's multiple comparison test (** $p \leq 0.001$, **** $p \leq 0.0001$).

Figure 4. 11: Hepatic deletion of *Trib1* increases *Atf3* mRNA and protein levels in a CEBPA dependent manner

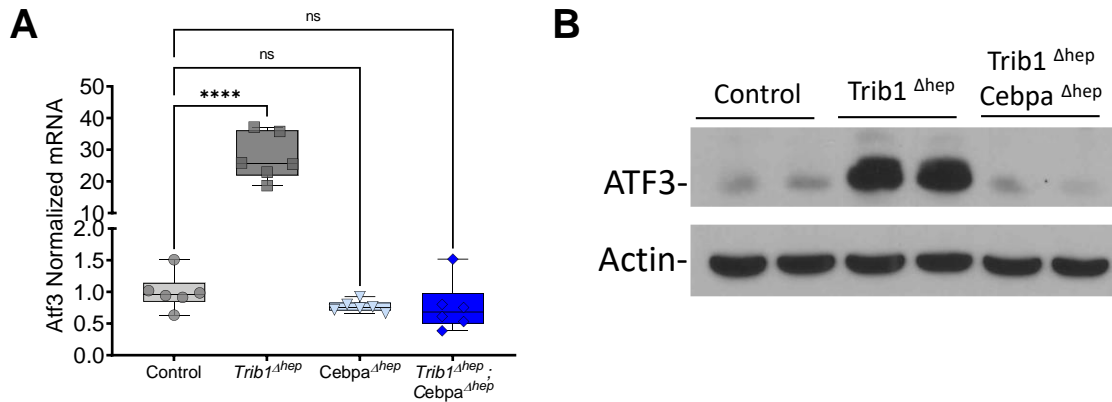


Figure 4.11: A. Hepatic transcript levels of ATF3 in chow-fed male mice (n=6 per group) 4 weeks after injection AAV-CRE. **B.** Immunoblot of hepatic ATF3 and β -actin, replicated in 3 independent cohorts. Box plots indicate median, 25th and 75th percentiles with whiskers extending to minimum and maximum values. Symbols indicate single values. Significance was determined by one-way ANOVA with Tukey's multiple comparison test (**** $p \leq 0.0001$).

Figure 4. 12: Ingenuity pathways analysis plot of *Atf3* downstream regulated factors in RNAseq cohort samples

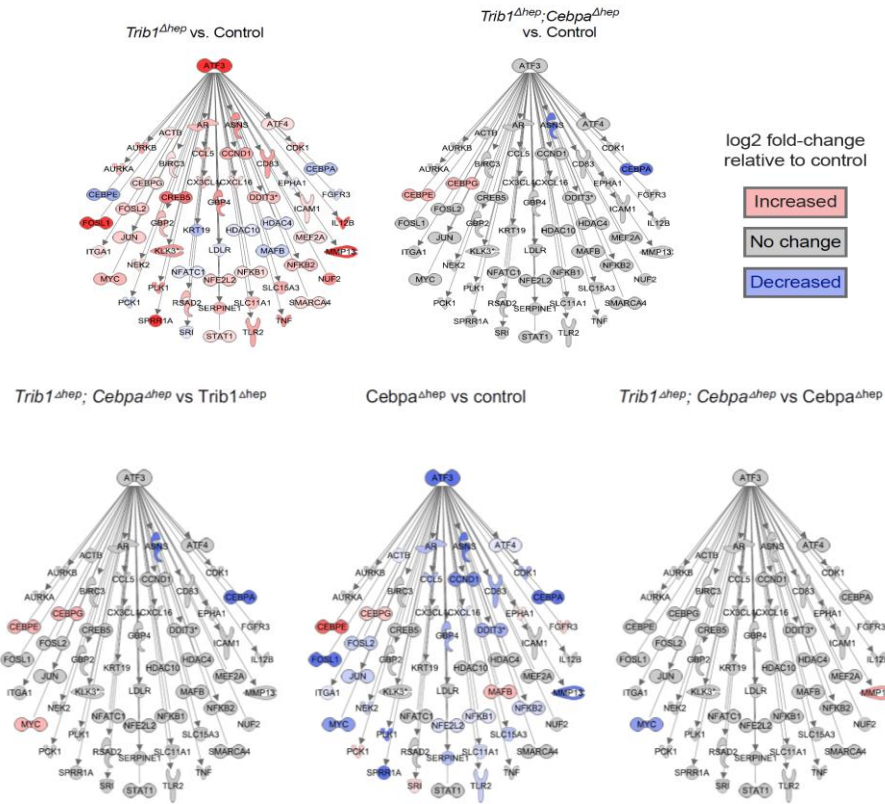


Figure 4.12: Ingenuity pathways analysis plot of *Atf3* downstream regulated factors in RNAseq cohort samples comparing Trib1^{Δhep} mice to control mice (A), Trib1^{Δhep} : Cebpa^{Δhep} mice to control mice (B), Trib1^{Δhep};Cebpa^{Δhep} compared to Trib1^{Δhep} mice (C), Cebpa^{Δhep} as compared to control mice (D) and Trib1^{Δhep};Cebpa^{Δhep} as compared to Cebpa^{Δhep} mice (E). Color overlays reflect the ratio of the differentially expressed transcript: for example, *Cepbe* is up-regulated (red), and *Cebpa* down-regulated (deleted, blue) in Trib1^{Δhep};Cebpa^{Δhep} compared to Trib1^{Δhep} (leftmost figure). Analysis was performed in chow fed mice 4 weeks after AAV8-CRE injection (n=6).

Figure 4. 13: *Atf3* siRNA deletion efficiency.

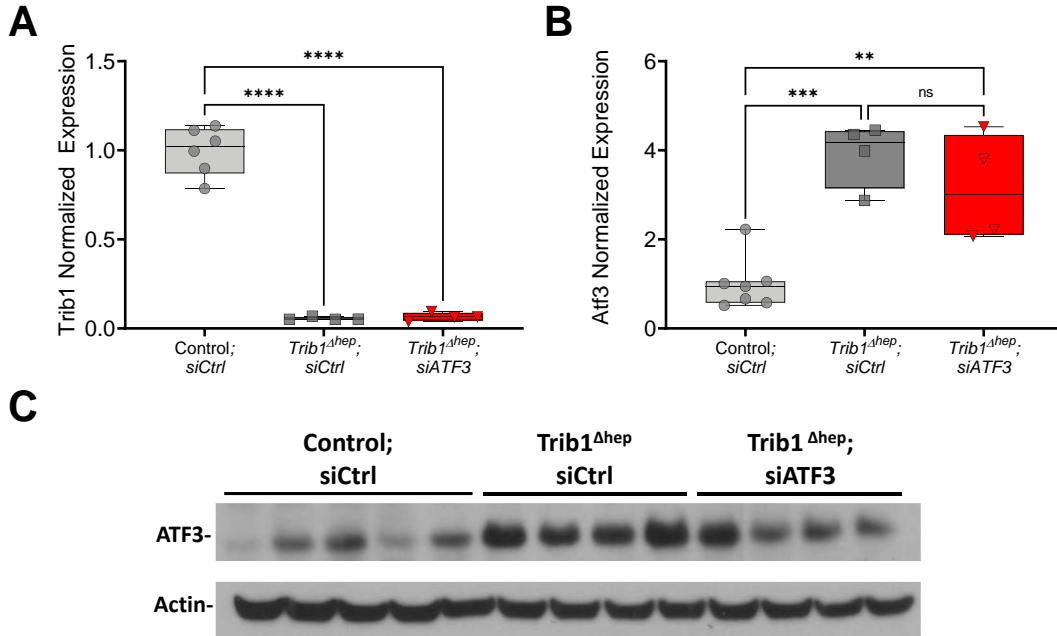


Figure 4.13: A-B. Hepatic transcript levels of Trib1 and Atf3 in 7 controls, 4 *Trib1*^{Δhep} Luciferase and 4 *Trib1*^{Δhep} Atf3 siRNA. **C.** Immunoblot of hepatic ATF3 and β-actin. Box plots indicate median, 25th and 75th percentiles with whiskers extending to minimum and maximum values. Symbols indicate single values. Significance was determined by one-way ANOVA with Tukey's multiple comparison test (**p ≤ 0.01, ***p ≤ 0.001, ****p ≤ 0.0001).

Figure 4. 14: Downregulation of *Atf3* in *Trib1*^{Δhep} mice reduces total cholesterol and HDL-C

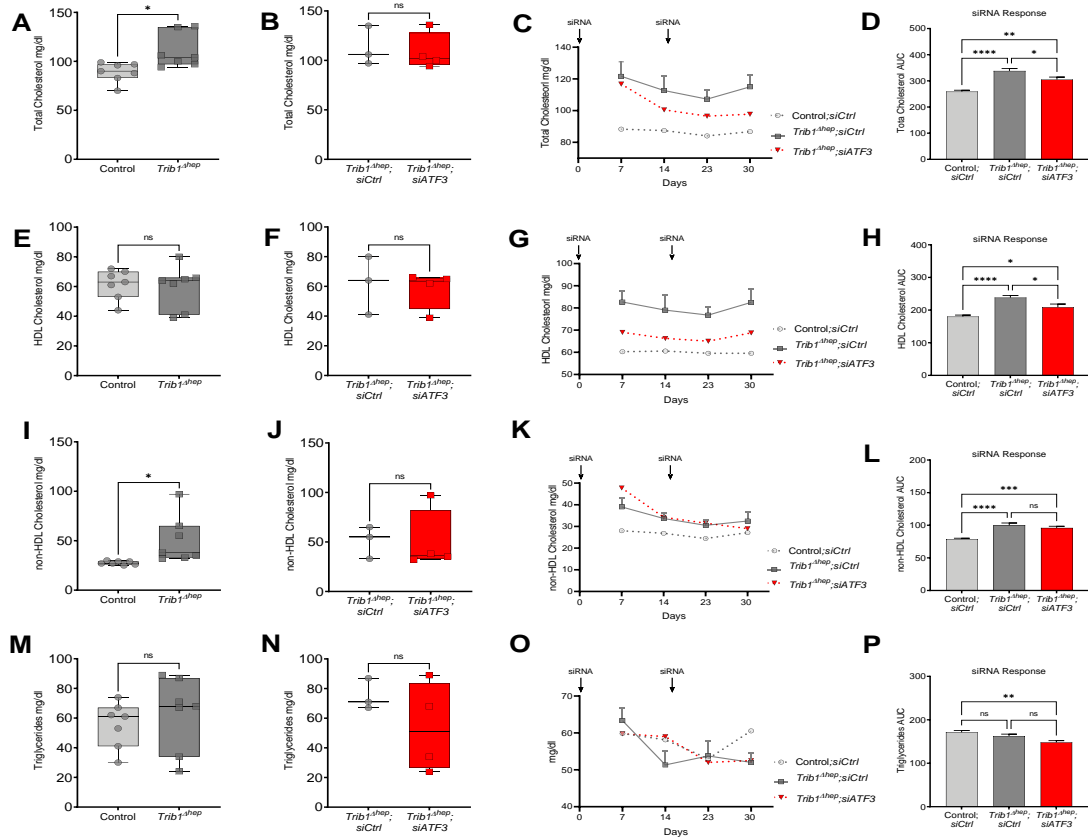


Figure 4.14: A, E, I, M. Total cholesterol, HDL cholesterol, non HDL cholesterol and triglycerides in control and *Trib1*^{Δhep} 2 weeks after AAV injection and prior to siRNA treatment (n=7 each). **B, F, J, N.** Total cholesterol, HDL cholesterol, non HDL cholesterol and triglycerides prior to siRNA treatment in *Trib1*^{Δhep} mice divided by eventual siRNA group (3 *Trib1*^{Δhep}; siCtrl and 4 *Trib1*^{Δhep}; siATF3). **C, G, K, O.** Time course of plasma total cholesterol, HDL cholesterol, non HDL cholesterol and triglycerides in siRNA injected mice. **D, H, L, P.** Area under the curve of the siRNA treatment time course in panel C,

G, K, O; y-axis, arbitrary units. Box plots indicate median, 25th and 75th percentiles with whiskers extending to minimum and maximum values. Symbols indicate individual values. Data are expressed as mean \pm s.e.m for the experimental group. Significance was determined by two-tailed, unpaired t-test and by one-way ANOVA with Tukey's multiple comparison test (* $p \leq 0.05$; ** $p \leq 0.01$; *** $p \leq 0.001$).

Figure 4. 15: Effects of downregulation of *Atf3* in *Trib1^{Δhep}* mice on lipoprotein distribution.

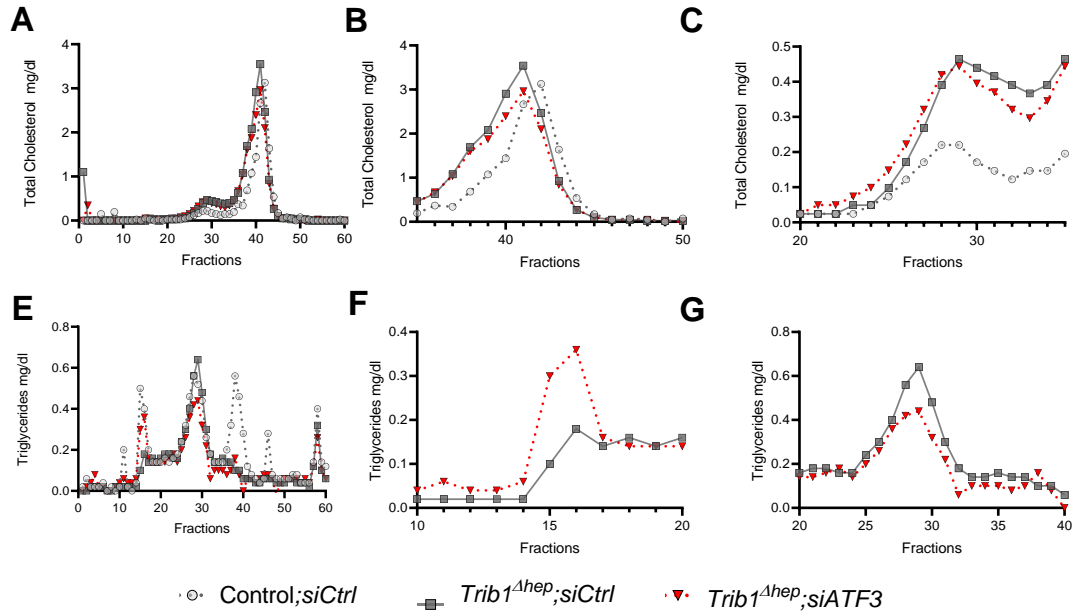


Figure 4.15: A. Total cholesterol distribution in FPLC-fractionated from day 30 pooled plasma. B-C. Zoomed in plots of A. E. Triglyceride distribution in FPLC-fractionated from day 30 pooled plasma. F-G. zoomed in plots of E.

Figure 4. 16: Downregulation of *Atf3* in *Trib1*^{Δhep} mice increases LDLR protein levels.

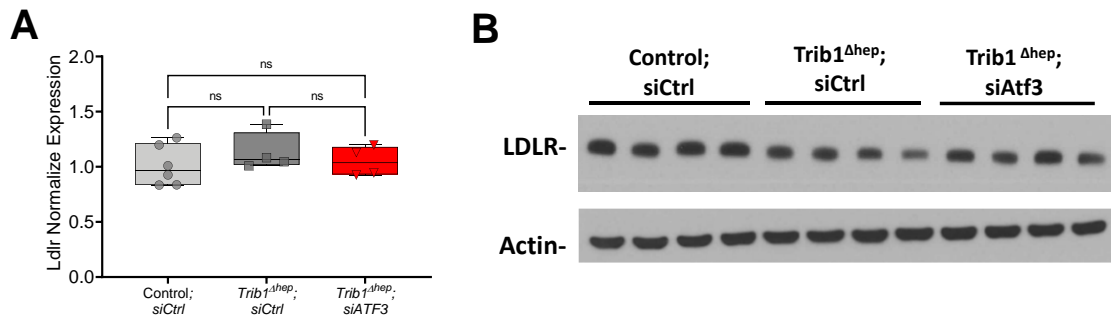


Figure 4.16: A. Hepatic transcript levels of *Ldlr* in 7 controls, 4 *Trib1*^{Δhep} Luciferase and 4 *Trib1*^{Δhep} *Atf3* siRNA. **B.** Immunoblot of hepatic LDLR and β -actin. Box plots indicate median, 25th and 75th percentiles with whiskers extending to minimum and maximum values. Symbols indicate single values. Significance was determined by one-way ANOVA with Tukey's multiple comparison test.

Figure 4. 17: Proposed mechanistic model of how *Trib1* regulates the LDLR in a CEBPa dependent manner.

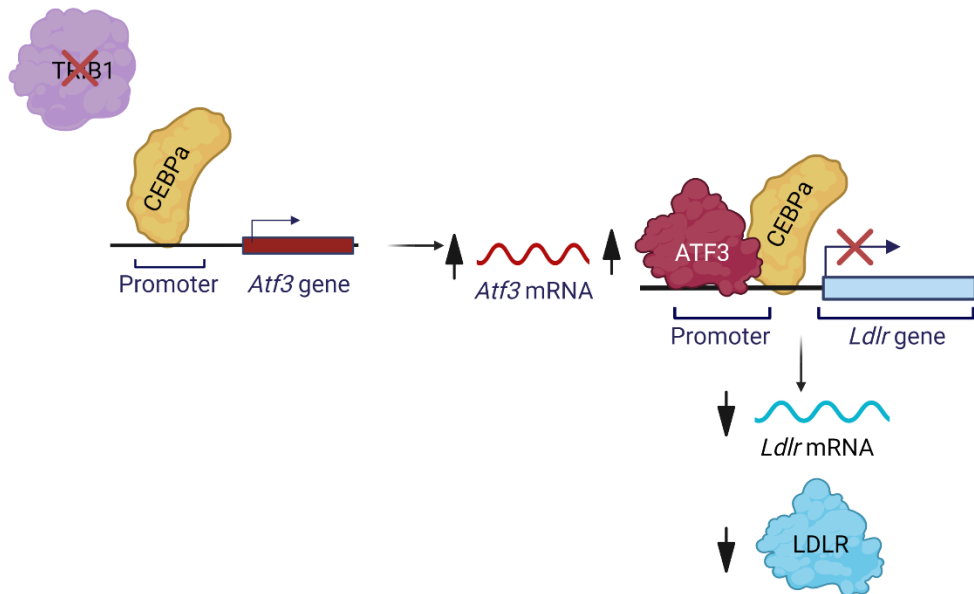









Figure 4.17: Our results are consistent with a model in which the hepatic deletion of *Trib1* allows CEBPa protein to escape targeted proteolysis, resulting in increased CEBPa protein. The increased CEBPa protein directly interacts with the *Atf3* promoter and leads to its transcriptional upregulation. The ATF3 protein (which CEBPa also binds directly) binds the *Ldlr* promoter and represses its transcription thereby resulting in the downregulation of LDLR mRNA and consequently of LDLR protein.

Table 2. Motif enrichment analysis of CEPBA ChIP-seq in liver from Trib1^{Δhep} mice.

Motif	Gene	Overlap	Adj P-Val
	ATF3	14.9%	1E-43
	CEBP	62.8%	1E-1016
	ATF4	27.2%	1E-408
	ATF1	16.71%	1E-68
	ATF7	11.36%	1E-47
	CHOP	21.19%	1E-313
	NFIL3	42.33%	1E-563

CHAPTER 5:

Constitutive deletion of *Trib1* in mice leads to highly penetrant neonatal lethality due to impaired glucose metabolism.

ABSTRACT

The effects of hepatic *TRIB1* on plasma lipid metabolism have been broadly studied, however not a lot of work has been done in determining the effects of extra-hepatic *TRIB1* on plasma lipids and other metabolic traits. To explore the extra-hepatic effects of *TRIB1*'s on lipid metabolism we acquired a mice line homozygous for *Trib1* whole body deletion (*Trib1* KO) on a pure C57BL/6 background, however we found that this model presented a highly penetrant lethal phenotype of unknown etiology. The goal of these studies was to determine the developmental stage at which lethality was occurring, as well as to determine the physiological mechanism leading to the lethal phenotype. Our studies determined that *Trib1* KO mice develop normally in uterus and that the period of lethality was post-natal, between day 0 and day 1 after birth. We hypothesized that this was likely due to severely low blood glucose levels compared to control mice. We also determined that about 5% of *Trib1* KO mouse survive the neonatal lethally period and make it to adulthood and that similar to *Trib1*^{Δhep} mice, *Trib1* KO have increased plasma lipids and impaired postprandial lipemia. I also demonstrated that *Trib1* KO mice have decreased fasting glucose levels, and that their glucose and insulin tolerance is improved compared to wild type and heterozygous mice. *Trib1*^{Δhep} mice also had improved glucose tolerance with no changes in insulin tolerance. The results from these studies suggest that additional

to regulating plasma lipids, *Trib1* is involved in the regulation of glucose metabolism, an association that has not been previously reported. However, questions regarding which tissues and the specific molecular mechanism by which *Trib1* regulates glucose phenotypes in mice remain unanswered.

INTRODUCTION

To explore the extra-hepatic effects of *TRIB1*'s on lipid metabolism we acquired a mice line homozygous for *Trib1* whole body deletion (Trib1 KO) on a pure C57BL/6 background, however we found that this model presented a highly penetrant lethal phenotype of unknown etiology. Based on this finding, we sought to investigate at which stages of development was the lethality occurring, as well as which physiological mechanism was impaired in these mice causing lethality.

The mouse is the most used model to study the genetic effects of mammalian gene mutation on biological function, however, it presents certain challenges that make their study difficult. One of the main challenges is that many mutations produced through genetic engineering can affect the developmental processes of the mutant embryos and compromise their survival rates [178]. Additional to affecting embryonic and fetal development, some mutations also intervene with survival at neonatal stages [179], which represents a limitation for understanding the physiological effects to certain genetic mutations in mice.

The lethality phenotypes at each stage of development are characterized by different physiological manifestations. At the embryonic/fetal state lethality can occur at early

stages of fertilization or implantation, or later stages of development [178]. Appropriate development through implantation depends on the development of extraembryonic tissues like the trophoblast, a layer of tissue on the outside of a mammalian blastula, which supplies the embryo with nourishment [180-182]. The process of gastrulation is also very crucial in these early stages, which will result in the formation of the primary germ layers and extraembryonic structures that will contribute to the yolk sac and the placenta [180-182]. Neural, lung, cardiovascular and renal development occur to fulfill appropriate development these tissues and organs that are required for life, and mutations or physiological deformities that affect any of these systems have been associated with deathly phenotypes in mice [178].

If the mice form normally and make it through the whole term, then it must overcome the process of parturition which is highly stressful for newborn pups. During gestation, the fetus depends on the placenta to supply nutrients, metabolic exchange and waste disposal; and glucose is the main energy source for fetal development [183, 184]. This stage of development for the fetus is characterized by high plasma insulin and low plasma glucagon levels [185, 186]. High levels of insulin signals to the liver that blood glucose is high, which causes tissues to absorb glucose and store it as glycogen, the primary carbohydrate stored in the liver and muscle cells of animals [187-190]. When blood sugar levels drop, glucagon signals the liver to break down glycogen into glucose, a process called glycogenolysis, causing blood sugar levels to increase [191]. Before birth, the expression of hepatic glycogen synthase is increased to promote tissue glycogen storage to endure the postnatal survival of the newborn [127, 192].

Soon after birth, the mice go through a period of starvation that is associated with the abrupt cessation of maternal nutrient supply previously provided through the umbilical cord, and neonatal metabolism must adapt to survive [193, 194]. In these early stages of life, glucose is still one of the most important sources of energy for the brain and vital organs, and the body undergoes many metabolic and hormonal changes to stabilize glucose levels [193]. The period right after birth and before suckling is characterized by an increase in glucagon and glucagon receptors and a decrease of insulin levels [179, 193]. This low insulin/high glucagon molar ratio is essential to produce glucose through glycogenolysis and gluconeogenesis, the latter which is metabolic pathway that results in the generation of glucose from non-carbohydrate carbon substrates [195]. In humans the main gluconeogenic precursors are lactate, glycerol, alanine and glutamine, which account for ~90% of gluconeogenic substrates [191]. The early postnatal stage is also characterized by an increased in glucocorticoids, which together with the increase in glucagon and catecholamine, promotes lipolysis and muscle protein breakdown, which increases the availability of gluconeogenic substrates [195]. Also, an increase in long chain fatty acid oxidation and ketone body production during the first 24 h following birth has been reported to contribute as alternative fuels to spare glucose requirements of neonates [196]. Any mutations that disrupt glucose homeostasis or the normal development of the liver or pancreas (which is crucial for the production of insulin) are associated with an array of developmental diseases and death due to their possible effects on energy balance.

Neonatal lethality due to hypoglycemia has been studied in several mouse models and has been associated with multiple physiological mechanism [127, 197-201]. Following

birth neonates go through transient hypoglycemia until glycogenolysis and gluconeogenesis are activated in the liver, but improper activation of any of these pathways could lead to severe hypoglycemia and neonatal lethality. It has also been shown that autophagy is a critical source of energy in these early stages of life, which is induced in response to starvation within 3-6 hours after birth [200]. This was confirmed in *Atg5* KO and *Atg7* KO mice, in which autophagosome fusion is blocked, and these mice die within 12 hours of birth with their energy levels depleted [200]. Another gene studied for its effect in neonatal lethality is *CEBPa*, which is a gene highlighted in my research. *Cebpa* mutant neonates show reduced glucose levels and die within 8 hours of birth due to their inability to store glycogen in the liver prior to birth and exhibited a remarkable lack of lipids in their hepatocytes and adipocytes [127]. Neonatal hypoglycemia can also result from increased insulin sensitivity, and it is associated with cyanosis and lethargy in mice with mutations in the *Ship2/phx2a* loci [197]. Other causes for neonatal hypoglycemia can be associated with respiratory distress and abnormal feeding [179].

The results from our studies suggest that the lethal phenotype in *Trib1* KO mice occurs postnatally due to severe hypoglycemia, and that the small percentage of *Trib1* KO mice that survives postnatal lethality (~5% survival rate) also present phenotypes of reduced glucose levels due to improved glucose tolerance and higher insulin sensitivity. The *TRIB1* gene has been broadly associated with multiple cardiometabolic traits, however glucose metabolism is not one of them. The results from these studies suggest a novel physiological association with *TRIB1* and glucose regulation mice, however questions regarding the molecular mechanism by which *Trib1* regulates glucose phenotypes in mice remain unanswered.

RESULTS

***Trib1* KO mice have normal embryonic development but die postnatally.**

In order to study the extra-hepatic effects of *Trib1* on plasma lipid metabolism, we acquired a mice line homozygous for *Trib1* whole body deletion (*Trib1* KO) on a pure C57BL/6 background, however we found that this model presented a highly penetrant lethal phenotype of unknown etiology. Previous unpublished studies from Rob Bauer in our lab focused in determining the developmental stage at which *Trib1* whole body deletion leads to lethality. Death due to genetic mutations can occur at different developmental stages, during fetal development (fetal death), within one day after birth (neonatal death) or after the first day of birth (postnatal death). Dr. Bauer previously studied several stages of embryonic development and was able to find that *Trib1* KO mice are present at every stage in utero, and they had no differences in gross appearance or any visible morphological defects. These mice also had normal development of cardiovascular and pulmonary systems compared to control mice. These data suggested that *Trib1* KO mice have normal embryonic development and perish on their neonatal or postnatal period after birth. The mice were followed after birth, and we were able to determined that the time of death ranges between neonatal day 0 and neonatal day 1. *Trib1* KO mice were born in a normal Mendelian ratio, showed no visual developmental deformities and nursed at normal rates compared to wild type mice, however they rarely survive to adult stages (weaning at 4 weeks). These observations led us to further hypothesis that the physiological mechanism leading to neonatal death is due to a metabolic disorder, likely due to improper adaptation to new metabolic needs after birth.

***Trib1* KO neonate mice have severe hypoglycemia.**

As discussed earlier, glucose is one of the most important sources of energy for early neonates and regulating glucose levels is crucial to ensure survival. To determine if *Trib1* KO mice have impaired glucose levels at early stages of life, mice were collected right after birth to collect blood and tissues. I measure glucose levels in all mice at the moment of death and discovered that *Trib1* KO mice have striking low levels of glucose compared to wild type mice (Figure 5.1). *Trib1* heterozygous mice presented intermedium glucose levels between wild type and KO mice (Figure 5.1), suggesting that the effect of *Trib1* on glucose levels is gene-dose dependent. Based on how important glucose homeostasis is for survival, we strongly believe that severe hypoglycemia is the cause of death on *Trib1* KO mice. Regulation of insulin levels in the circulation is crucial to maintain euglycemia; and concentration in the plasma is largely determined by the rate of secretion from beta cells in the pancreas [202]. Failure to regulate insulin production and secretion or insulin clearance can result in increased plasma insulin levels, which could lead to the hypoglycemic phenotype in *Trib1* KO mice. We tried measuring insulin levels in *Trib1* KO mice compared to wild type and heterozygous mice, however insulin levels were undetected in all the groups. It is possible that at this early-stage of development insulin levels are too low in these mice to be detected, for which reason it couldn't be detected by our assay.

***Trib1* KO neonate mice have normal liver lipids and ketones but decreased lactate and glycogen levels.**

As *Trib1* is known for its effects on hepatic lipid metabolism, we decided to explore hepatic levels of triglycerides and cholesterol and saw no differences between the groups (Figure

5.2 A-B), suggesting that hepatic lipid levels are not contributing to the metabolic effects observed in *Trib1* KO mice. Ketone body production is known to increase substantially during the first 24 h following birth and to contribute as fuel for glucose requirements on neonates, however, no differences were observed between the groups (Figure 5.2 C). Lactate, which is a key substrate for gluconeogenesis, was significantly decreased in a dose dependent manner on *Trib1* Het and *Trib1* KO mice (Figure 5.2 D). Additionally, glycogen, which is highly important for glucose production in early neonates, was strikingly reduced in both *Trib1* Het and *Trib1* KO mice, however not in a dose dependent manner (Figure 5.2 E). The decrease in ketones and glycogen can both be causing or contributing to the hypoglycemic phenotype in *Trib1* KO mice, however more experiments are needed to determine the exact mechanism leading to neonatal hypoglycemia and death.

***Trib1* KO neonate mice have increased levels of lipogenic genes.**

As *Trib1* is known for its effects on lipogenic gene expression, we decided to explore for changes in expression in some target genes. First, we were able to confirm complete knockout of *Trib1* in *Trib1* KO mice, as well as intermedium knockout in *Trib1* het mice (Figure 5.3 A). We also observed a significant reduction on *Cebpa* mRNA levels (Figure 5.3 B), like what has been shown in *Trib1*^{Δhep} mice. I observed an increase in the expression of Fatty Acid Synthase (*Fasn*) and Acetyl-CoA Carboxylase Alpha (*ACACA*) (Figure 5.3 C-D), both genes which are involved in the synthesis of fatty acids. These data show that even at this young age, *Trib1* KO mice present similar gene expression to *Trib1*^{Δhep} mice. Even though the increased of these genes is associated with increased hepatic lipids in *Trib1*^{Δhep} mice, this phenotype is not recapitulated right after birth in neonates.

***Trib1* KO neonate mice have normal levels of glucogenic genes.**

As *Trib1* KO mice suffer from severe hypoglycemia, we decided to explore if there were any changes in expression on genes associated with the process of glucose production in the liver. I explore for changes in Phosphoenolpyruvate carboxykinase (PEPCK), which encodes an enzyme that catalyzes the rate-limiting step of gluconeogenesis; Glucose-6-phosphatase catalytic subunit (G6pc), which encodes a key enzyme in glucose homeostasis which functions in gluconeogenesis and glycogenolysis; and Glycogen synthase 1 (Gys1), which encodes a key enzyme for glycogen production [191]. However, no changes in mRNA expression were observed in any of these genes when comparing *Trib1* KO to control mice (Figure 5.4).

Adult *Trib1* KO mice have increased plasma lipids and impaired postprandial triglyceride clearance.

In my time breeding these mice we have found out that about 5% of *Trib1* KO mice are able to survive the neonatal lethally period and make it to adulthood. I studied 3 surviving *Trib1* KO together with wild type and heterozygous adult age matched mice and phenotype them for changes in plasma lipid metabolism. *Trib1* KO mice presented with low triglyceride levels, increased total cholesterol, no changes in HDL cholesterol and increased non-HDL cholesterol and plasma ALTs (Figure 5.5). *Trib1* KO mice also presented highly impaired triglyceride clearance phenotype after a high lipid load (Figure 5.6 A), which was confirmed by calculating the area under the curve (Figure 5.6 B). These results from adult *Trib1* KO mice are similar to what was observed in the *Trib1*^{hep} mice, suggesting that hepatic *Trib1* is mostly contributing to the plasma lipid metabolism

phenotypes observed. More interestingly, *Trib1* Het mice did not show differences in plasma lipids or postprandial lipemia compared to control, suggesting that 50% expression of *Trib1* is sufficient to maintain a normal plasma lipid phenotype in these mice.

Adult *Trib1* KO mice have reduced glucose, increased lactate, and normal ketone plasma levels.

As *Trib1* KO neonate mice die from severe hypoglycemia, we decided to explore if the surviving adult *Trib1* KO mice have any impairment in glucose metabolism. We measured glucose levels at different fed and fasted times in mice and showed that fed *Trib1* KO mice have normal glucose levels compared to wild type and heterozygous mice, however, short time fasting of 4 and 6 hours significantly reduces glucose levels in *Trib1* KO mice and that in overnight fasted *Trib1* KO mice glucose levels are back to normal (Figure 5.7 A). Overall, all groups presented a reduction in glucose overtime, this likely due to the lack of nutrient uptake. These results suggest that similar to neonate mice, adult *Trib1* KO mice have an impaired regulation of glucose levels. We also explore for changes in lactate levels and observed that *Trib1* KO mice have normal levels at fed and 4-hour fasting, but that lactate levels are significantly increased after overnight fasting (Figure 5.7 B). Ketones levels in *Trib1* KO mice were comparable to control and *Trib1* Het mice, however overnight fasting strikingly increased ketone levels in all groups, this likely due to the low levels of glucose which induce fatty acid breakdown and ketone body formation as an alternative source of energy.

Adult *Trib1* KO mice have improved glucose and insulin tolerance, and Adult *Trib1*^{hep} mice have improved glucose tolerance with no changes in insulin tolerance.

Increased plasma and hepatic lipids are usually associated with defects in glucose tolerance and insulin sensitivity in mammals. I performed glucose tolerance test (GTT) and insulin tolerance test (ITT) in this cohort to determine if there were any defects in *Trib1* KO mice. Surprisingly, *Trib1* KO mice have improved glucose clearance after glucose or insulin bolus infusions, which means they have improved insulin sensitivity to glucose (Figure 5.8). These studies were performed in *Trib1*^{hep} mice, which showed improved glucose sensitivity, but no changes in insulin sensitivity (Figure 5.9). These results suggest that *Trib1* effects on insulin sensitivity to glucose are mediated by extra-hepatic tissues, with the pancreas being the most obvious target as it regulates the production and secretion of insulin. It was surprising to see that even though these mice have increased lipids, which in human usually leads to insulin resistance and diabetes, both *Trib1* KO and *Trib1*^{hep} mice have improved glucose sensitivity. It would be interesting to further study the mechanisms that lead to these phenotypes. Overall, the findings from these studies further solidify our hypothesis that *Trib1* is associated with the regulation of glucose metabolism both in early stages of development and in adulthood in mice.

Adult *Trib1* het and KO mice have similar mRNA expression pattern as *Trib1*^{hep} mice.

Even though they survive neonatal lethality due to hypoglycemia, adult *Trib1* KO mice have higher mortality rates associated with the development of prolapse rectum. From the cohort I followed, 2 out of 3 *Trib1* KO mice developed prolapsed rectum and die because

of it. From previous cohort with sporadic surviving Trib1 KO mice, the development of prolapsed rectum was observed often, but not quantified. For this reason, they needed to be euthanized at an earlier age, which made it challenging to match them to control and het mice for long term experiment and collect tissues for mRNA and protein studies. I collected tissue from 1 surviving *Trib1* KO mouse and compared it to its match wild type and het mice. Overall, *Trib1* KO mice showed a trend of hepatic mRNA expression very similar to *Trib1*^{Δ_{hep}} mice. *Trib1* expression was undetected and *Cebpa* expression was reduced to about 50% of wild type mice. *Trib1* KO mice showed increased expression of lipogenic genes such as *Dgat2*, *Fasn* and *Acaca* (Figure 5.10). There were no differences in *Ldlr* expression but increased *Atf3* expression (Figure 5.10). The results from these studies are interesting, however limited interpretation can be done as it is based on only one *Trib1* KO mouse. It will be necessary to further breed these mice to obtain more *Trib1* KO mice for analysis of hepatic and extra-hepatic gene expression of genes associated with glucose and plasma lipid metabolism.

DISCUSSION

The *TRIB1* gene, which encodes Tribbles homolog 1 protein (TRIB1), has been suggested as causal for the highly robust genome-wide association study (GWAS) signal at human chromosomal locus 8q24 for a remarkable number of cardiometabolic traits, including plasma lipids and lipoproteins, hepatic steatosis, adiponectin levels, and coronary artery disease [69, 124, 146, 148]. However, no previous association with glucose metabolism has been described.

In our studies we explore *Trib1* whole body deletion effect on the pure C57BL/6 background mice, as this background is the most used to study metabolic traits in mice. However, we demonstrated that *Trib1* whole body deletion in this background leads to a highly penetrant neonatal lethality, with only about 5% of *Trib1* KO mice making it to adult stages. Other models of whole body *Trib1* deletion on mixed backgrounds have been used, and even though they are viable, unofficial reports of decreased survival have been cited and not fully described. We show that *Trib1* KO mice die at neonatal stages, which usually is associated with defects in adjusting to new metabolic needs after birth.

Soon after birth, mammals go through a period of starvation that is associated with the abrupt cessation of maternal nutrient supply and adaptation to new metabolic needs to regulate their own homeostasis [186, 193]. In these early stages of life, glucose is one of the most important sources of energy for the brain and vital organs and the body undergoes many metabolic and hormonal changes to stabilize glucose levels. Before birth, glycogen synthase expression is increased in the liver to promote glycogen storage that will allow survival of the newborn during postnatal starvation [192]. The period right after birth is characterized by an increase in glucagon and a decreased in insulin levels, which induces hepatic glycogenolysis and gluconeogenesis to produce glucose from the stored glycogen and other non-carbohydrate carbon substrates, respectively [185, 186, 191-193, 195, 196].

Our studies show that *Trib1* KO mice have significantly low levels of glucose compared to control mice, and that *Trib1* Het mice have an intermedium phenotype between KO and wild type mice. We decided to measure insulin levels in these mice, as insulin is highly important in the regulation of glucose, and low levels are necessary to promote survival at

this early stage. However, our assay was unable to detect plasma insulin in any of the mice. It is possible that the stage at which the mice are collected plasma insulin levels are too low to be detected. Due to the limited amount of plasma collected from these mice, this test was performed only once on pooled plasma from several mice, and the plasma was thawed twice. It is possible that the already low levels of insulin quickly degraded after being collected and processed. Either way, this test needs to be repeated with fresh samples to confirm this result.

Additional to having severely low glucose levels, *Trib1* KO neonates also had significantly low levels of lactate, with *Trib1* Het mice presenting an intermedium phenotype between *Trib1* KO and wild type mice, a similar trend to the one observed for glucose. Lactate serves as a precursor for gluconeogenesis in the liver, which induces the production of glucose [195]. Low levels of lactate could result in decreased gluconeogenesis and decreased glucose levels in mice, which could be causing the severe hypoglycemia in *Trib1* KO mice. Additional to low lactate levels, *Trib1* KO mice also have significantly low levels of hepatic glycogen, which is crucial to maintain euglycemia at these early stages. Because *Trib1* Het mice also have low levels of glycogen comparable to *Trib1* KO mice, we don't think that this alone could be causing neonatal lethality. However, the decreased in both lactate and glycogen in *Trib1* KO mice could be causing or strongly contributing to the severe hypoglycemic phenotype in these mice. Replicating these finding in a bigger cohort is necessary to corroborate these results. Additionally, glycogen staining in the livers of these mice should be performed, as it is a more reliable measurement for glycogen levels.

Further, we decided to explore if there were any changes in expression on certain genes associated with the process of glucose production. We looked for changes in *Pepck*, *G6pc* and *Gys1* and observed no differences on the mRNA of these genes that are involved in the processes of gluconeogenesis and glycogenolysis. However, it is possible that the phenotypes in *Trib1* KO mice are regulating by other genes. A better approach to identify candidate genes regulating *Trib1* KO glucose phenotypes would be to perform unbiased RNA sequencing in the liver and pancreas of these mice, which are two of the most important tissues regulating glucose metabolism. The results from the RNA sequencing would provide with an array of candidates to study for this purpose. Our studies suggest that severe hypoglycemia in *Trib1* KO neonates is caused by decreased levels of lactate and glycogen, however, more studies are necessary to confirm this as well as to determine the molecular mechanism leading to these phenotypes.

While breeding *Trib1* KO mice we discovered that about 5% of *Trib1* KO mouse survive the neonatal lethally period and make it to adulthood. I studied these mice together with wild type and heterozygous adult mice and determined that like *Trib1*^{hep} mice, they have increased plasma lipids and impaired postprandial lipemia, which suggested that hepatic *Trib1* is solely responsible for the regulation of plasma lipids in these mice. I also demonstrated that *Trib1* KO mice have decreased glucose levels during short time fasting and that they have improved glucose and insulin tolerance compared to *Trib1* wild type and heterozygous mice. I also demonstrated that *Trib1*^{hep} mice also had improved glucose tolerance with no changes in insulin tolerance, suggesting that *Trib1* effect on insulin response is mediated by extra-hepatic tissues. A possible candidate tissue will be the pancreas, as it is the main tissue regulating the production and secretion of insulin. These

results confirmed our hypothesis that additional to regulating lipid metabolism, *Trib1* serves a regulator of glucose metabolism in mice, an association that had not previously been described or tested. However, Additional studies to determine the molecular mechanism leading to trib1 regulation of glucose levels are necessary to fully understand these phenotypes.

FIGURES

Figure 5. 1: Trib1 KO neonate mice have decreased plasma glucose levels.

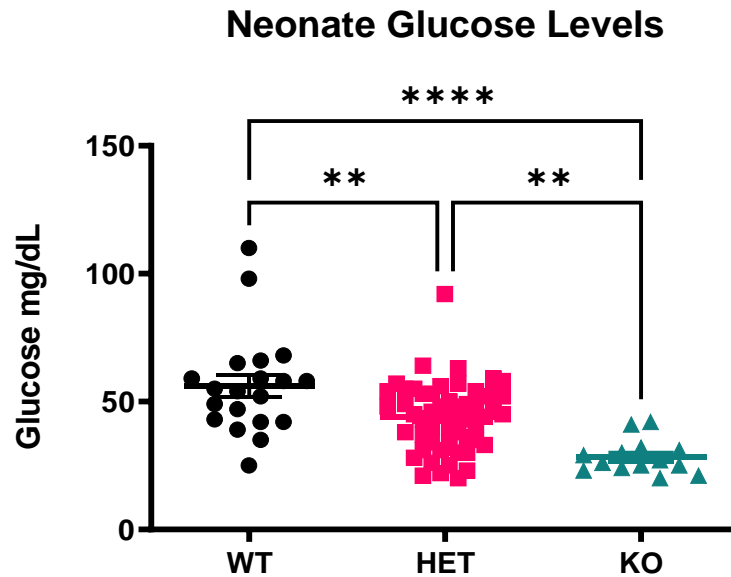


Figure 5.1: Plasma glucose levels were measured at postnatal day 0 in several cohorts of mice (n= 20 controls, 54 HET and 14 KO). Data indicate individual values with mean \pm s.e.m. Significance was determined by One-Way ANOVA multiple comparison (** $P \leq 0.01$, **** $P \leq 0.0001$).

Figure 5. 2: Trib1 KO mice have normal hepatic lipids and plasma ketones, but reduced plasma lactate and hepatic glycogen levels.

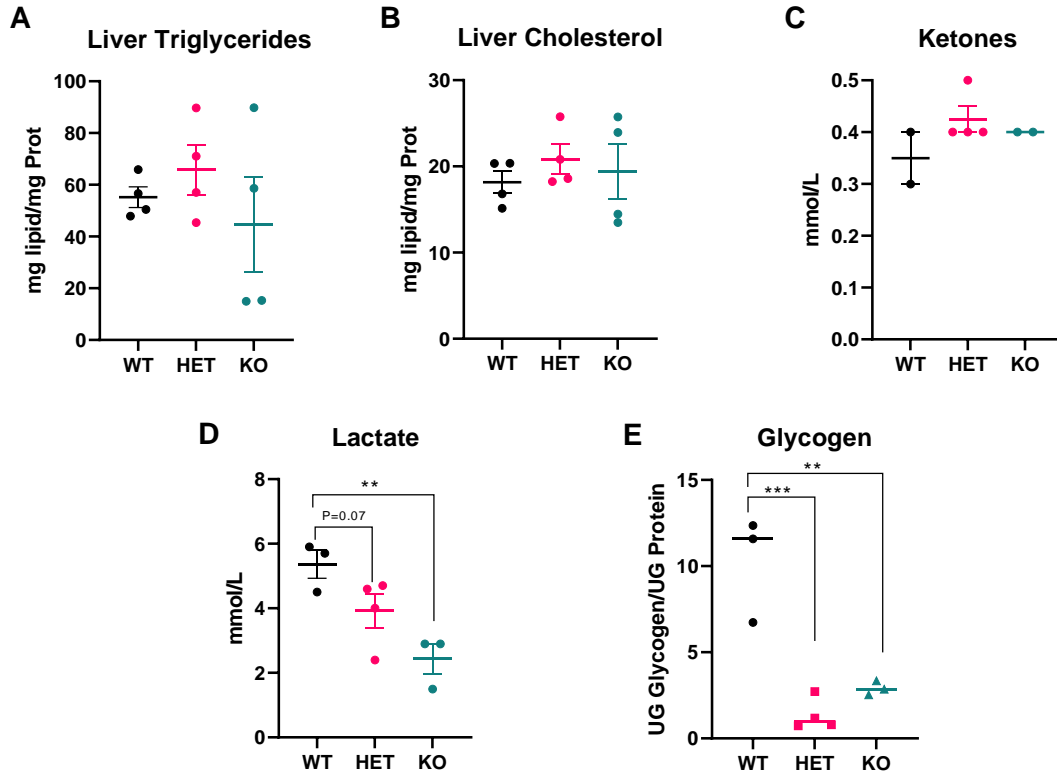


Figure 5.2: A-B. Hepatic triglycerides and total cholesterol in neonate mice right after birth. **C.** Plasma ketone levels in neonate mice right after birth. **D.** Plasma lactate levels in neonate mice right after birth. **E.** Hepatic levels of glycogen in neonate mice right after birth. Data indicate individual values with mean \pm s.e.m. Significance was determined by One-Way ANOVA multiple comparison (** $P \leq 0.01$, *** $P \leq 0.001$).

Figure 5. 3: Hepatic gene expression of lipogenic genes in neonate mice.

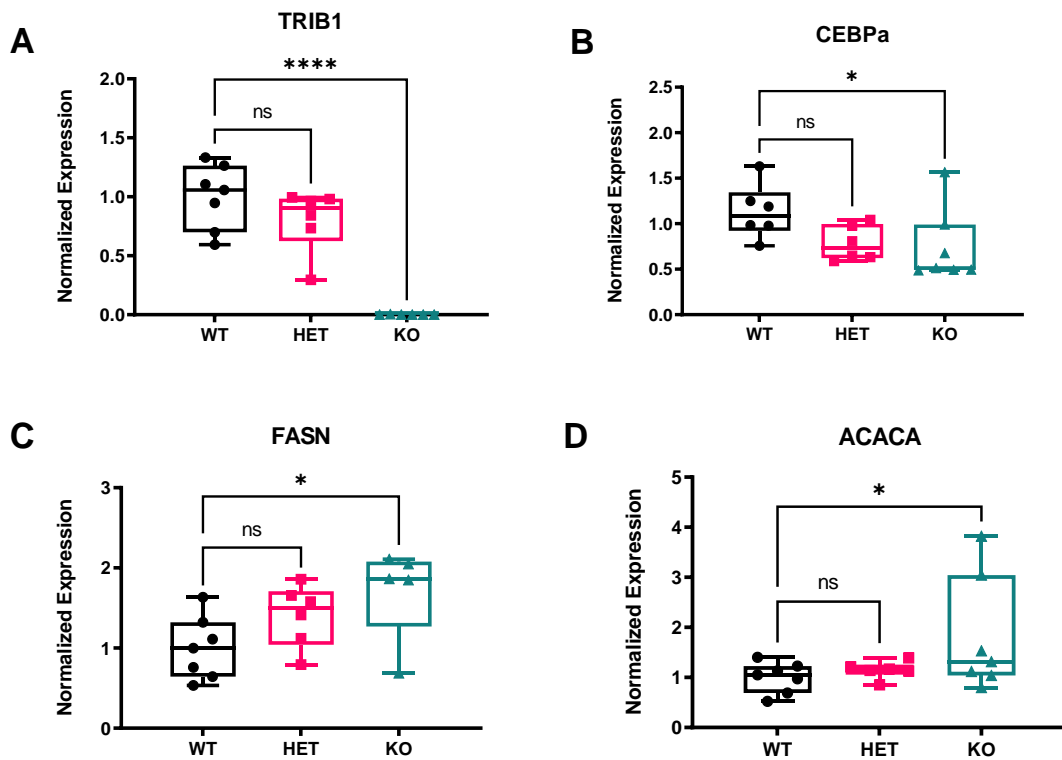


Figure 5.3: A-D. Hepatic transcript levels of Trib1, Cebppa, FasN and Acaca in Trib1 WT, HET and KO mice right after birth. Box plots indicate median, 25th and 75th percentiles with whiskers extending to minimum and maximum values. Symbols indicate single values. Significance was determined by One-Way ANOVA multiple comparison (* $P \leq 0.05$, **** $P \leq 0.0001$).

Figure 5. 4: Hepatic gene expression of glucogenic genes in neonate mice.

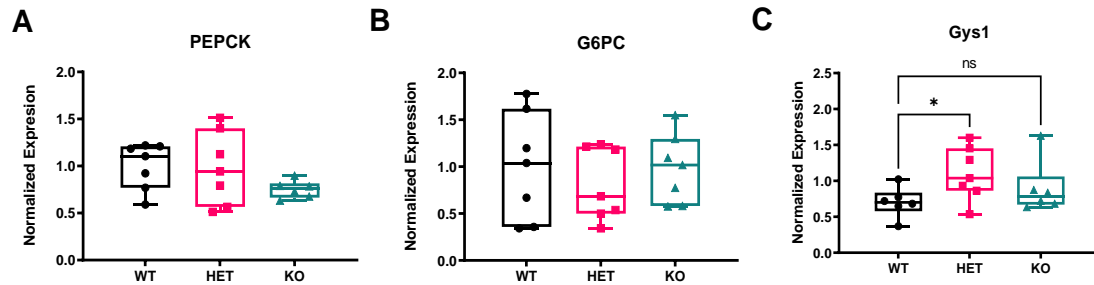


Figure 5.4: A-D. Hepatic transcript levels of *Pepck*, *G6pc* and *Gys1* in *Trib1* WT, HET and KO mice right after birth. Box plots indicate median, 25th and 75th percentiles with whiskers extending to minimum and maximum values. Symbols indicate single values. Significance was determined by One-Way ANOVA multiple comparison (* $P \leq 0.05$)

Figure 5. 5: Adult Trib1 KO mice have increased levels of plasma total cholesterol, non-HDL cholesterol and ALTs.

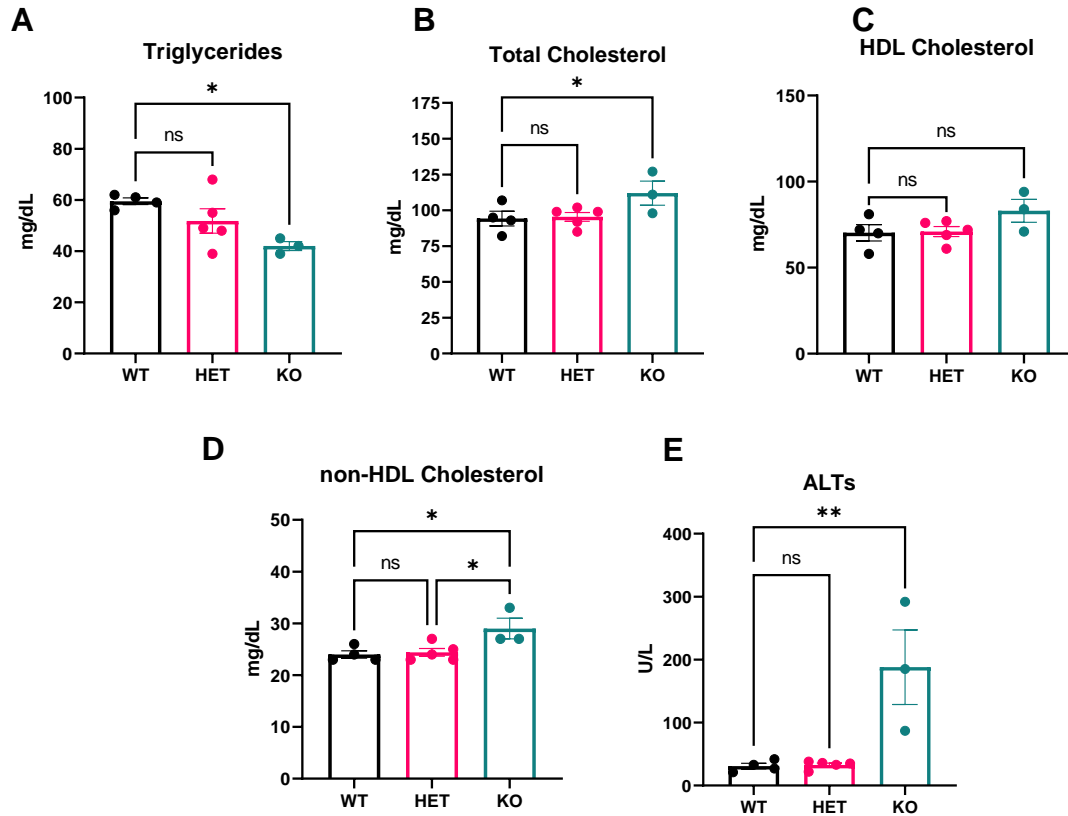


Figure 5.5: A-E. Plasma triglycerides, total cholesterol, HDL cholesterol, non-HDL cholesterol and ALTs in adult Trib1 WT, HET and KO mice after 4 hours fasting. Data indicate individual values with mean \pm s.e.m. Significance was determined by One-Way ANOVA multiple comparison (* $P \leq 0.05$, ** ≤ 0.01).

Figure 5. 6: Adult Trib1 KO mice have impaired postprandial triglyceride clearance.

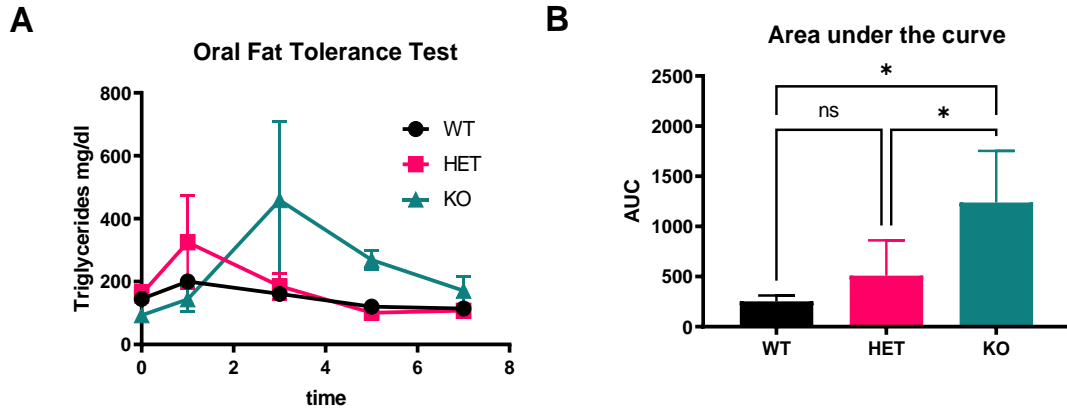


Figure 5.6: A. Oral fat tolerance test in adult Trib1 KO mice after overnight fasting. **B.** Area under the curve from A (n=3 WT, 4 HET, 2 KO). Data are expressed as mean \pm s.e.m for the experimental group. Significance was determined by One-Way ANOVA multiple comparison (* $P \leq 0.05$).

Figure 5. 7: Adult Trib1 KO mice have decreased fasting glucose and increased fasting lactate, with normal ketone levels.

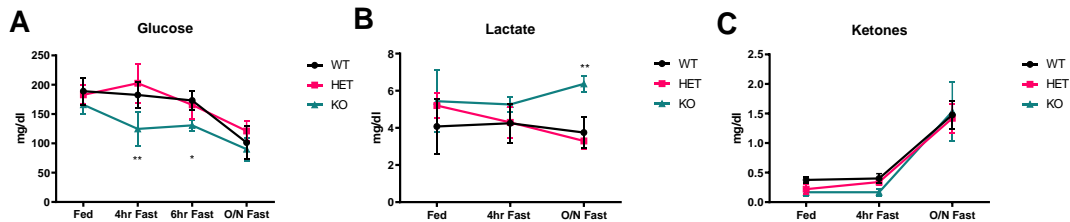


Figure 5.7: A-C. Plasma glucose, lactate and ketone levels at indicated fasting time in adult Trib1 KO mice compared to Trib1 WT and HET mice (n=5 WT, 5 HET, 3 KO). Data are expressed as mean \pm s.e.m for the experimental group. Significance was determined by Two-Way ANOVA multiple comparison (* $P \leq 0.05$, ** $P \leq 0.01$).

Figure 5. 8: Adult Trib1 KO mice have improved glucose and insulin tolerance.

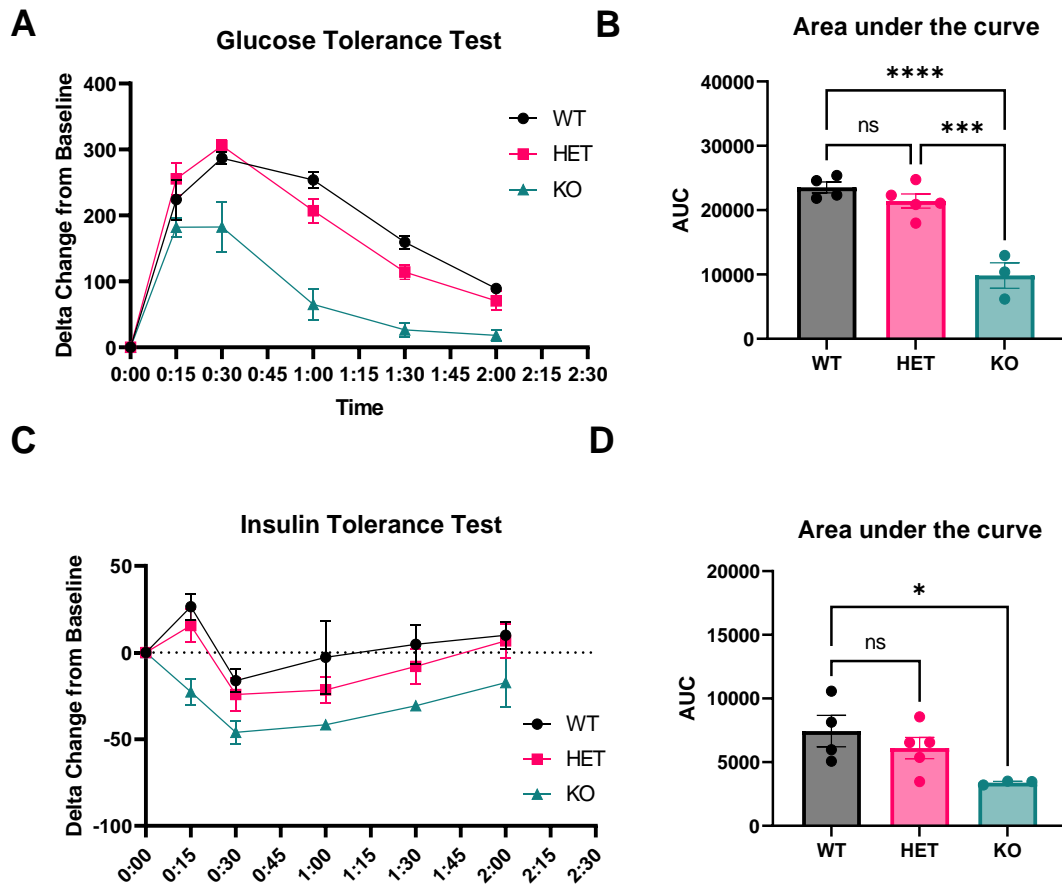


Figure 5.8: A-B. Glucose tolerance test in mice after overnight fasting (n= 4 WT, 4 HET and 3 KO). **C-D.** Insulin tolerance test in mice after 6 hours fasting (n= 4 WT, 4 HET and 3 KO). Data are expressed as mean \pm s.e.m for the experimental group. Significance was determined by One-Way ANOVA multiple comparison (* $P \leq 0.05$, *** $P \leq 0.001$, **** $P \leq 0.0001$).

Figure 5. 9: Hepatic deletion of Trib1 improves glucose tolerance with no changes in insulin tolerance.

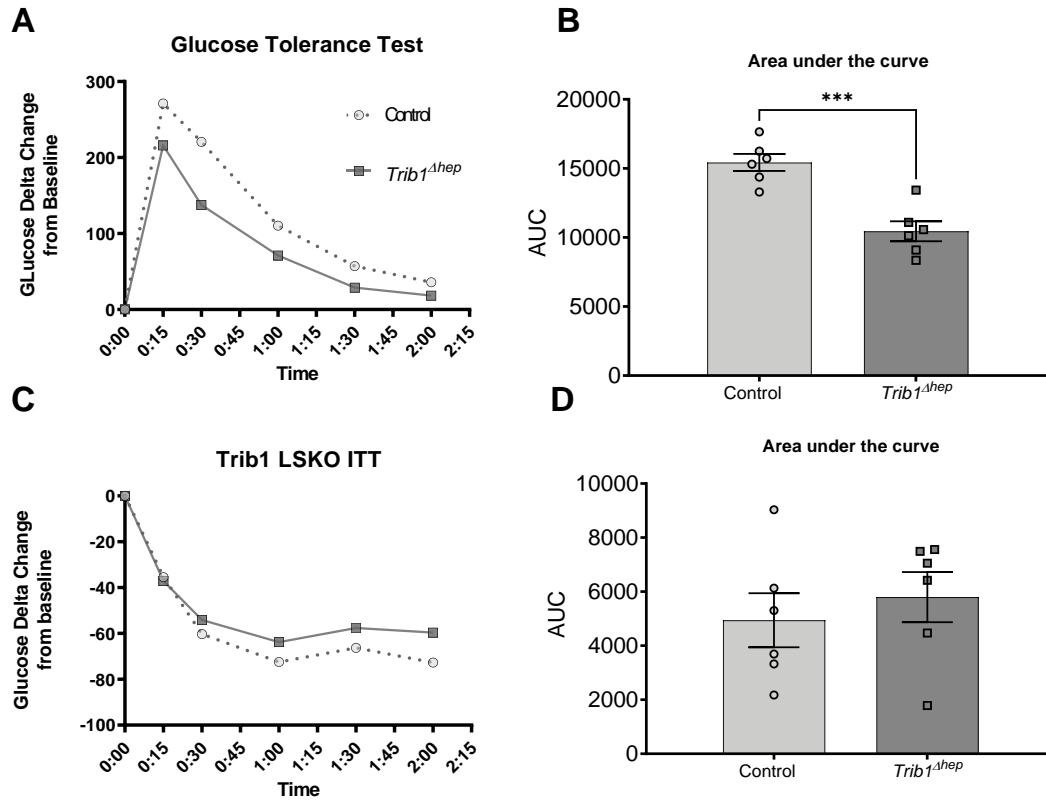


Figure 5.9: A-B. Glucose tolerance test in mice after overnight fasting (n= 6 each). **C-D.** Insulin tolerance test in mice after 6 hours fasting (n= 6 each). Data are expressed as mean \pm s.e.m for the experimental group. Significance was determined by One-Way ANOVA multiple comparison (* $P \leq 0.05$, *** $P \leq 0.001$, **** $P \leq 0.0001$).

Figure 5. 10: Hepatic gene expression in adult Trib1 KO mice.

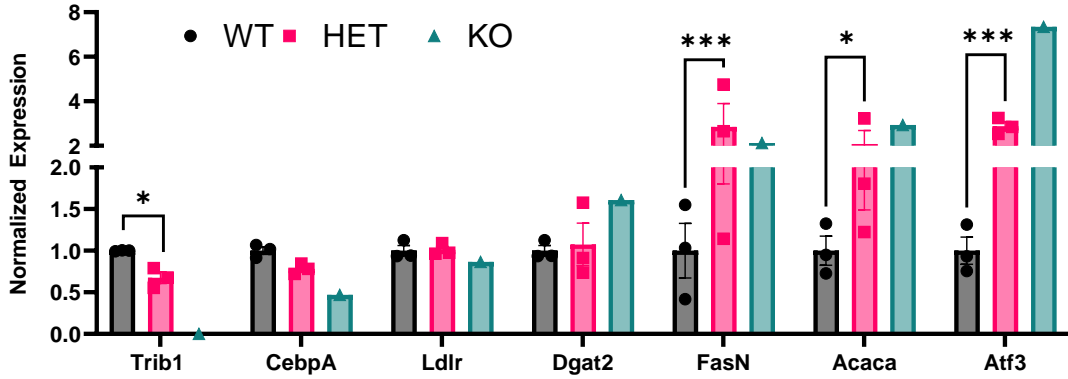


Figure 5.10: Hepatic transcript levels of *Trib1*, *Cebpa*, *Ldlr*, *Dgat2*, *FasN*, *Acaca* and *Atf3* in adult Trib1 KO mice (n=1), compared to wild type (n=3) and heterozygous mice (n=3). Data indicate individual values with mean \pm s.e.m. Significance was determined by Two-Way ANOVA multiple comparison (* $P \leq 0.05$, *** $P \leq 0.001$). No statistical significance was determined on *Trib1* KO mouse because of having only one mouse.

SUMMARY AND FUTURE DIRECTIONS

The goal of this dissertation was to functionally characterize the gene *TRIB1*, a GWAS locus that has been broadly associated with multiple cardiometabolic traits such as plasma triglycerides, total cholesterol, LDL cholesterol, HDL cholesterol and ALTs, as well as hepatic lipids and the development of hepatic steatosis. Lipids are essential to support life, as they accomplish a variety of biological functions such as energy storage, phospholipid bi-layer formation, signaling, and transport [1, 5]. However, their improper metabolism and accumulation could lead to the development of cardiovascular diseases with high rates of mortality [28, 85]. For this reason, it is crucial to understand all the genetic players and mechanisms that regulate plasma lipid metabolism, which could lead to the development of improved treatments for disease.

The *TRIB1* gene was one of the first novel genes identified by GWAS studies to be involved in the regulation of plasma lipids and cardiovascular disease traits [69, 79]. The *Tribbles* gene was originally identified in *Drosophila melanogaster* as a regulator of cell division and cell migration, and since its original discovery 3 human homologs have been described (*TRIB1 1-3*) [88, 89, 91]. Prior to GWAS association of *TRIB1* with plasma lipid metabolism, most of the studies for this family members were aimed to determine their function on myeloid cell development through the interactions of their C terminal binding domains (COP1 and MEK1) with other proteins such as CEBPa, which has shown that these proteins serve as signal transduction modulators and to target other proteins for degradation and proteasomal degradation [92, 93, 100-102, 112, 203].

Previous work from our laboratory was focused on validating the *TRIB1* association with plasma lipids, as well as investigating possible mechanism of action using different mouse

models. Our group was the first one to determine that *Trib1* overexpression in mice reduces plasma lipids, hepatic *de novo* lipogenesis and VLDL secretion and conversely, *Trib1* hepatic deletion in mice increases plasma lipids, hepatic fat and *de novo* lipogenesis [104, 125]. It was also demonstrated that *Trib1* effect on hepatic lipogenesis and hepatic lipids was mediated through an increase in CEBPa protein [104], however CEBPa involvement in regulating plasma lipids was not explored. Additionally, more questions regarding what other physiological mechanism of plasma lipid regulation, *TRIB1* could be affecting remained unanswered.

The first goal of my dissertation was to explore possible physiological mechanisms by which hepatic *TRIB1* regulates plasma lipids. Using a *Trib1* hepatocyte-specific knockout model, I confirmed the previously published increased total cholesterol, HDL cholesterol and non-HDL cholesterol in mice and demonstrated that challenging these mice with WTD (high fat, high carbohydrate) further exacerbated these phenotypes (Figure 3.2). However, we were not able to observe changes in plasma triglyceride levels in any of the diets, a phenotype that has been previously reported. Our results did suggest that *Trib1*^{Δhep} mice accumulate total cholesterol and triglycerides on the LDL lipoprotein fractions, and that they have increased apoB protein levels, the main apolipoprotein in LDL (Figures 3.4-3.6). Our studies also demonstrated that hepatic deletion of *Trib1* in mice impairs postprandial lipemia, which is likely leading to accumulation of triglycerides in the LDL lipoprotein fractions, and that the accumulation of total cholesterol in the LDL lipoprotein fractions *Trib1*^{Δhep} mice is due to the improper catabolism of LDL and VLDL lipoproteins due to a decrease of the *Ldlr* mRNA and protein levels (Figures 3.8-3.11). I further explore the effects of hepatic *trib1* on plasma lipids using an *Ldlr* KO mouse model and I demonstrated

that hepatic *Trib1* is able to regulate the clearance of apoB containing lipoproteins through its regulation of LDLR, but that steady state plasma lipids are regulated independently of the LDLR, specifically through the secretion of apoB containing lipoproteins from the liver (Figures 3.12-3.14).

The results from our newly synthesized apoB secretion studies showed that *Trib1*^{Δ*hep*} mice have increased secretion of apoB containing lipoproteins with no changes in triglyceride secretion, which suggest that hepatic deletion of *Trib1* leads to the secretion of triglyceride depleted apoB containing lipoproteins (Figure 3.14). This is a novel finding that has not been previously reported in any model study for hepatic lipoprotein secretion. Usually, an increased secretion in apoB protein is accompanied by increased triglyceride secretion, or there is increased triglyceride secretion with no changes in apoB protein, which means that the lipoproteins secreted are lipid rich [147]. This is because the secretion of VLDL-apoB from the liver is a tightly regulated process by the Endoplasmic-reticulum-associated protein degradation (ERAD) complex, which targets improperly folded or improperly lipidated apoB proteins for ubiquitination and proteasomal degradation [204]. My data shows that *Trib1*^{Δ*hep*} mice have increased levels of triglycerides in their hepatocytes, however this triglyceride is not being incorporated into the newly formed VLDL particles (Figures 3.7, 3.14).

The findings from these studies are fascinating and future studies will aim to elucidate the mechanisms that lead to these phenotypes. Because the ER stress response is highly important in the regulation of VLDL-apoB secretion, I measured for changes in ER stress markers such as pEF2a and observed that this was increased in *Trib1*^{Δ*hep*} mice. It is possible that changes in the increased hepatic lipogenesis and hepatic steatosis

development in *Trib1*^{Δ_{hep}} mice are causing increased ER stress, which has been shown to affect the rates of lipoprotein secretion from the liver [147], however, more studies would be necessary to determine the mechanism of this effect and what other genes might be involved in this regulation. Additionally, the development of hepatic steatosis mediated by *Trib1* deletion is a process that has not been fully studied. Increased CEBPα protein in *Trib1*^{Δ_{hep}} mice leads to increase de novo lipogenesis and increased liver lipids, however, other players might be affecting this phenotype but have not been fully described in *in vivo* models. Some examples previously mentioned included HNF4a, SIN3A and ERK1/2 [132, 133, 136, 137] and elucidating the molecular mechanisms by *TRIB1* is regulating these genes *in vivo* and their effects on plasma lipids and cardiovascular disease, will further share light into all the potential mechanism by which *TRIB1* is regulating multiple cardiometabolic traits.

My experiments in *Trib1*^{Δ_{hep}} mice also revealed that they are resistant to diet induced obesity even though they develop hyperlipidemia (Figure 3.7). Previous research has suggested that reduced expression of *Trib1* in white adipose tissue (WAT), leads impaired cytokine gene expression which protects the mice from weight gain and adiposity when fed a high fat diet [149], however the effects of hepatocyte specific *Trib1* deletion on obesity are novel. It is crucial to determine the effects of hepatic *Trib1* deletion on cytokine expression and inflammation, which could help determining the mechanism by which these mice are resistant to diet induced obesity, as well as it could help explain the mechanism by which hepatic deletion of *Trib1* leads to the development of hepatic steatosis, a disease that is characterized by inflammatory responses and cytokine release. If changes in inflammatory responses and cytokine release are not responsible for the

differences in body weight in response to diet in *Trib1^{Δhep}* mice, it is possible that these phenotypes are caused by different patterns of food consumption or energy expenditure in these mice, which could be determined by performing *in vivo* behavioral and metabolic experiments in these mice. These experiments will help determine if *Trib1^{Δhep}* mice are consuming less food or if they are having the same nutrient intake, but expend more energy compared to control mice.

Overall, the main next question resulting from our studies was determining the molecular mechanism by which hepatic *Trib1* regulates the *LDLR*. Because *Trib1* has an established role in regulating the transcription factor CEBPa by targeting it for ubiquitination and proteasomal degradation, we decided to explore if *Trib1* effects on plasma lipids and *LDLR* regulation are mediated dependently or independently of CEBPa regulation. To do this, we crossed our *Trib1^{flox;flox}* mice to an *Cebpa^{flox;flox}* with the goal of creating a double knockout mouse after injection with AAV-CRE (*Trib1^{Δhep};Cebpa^{Δhep}*/DKO mice). The results from my studies showed that simultaneous deletion of *Cebpa* in *Trib1^{Δhep}* mice eliminated the effects of hepatic deletion of *Trib1* on plasma lipids, hepatic lipids, ALTs, triglyceride catabolism, apoB catabolism and hepatic *LDLR* regulation, suggesting that increased CEBPa protein is necessary for the effects of hepatic *Trib1* deletion (Figures 4.2-4.6). We also identified the Activating Transcription Factor 3 (*Atf3*) as a possible target mediating *Trib1*'s CEBPa dependent regulation of the *LDLR* (Figures 4.9, 4.11-4.12). ATF3 is a stress-inducible transcriptional repressor that has been shown to interact with the promoter region of *LDLR* and represses its expression; furthermore, ATF3 directly binds to the CEBPA protein [164, 166, 167]. Our RNA sequencing analysis showed that ATF3 was highly upregulated in the livers of *Trib1^{Δhep}* but not in DKO mice, which was confirmed

by qPCR and western blot (Figure 4.11). We also demonstrated that downregulating *Atf3* in *Trib1^{Δhep}* mice reduced the levels of total cholesterol, HDL- cholesterol and LDL- cholesterol, and partially attenuated the effects on the LDLR (Figures 4.13-4.16).

The results from these studies suggested a partial effect of ATF3 downregulation mediating a decrease in plasma lipids and increased LDLR protein, which might be due to several reasons. We performed this siRNA knockdown pilot experiment once using the highest dose recommended by the manufacturer, however *Atf3* mRNA expression and protein levels were not fully knockdown (Figure 4.13), suggesting we might need a higher dose to achieve proper knockdown and observe more striking phenotypes. Additionally, we could acquire an *Atf3* knockout mice line and cross it to our *Trib1^{flox;flox}* mice, which will ensure complete lack of expression of *Atf3*. In both models, it would be crucial to perform oral fat tolerance test, LDL and VLDL apoB kinetics and apoB secretion studies, which would give us more concise answers as to what is the involvement of *Atf3* in the regulation of plasma lipids and LDLR in *Trib1^{Δhep}* mice. It is also possible that *Atf3* itself is not the only factor contributing to *Trib1* regulation of plasma lipid and the LDLR in a CEBPa dependent manner, and that other factors are also involved in this regulation. If that is the case, we will use the results from our RNA sequencing experiments for further identify other mechanistic links by which hepatic *Trib1* deletion is leading to the regulation of apoB catabolism and the LDLR.

In these studies, I also compared our results to *Cebpa^{Δhep}* mice, which showed that *Cebpa* deletion by itself decreases plasma lipids and plasma LDL in the cholesterol and triglycerides fractions, had improved triglyceride clearance after fat load and had no differences in VLDL or LDL apoB clearance (Figures 4.2- 4.6). These results confirm the

fact that *Cebpa* is highly involved in the regulation of plasma lipids and provide us with a model for further studying *Cebpa* hepatic deletion effects independently of its *Trib1* regulation.

The third goal of this dissertation was to explore the physiological mechanism by which *Trib1* whole body deletion on a pure C57BL/6 background leads to a highly penetrant lethal phenotype in mice. Our studies determined that *Trib1* KO mice develop normally in uterus and that the period of lethality was post-natal, between day 0 and day 1 after birth, likely due to severely low blood glucose levels compared to control mice. The decrease in glucose levels was accompanied by decrease glycogen and lactate levels, both of which are substrates for glucose production by glycogenolysis and gluconeogenesis, respectively (Figures 5.1- 5.2). *Cebpa* deficient mice die postnatally due to severely low levels of hepatic glycogen [127], so it is possible that the decreased in hepatic glycogen combined with decreased plasma lactate are causing or contributing to the severe hypoglycemic phenotype in *Trib1* KO neonates. In the future we will be performing glycogen staining in the livers of *Trib1* KO neonate mice to further characterize this phenotype, if the changes are drastically different comparing *Trib1* KO mice to control and het mice, it is likely that this might explain the severe hypoglycemia in *Trib1* KO mice. If we don't observed differences in hepatic glycogen content, we would consider measuring plasma insulin levels again in these mice, as it has been broadly demonstrated that high levels of insulin (hyperinsulinemia) can lead to severe hypoglycemia and neonatal death [202, 205-209]. In our studies we also determined that about 5% of *Trib1* KO mouse survive the neonatal lethally period and make it to adulthood, and that similar to *Trib1*^{hep} mice, adult *Trib1* KO have increased plasma lipids and impaired postprandial lipemia

(Figures 5.5-5.6). I also demonstrated that *Trib1* KO mice have decreased glucose levels depending on their fasting time, and that their glucose and insulin tolerance is improved compared to wild type and heterozygous mice (Figures 5.7- 5.8). *Trib1*^{hep} mice also had improved glucose tolerance with no changes in insulin tolerance (Figure 5.9).

The results from these studies suggest that additional to regulating plasma lipids, *Trib1* is involved in the regulation of glucose metabolism, an association that has not been previously reported. In humans, cardiovascular diseases and high concentration of lipids are associated/correlated with the development of type 2 diabetes (T2D), which is characterized by increased plasma glucose levels due to decrease insulin or impaired insulin sensitivity [210]. Our results showed that even though *Trib1* KO mice are characterized by increased lipids, their glucose and insulin tolerance is improved, which are phenotypes that are protective against the development of T2D in humans. These findings are striking and present a novel association of *Trib1* with another cardiometabolic trait associated with disease. To determining the molecular mechanisms by which *Trib1* is regulating glucose metabolism genes, we should perform RNA sequencing studies in tissues such as the liver and pancreas from these mice, both of which are critical in the regulation of plasma glucose in mammals. The results from these studies will provide with an array of unbiased targets which could explain how *Trib1* deletion is leading to changes in glucose metabolism and neonatal lethality in mice.

In summary, I have shown that *Trib1* plays a crucial role mediating the regulation of multiple physiological pathways that regulate plasma lipid metabolism, all of which are associated with the development of cardiometabolic disease. Additionally, my studies have opened future paths of investigation of *Trib1* and other novel cardiometabolic traits

such glucose metabolism and T2D, both of which have not been previously described. Overall, the results from my studies highlight the fact GWAS findings combined with experimental validation can lead to novel biological insights and better understanding of how natural genetic variation can impact human disease.

APPENDIX

Hepatocyte deletion of *Trib1* leads to the plasma secretion of an unidentified protein of approximately 20 kDA.

While performing the newly synthesized apoB secretion experiments, I discovered that plasma from *Trib1*^{Δ_{hep}} mice contains a prominent protein band visible by autoradiography between the molecular weight markers of 15-25kD (Figure 6.1 A). The relative abundance of this protein was significantly higher in *Trib1*^{Δ_{hep}} plasma compared to control mice (Figure 6.1 B). Additionally, this unidentified protein was visible by Ponceau S staining in plasma from 4 hour-fasted *Trib1*^{Δ_{hep}} mice, but was very minimally or not expressed in control mice (Figure 6.1 C). To further investigate the identity and possible role of this protein with *Trib1* effects on plasma lipids, we performed Mass Spectrometry on the bands of interest. We submitted a Coomassie stained gel containing Control and *Trib1*^{Δ_{hep}} samples loaded in equal volumes (Figure 6.1 D) and tested one sample of each condition as an initial exploratory approach. Interestingly, the assay identified 116 proteins in samples from control and 126 proteins in samples from *Trib1*^{Δ_{hep}} mice (Figure 6.1 E), with not all of them matching the size range of the visualized protein bands. We identified 23 proteins that were approximately the same molecular weight as the visualized bands, and that were more abundant in *Trib1*^{Δ_{hep}} mice (Table 3). A pivotal result from this pilot study was the increased abundance of the Mayor Urinary Protein (MUPs) family, specifically MUP 1, 2, 3 AND 17. More interesting, several MUPs family members are also increased at the mRNA level in *Trib1*^{Δ_{hep}} mice based on the RNA Seq data, including *Mup* 2, 6, 8, 9, 17 and others. MUPs are a subfamily of proteins synthesized in the liver, secreted through the

kidneys, and excreted in urine [211, 212]. MUPS are present in many species, however they are not conserved in humans, which presents a challenge in translating these findings to any human disease significance [213].

Another limitation of this study is that the results are based on a pilot study from only one sample. We would need to repeat this study with additional biological replicates to confirm the results and to gain more confidence in the possible identity of the protein. Another way of reducing nonspecific detection of proteins is to use depletion columns for highly expressed plasma proteins such as Albumin and IgGs. This will ensure higher detection of smaller, lower expressed proteins. In the case that we identify other highly represented proteins, or that MUPs are still the most represented upregulated proteins, follow up studies would be necessary to corroborate their identity, such as western blots.

To investigate the relevance of this unidentified protein in humans, we could acquire plasma samples from human carriers of *TRIB1* mutations and perform Coomassie staining as I did for the mouse samples. In the case that this band is also present in human samples, it would suggest that the protein is not a MUP and that it might be biologically important in the regulation of lipids in humans too. These samples could also be used for mass spectrometry as well proteomic analysis with the goal of identifying the specific protein of interest.

Figure 6. 1. Trib1^{Δhep} mice secrete an unidentified protein of around 15-25 kDa.

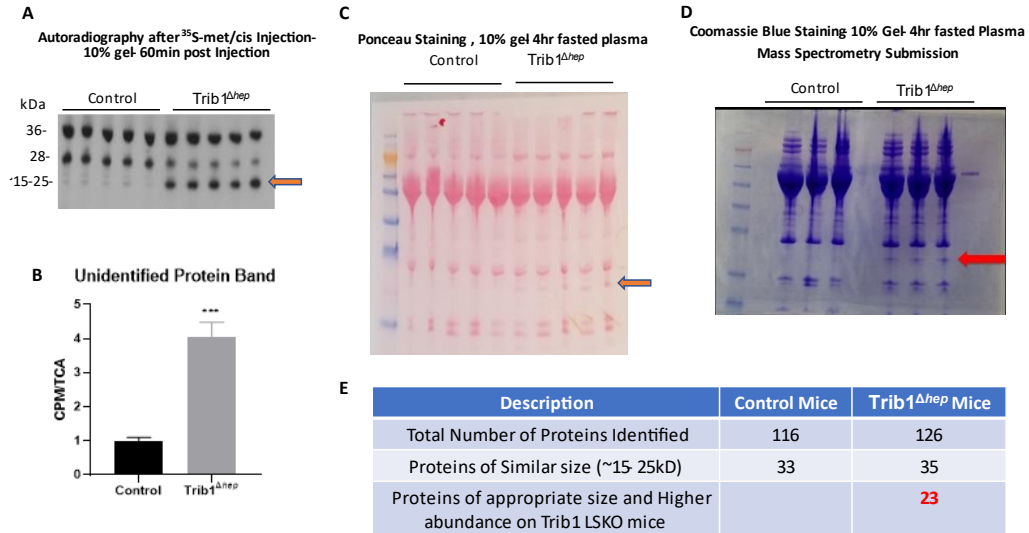


Figure 6.1: A. Autoradiography of plasma from *Trib1^{Δhep}* and control mice 60 minutes after injection with ³⁵S-met/cis and pluronic injection. **B.** Quantification of an unidentified protein counts normalized to total precipitable protein count. **C.** Ponceu staining of 4hr fasted plasma from *Trib1^{Δhep}* and control mice. **D.** Coomassie blue staining of 4hr fasted plasma from *Trib1^{Δhep}* and control mice of samples that were submitted for mass spectrometry analysis. **E.** summary table of mass spectrometry results analysis.

Table 3. Selected mass spectrometry results based on the size of the unidentified protein band and higher abundance on Trib1^{Δhep} vs control mice

Protein	MW kDa	Coverage %	Abundance - Control	Abundance - Trib1 LSKO	Relative Abundance- Trib1 LSKO/Control
Mucin-like protein 2	14.8	9	9933	76938	7.7
Serum amyloid A-4 protein	15.1	27	3384727	5102911	1.5
Ig heavy chain V region 93G7	15.5	10	93191	129524	1.4
Transthyretin	15.8	41	190931699	315554829	1.7
Lysozyme c-1	16.8	8	243167	309396	1.3
Immunoglobulin J chain	18	21	2467437	32156859	13.0
cathelicidin antimicrobial peptide	19.4	22	202945	490280	2.4
Actin-related protein 2/3 complex subunit 4	19.7	14	664496	1139557	1.7
Major urinary protein 1	20.6	67	60925563	324867934	5.3
Major urinary protein 17	20.6	16	16813090	132962899	7.9
Major urinary protein 2	20.7	73	231285	2307170	10.0
Cerebellin-1	21.1	4	189533	449446	2.4
apolipoprotein M	21.3	36	38194963	50579485	1.3
Major urinary protein 3	21.5	11	156851	546053	3.5

Angiopoietin-like protein 8	22.1	5	0	34584	100.0
Receptor expression-enhancing protein 6	22.2	6	0	34542	100.0
Secreted phosphoprotein 24	23.1	6	116479	464715	4.0
Retinol-binding protein 4	23.2	37	121482728	272297637	2.2
Alpha-1-acid glycoprotein 3	24.1	10	0	196940	100.0
BPI fold-containing family A member 2	24.7	6	29887	161626	5.4
Glutathione peroxidase 3	25.4	21	1034408	4396303	4.3
Proteasome subunit beta type-6	25.4	5	11754	589704	50.2
Complement C1q subcomponent subunit A	26	6	47896	92993	1.9

BIBLIOGRAPHY

1. Griffin, B.A., *Lipid metabolism*. 2013, Elsevier Ltd. p. 267-272.
2. Spector, A.A., *Plasma lipid transport*. Clin Physiol Biochem, 1984. **2**(2-3): p. 123-34.
3. Goldstein, J.L. and M.S. Brown, *The LDL receptor*. Arteriosclerosis, thrombosis, and vascular biology, 2009. **29**(4): p. 431-438.
4. Goldstein, J.L., M.S. Brown, and N.J. Stone, *Genetics of the LDL receptor: Evidence that the mutations affecting binding and internalization are allelic*. Cell, 1977. **12**(3): p. 629-641.
5. Feingold, K.R. and C. Grunfeld, *Introduction to Lipids and Lipoproteins*. 2000: MDTText.com, Inc.
6. Mahley, R.W., et al., *Plasma lipoproteins: apolipoprotein structure and function*. J Lipid Res, 1984. **25**(12): p. 1277-94.
7. Desvergne, B., L. Michalik, and W. Wahli, *Transcriptional Regulation of Metabolism*. the american physiological society, 2006: p. 465-514.
8. Virani, S.S., et al., *Heart Disease and Stroke Statistics—2021 Update*. Circulation, 2021. **143**(8): p. e254-e743.
9. *Coronary Artery Disease: Causes, Diagonosis & Prevention* | cdc.gov.
10. Liu, M., et al., *Hepatic ABCA1 and VLDL triglyceride production*. Biochimica et biophysica acta, 2012. **1821**(5): p. 770-777.
11. Hooper, A.J., J.R. Burnett, and G.F. Watts, *Contemporary aspects of the biology and therapeutic regulation of the microsomal triglyceride transfer protein*. Circ Res, 2015. **116**(1): p. 193-205.
12. Reiner, Ž., *Hypertriglyceridaemia and risk of coronary artery disease*. Nature Reviews Cardiology, 2017. **14**(7): p. 401-411.
13. Borén, J., et al., *The molecular mechanism for the genetic disorder familial defective apolipoprotein B100*. J Biol Chem, 2001. **276**(12): p. 9214-8.
14. Whitfield, A.J., et al., *Four novel mutations in APOB causing heterozygous and homozygous familial hypobetalipoproteinemia*. Hum Mutat, 2003. **22**(2): p. 178.
15. Olivecrona, G., *Role of lipoprotein lipase in lipid metabolism*. Curr Opin Lipidol, 2016. **27**(3): p. 233-41.
16. Zechner, R., et al., *The role of lipoprotein lipase in adipose tissue development and metabolism*. International journal of obesity and related metabolic disorders : journal of the International Association for the Study of Obesity, 2000. **24 Suppl 4**: p. S53-S56.
17. Mead, J.R., S.A. Irvine, and D.P. Ramji, *Lipoprotein lipase: Structure, function, regulation, and role in disease*. Journal of Molecular Medicine, 2002. **80**(12): p. 753-769.
18. Lun, Y., et al., *Severe hypertriglyceridemia due to two novel loss-of-function lipoprotein lipase gene mutations (C310R/E396V) in a Chinese family associated with recurrent acute pancreatitis*. Oncotarget, 2017. **8**(29): p. 47741-47754.
19. Breckenridge, W.C., et al., *Hypertriglyceridemia associated with deficiency of apolipoprotein C-II*. N Engl J Med, 1978. **298**(23): p. 1265-73.

20. Priore Oliva, C., et al., *Inherited apolipoprotein A-V deficiency in severe hypertriglyceridemia*. *Arterioscler Thromb Vasc Biol*, 2005. **25**(2): p. 411-7.
21. Zhang, R., *The ANGPTL3-4-8 model, a molecular mechanism for triglyceride trafficking*. *Open Biology*, 2016. **6**(4): p. 150272-150272.
22. Larsson, M., et al., *Apolipoprotein C-III inhibits triglyceride hydrolysis by GPIIIBP1-bound LPL*. *Journal of lipid research*, 2017. **58**(9): p. 1893-1902.
23. Dijk, W. and S. Kersten, *Regulation of lipid metabolism by angiotensin-like proteins*. *Curr Opin Lipidol*, 2016. **27**(3): p. 249-56.
24. Pollin, T.I., et al., *A null mutation in human APOC3 confers a favorable plasma lipid profile and apparent cardioprotection*. *Science (New York, N.Y.)*, 2008. **322**(5908): p. 1702-1705.
25. Romeo, S., et al., *Rare loss-of-function mutations in ANGPTL family members contribute to plasma triglyceride levels in humans*. *J Clin Invest*, 2009. **119**(1): p. 70-9.
26. Mahley, R.W., *Apolipoprotein E: from cardiovascular disease to neurodegenerative disorders*. *Journal of molecular medicine (Berlin, Germany)*, 2016. **94**(7): p. 739-746.
27. van de Sluis, B., M. Wijers, and J. Herz, *News on the molecular regulation and function of hepatic low-density lipoprotein receptor and LDLR-related protein 1*. *Current opinion in lipidology*, 2017. **28**(3): p. 241-247.
28. Castelli, W.P., et al., *Lipids and risk of coronary heart disease. The Framingham Study*. *Ann Epidemiol*, 1992. **2**(1-2): p. 23-8.
29. Benjamin, E.J., et al., *Heart Disease and Stroke Statistics-2019 Update: A Report From the American Heart Association*. *Circulation*, 2019. **139**(10): p. e56-e66.
30. Ivanova, E.A., et al., *Small Dense Low-Density Lipoprotein as Biomarker for Atherosclerotic Diseases*. *Oxid Med Cell Longev*, 2017. **2017**: p. 1273042.
31. Hansson, G.K., *Inflammation, Atherosclerosis, and Coronary Artery Disease*. *n engl j med*, 2005. **352**16(21).
32. Meeusen, J.W., L.J. Donato, and A.S. Jaffe, *Lipid Biomarkers for Risk Assessment in Acute Coronary Syndromes*. *Current Cardiology Reports*, 2017. **19**(6): p. 48-48.
33. Bentzon, J.F., et al., *Mechanisms of plaque formation and rupture*. *Circulation Research*, 2014. **114**(12): p. 1852-1866.
34. Gu, H.-M. and D.-W. Zhang, *Hypercholesterolemia, low density lipoprotein receptor and proprotein convertase subtilisin/kexin-type 9*. *Journal of biomedical research*, 2015. **29**(5): p. 356-361.
35. Brown, M.S. and J.L. Goldstein, *The SREBP Pathway: Regulation Review of Cholesterol Metabolism by Proteolysis of a Membrane-Bound Transcription Factor*. 1997. p. 331-340.
36. Horton, J.D., J.L. Goldstein, and M.S. Brown, *SREBPs: activators of the complete program of cholesterol and fatty acid synthesis in the liver*. *The Journal of clinical investigation*, 2002. **109**(9): p. 1125-1131.
37. Scotti, E., et al., *IDOL Stimulates Clathrin-Independent Endocytosis and Multivesicular Body-Mediated Lysosomal Degradation of the Low-Density Lipoprotein Receptor*. *Molecular and Cellular Biology*, 2013. **33**(8): p. 1503-1514.
38. Sorrentino, V., et al., *The LXR-IDOL axis defines a clathrin-, caveolae-, and dynamin-independent endocytic route for LDLR internalization and lysosomal degradation*. *J Lipid Res*, 2013. **54**(8): p. 2174-2184.

39. Lagace, T.A., *PCSK9 and LDLR degradation: Regulatory mechanisms in circulation and in cells*. 2014, Lippincott Williams and Wilkins. p. 387-393.
40. Zhao, Z., et al., *Molecular characterization of loss-of-function mutations in PCSK9 and identification of a compound heterozygote*. American journal of human genetics, 2006. **79**(3): p. 514-523.
41. DuBroff, R. and M. de Lorgeril, *Cholesterol confusion and statin controversy*. World journal of cardiology, 2015. **7**(7): p. 404-409.
42. Sirtori, C.R., *The pharmacology of statins*. Pharmacological Research, 2014. **88**: p. 3-11.
43. Nissen, S.E., et al., *Statin Therapy, LDL Cholesterol, C-Reactive Protein, and Coronary Artery Disease*. New England Journal of Medicine, 2005. **352**(1): p. 29-38.
44. Stancu, C. and A. Sima, *Statins: Mechanism of action and effects*. Journal of Cellular and Molecular Medicine, 2001. **5**(4): p. 378-387.
45. Ward, N.C., G.F. Watts, and R.H. Eckel, *Statin Toxicity*. Circulation Research, 2019. **124**(2): p. 328-350.
46. Ward, N.C., G.F. Watts, and R.H. Eckel, *Statin Toxicity: Mechanistic Insights and Clinical Implications*. 2019, Lippincott Williams and Wilkins. p. 328-350.
47. Thompson, P.D., et al., *Statin-associated side effects*. 2016, Elsevier USA. p. 2395-2410.
48. Hussain, M.M., *Intestinal lipid absorption and lipoprotein formation*. Current opinion in lipidology, 2014. **25**(3): p. 200-206.
49. Kindel, T., D.M. Lee, and P. Tso, *The mechanism of the formation and secretion of chylomicrons*. Atheroscler Suppl, 2010. **11**(1): p. 11-6.
50. Blanc, V. and N.O. Davidson, *Mouse and other rodent models of C to U RNA editing*. Methods in molecular biology (Clifton, N.J.), 2011. **718**: p. 121-135.
51. Greeve, J., et al., *Apolipoprotein B mRNA editing in 12 different mammalian species: hepatic expression is reflected in low concentrations of apoB-containing plasma lipoproteins*. J Lipid Res, 1993. **34**(8): p. 1367-83.
52. Wang, H. and R.H. Eckel, *Lipoprotein lipase: from gene to obesity*. Am J Physiol Endocrinol Metab, 2009. **297**(2): p. E271-88.
53. Kypreos, K.E. and V.I. Zannis, *LDL receptor deficiency or apoE mutations prevent remnant clearance and induce hypertriglyceridemia in mice*. Journal of Lipid Research, 2006. **47**(3): p. 521-529.
54. Castro-Orós, I.D., et al., *Common Genetic Variants Contribute to Primary Hypertriglyceridemia Without Differences Between Familial Combined Hyperlipidemia and Isolated Hypertriglyceridemia*. Circulation: Cardiovascular Genetics, 2014. **7**(6): p. 814-821.
55. Wang, S. and J.D. Smith, *ABCA1 and nascent HDL biogenesis*. BioFactors (Oxford, England), 2014. **40**(6): p. 547-554.
56. Smith, J.D., et al., *ABCA1 mediates concurrent cholesterol and phospholipid efflux to apolipoprotein A-I*. J Lipid Res, 2004. **45**(4): p. 635-44.
57. Brunham, L.R., et al., *Clinical, Biochemical, and Molecular Characterization of Novel Mutations in ABCA1 in Families with Tangier Disease*. JIMD reports, 2015. **18**: p. 51-62.
58. Jiang, X.-C., W. Jin, and M.M. Hussain, *The impact of phospholipid transfer protein (PLTP) on lipoprotein metabolism*. Nutrition & Metabolism, 2012. **9**(1): p. 75.

59. Ossoli, A., et al., *Role of LCAT in Atherosclerosis*. J Atheroscler Thromb, 2016. **23**(2): p. 119-27.
60. McIntyre, N., *Familial LCAT deficiency and fish-eye disease*. J Inherit Metab Dis, 1988. **11 Suppl 1**: p. 45-56.
61. Mabuchi, H., A. Nohara, and A. Inazu, *Cholesteryl ester transfer protein (CETP) deficiency and CETP inhibitors*. Molecules and cells, 2014. **37**(11): p. 777-784.
62. Acton, S., et al., *Identification of scavenger receptor SR-BI as a high density lipoprotein receptor*. Science, 1996. **271**(5248): p. 518-20.
63. Trigatti, B.L., M. Krieger, and A. Rigotti, *Influence of the HDL Receptor SR-BI on Lipoprotein Metabolism and Atherosclerosis*. Arteriosclerosis, Thrombosis, and Vascular Biology, 2003. **23**(10): p. 1732-1738.
64. Zwick, M.E., D.J. Cutler, and A. Chakravarti, *Patterns of genetic variation in Mendelian and complex traits*. Annu Rev Genomics Hum Genet, 2000. **1**: p. 387-407.
65. Visscher, P.M., et al., *10 Years of GWAS Discovery: Biology, Function, and Translation*. American Journal of Human Genetics, 2017. **101**(1): p. 5-22.
66. Frazer, K.A., et al., *Human genetic variation and its contribution to complex traits*. Nature Reviews Genetics, 2009. **10**(4): p. 241-251.
67. Bush, W.S. and J.H. Moore, *Chapter 11: Genome-wide association studies*. PLoS Comput Biol, 2012. **8**(12): p. e1002822.
68. Tam, V., et al., *Benefits and limitations of genome-wide association studies*. Nature Reviews Genetics, 2019. **20**(8): p. 467-484.
69. Teslovich, T.M., et al., *Biological, clinical and population relevance of 95 loci for blood lipids*. Nature, 2010. **466**(7307): p. 707-13.
70. Ioannidis, J.P., G. Thomas, and M.J. Daly, *Validating, augmenting and refining genome-wide association signals*. Nat Rev Genet, 2009. **10**(5): p. 318-29.
71. Korte, A. and A. Farlow, *The advantages and limitations of trait analysis with GWAS: a review*. Plant Methods, 2013. **9**(1): p. 29.
72. Edwards, A.O., et al., *Complement factor H polymorphism and age-related macular degeneration*. Science, 2005. **308**(5720): p. 421-4.
73. Katta, S., I. Kaur, and S. Chakrabarti, *The molecular genetic basis of age-related macular degeneration: an overview*. J Genet, 2009. **88**(4): p. 425-49.
74. Toomey, C.B., et al., *Regulation of age-related macular degeneration-like pathology by complement factor H*. Proceedings of the National Academy of Sciences of the United States of America, 2015. **112**(23): p. E3040-E3049.
75. Wellcome Trust Case Control, C., *Genome-wide association study of 14,000 cases of seven common diseases and 3,000 shared controls*. Nature, 2007. **447**(7145): p. 661-678.
76. Rioux, J.D., et al., *Genome-wide association study identifies new susceptibility loci for Crohn disease and implicates autophagy in disease pathogenesis*. Nat Genet, 2007. **39**(5): p. 596-604.
77. Zhao, Y., et al., *Gain-of-Function Mutations of SLC16A11 Contribute to the Pathogenesis of Type 2 Diabetes*. Cell Reports, 2019. **26**(4): p. 884-892.e4.
78. Yang, X., et al., *Validation of candidate causal genes for obesity that affect shared metabolic pathways and networks*. Nature genetics, 2009. **41**(4): p. 415-423.

79. Kathiresan, S., et al., *Six new loci associated with blood low-density lipoprotein cholesterol, high-density lipoprotein cholesterol or triglycerides in humans*. Nature Genetics, 2008. **40**(2): p. 189-197.
80. Willer, C.J., et al., *Newly identified loci that influence lipid concentrations and risk of coronary artery disease*. Nature genetics, 2008. **40**(2): p. 161-9.
81. Klarin, D., et al., *Genetics of blood lipids among ~300,000 multi-ethnic participants of the Million Veteran Program*. Nature Genetics, 2018. **50**(11): p. 1514-1523.
82. Below, J.E., et al., *Meta-analysis of lipid-traits in Hispanics identifies novel loci, population-specific effects, and tissue-specific enrichment of eQTLs*. Scientific reports, 2016. **6**: p. 19429-19429.
83. Peloso, G.M., et al., *Association of low-frequency and rare coding-sequence variants with blood lipids and coronary heart disease in 56,000 whites and blacks*. American journal of human genetics, 2014. **94**(2): p. 223-232.
84. Chasman, D.I., et al., *Forty-three loci associated with plasma lipoprotein size, concentration, and cholesterol content in genome-wide analysis*. PLoS Genet, 2009. **5**(11): p. e1000730.
85. Asselbergs, F.W., et al., *Large-scale gene-centric meta-analysis across 32 studies identifies multiple lipid loci*. American journal of human genetics, 2012. **91**(5): p. 823-838.
86. Willer, C.J., et al., *Discovery and refinement of loci associated with lipid levels*. Nat Genet, 2013. **45**(11): p. 1274-1283.
87. Edgar, B.A., D.A. Lehman, and P.H. O'Farrell, *Transcriptional regulation of string (cdc25): a link between developmental programming and the cell cycle*. Development (Cambridge, England), 1994. **120**(11): p. 3131-3143.
88. Rg Großhans, J. and E. Wieschaus, *A Genetic Link between Morphogenesis and Cell Division during Formation of the Ventral Furrow in Drosophila*. Cell, 2000. **101**: p. 523-531.
89. Seher, T.C. and M. Leptin, *Tribbles, a cell-cycle brake that coordinates proliferation and morphogenesis during Drosophila gastrulation*. Current Biology, 2000. **10**(11): p. 623-629.
90. Gong, L., et al., *Drosophila ventral furrow morphogenesis: a proteomic analysis*. Development, 2004. **131**(3): p. 643-656.
91. Juan Mata, S.C.A.E.P.R., *Tribbles Coordinates Mitosis and Morphogenesis in Drosophila by Regulating String/CDC25 Proteolysis*. Cell, 2000. **101**: p. 511-522.
92. Foulkes, D.M., et al., *Tribbles pseudokinases: novel targets for chemical biology and drug discovery?* Biochemical Society transactions, 2015. **43**(5): p. 1095-103.
93. Evers, P.A., et al., *Tribbles in the 21st Century: The Evolving Roles of Tribbles Pseudokinases in Biology and Disease*. Trends in Cell Biology, 2016: p. 686-693.
94. Hegedus, Z., A. Czibula, and E. Kiss-Toth, *Tribbles: Novel regulators of cell function; evolutionary aspects*. 2006. p. 1632-1641.
95. Rechsteiner, M. and S.W. Rogers, *PEST sequences and regulation by proteolysis*. Trends Biochem Sci, 1996. **21**(7): p. 267-71.
96. Boudeau, J., et al., *Emerging roles of pseudokinases*. Trends Cell Biol, 2006. **16**(9): p. 443-52.
97. Richmond, L., et al., *Pseudokinases: a tribble-edged sword*.
98. Lohan, F. and K. Keeshan, *The functionally diverse roles of tribbles*. Biochemical Society Transactions, 2013. **41**(4).

99. Yokoyama, T., et al., *Trib1 links the MEK1/ERK pathway in myeloid leukemogenesis*. *Blood*, 2010. **116**(15): p. 2768-2775.
100. Dobens, L.L. and S. Bouyain, *Developmental roles of tribbles protein family members*. *Developmental Dynamics*, 2012. **241**(8): p. 1239-1248.
101. Dedhia, P.H., et al., *Differential ability of Tribbles family members to promote degradation of C/EBP α and induce acute myelogenous leukemia*. *Blood*, 2010. **116**(8): p. 1321-1328.
102. Murphy, J.M., et al., *Molecular Mechanism of CCAAT-Enhancer Binding Protein Recruitment by the TRIB1 Pseudokinase*. *Structure/Folding and Design*, 2015. **23**: p. 2111-2121.
103. Naiki, T., et al., *TRB2, a mouse tribbles ortholog, suppresses adipocyte differentiation by inhibiting AKT and C/EBP*. *Journal of Biological Chemistry*, 2007. **282**(33): p. 24075-24082.
104. Bauer, R.C., et al., *Tribbles-1 regulates hepatic lipogenesis through posttranscriptional regulation of C/EBP α* . *Journal of Clinical Investigation*, 2015. **125**(10): p. 3809-3818.
105. Wedel, A. and H.W. Lömsziegler-Heitbrock, *The C/EBP Family of Transcription Factors*. *Immunobiology*, 1995. **193**(2): p. 171-185.
106. Keeshan, K., et al., *Co-operative leukemogenesis in acute myeloid leukemia and acute promyelocytic leukemia reveals C/EBP?? as a common target of TRIB1 and PML/RARA*. *Haematologica*, 2016. **101**(10): p. 1228-1236.
107. Satoh, T., et al., *Critical role of Trib1 in differentiation of tissue-resident M2-like macrophages*. *Nature*, 2013. **495**(7442): p. 524-528.
108. Nakamura, T., *The role of Trib1 in myeloid leukaemogenesis and differentiation*. *Biochemical Society Transactions*, 2015. **43**(5).
109. Jakobsen, J.S., et al., *Mutant CEBPA directly drives the expression of the targetable tumor-promoting factor CD73 in AML*. *Science Advances*, 2019. **5**(7): p. eaaw4304.
110. Reckzeh, K. and J. Cammenga, *Molecular mechanisms underlying deregulation of C/EBP α in acute myeloid leukemia*. *International Journal of Hematology*, 2010. **91**(4): p. 557-568.
111. Hughes, J.M., et al., *C/EBP α -p30 protein induces expression of the oncogenic long non-coding RNA UCA1 in acute myeloid leukemia*. *Oncotarget*, 2015. **6**(21): p. 18534-18544.
112. Yoshida, A., et al., *COP1 targets C/EBP α for degradation and induces acute myeloid leukemia via Trib1*. *Blood*, 2013. **122**(10): p. 1750-60.
113. O'Connor, C., et al., *The presence of C/EBP α and its degradation are both required for TRIB2-mediated leukaemia*. *Oncogene*, 2016. **35**(40): p. 5272-5281.
114. Ashton-Chess, J., et al., *Tribbles-1 as a novel biomarker of chronic antibody-mediated rejection*. *Journal of the American Society of Nephrology : JASN*, 2008. **19**(6): p. 1116-1127.
115. O'Connor, C., et al., *Trib2 expression in granulocyte-monocyte progenitors drives a highly drug resistant acute myeloid leukaemia linked to elevated Bcl2*. *Oncotarget*, 2018. **9**(19): p. 14977-14992.
116. Ohoka, N., et al., *TRB3, a novel ER stress-inducible gene, is induced via ATF4-CHOP pathway and is involved in cell death*. *EMBO Journal*, 2005. **24**(6): p. 1243-1255.

117. Yamamoto, M., et al., *Enhanced TLR-mediated NF-IL6 dependent gene expression by Trib1 deficiency*. The Journal of experimental medicine, 2007. **204**(9): p. 2233-2239.
118. Aimé, P., et al., *Trib3 Is Elevated in Parkinson's Disease and Mediates Death in Parkinson's Disease Models*. J Neurosci, 2015. **35**(30): p. 10731-49.
119. Borsting, E., et al., *Tribbles Homolog 3 Attenuates Mammalian Target of Rapamycin Complex-2 Signaling and Inflammation in the Diabetic Kidney*. Journal of the American Society of Nephrology, 2014. **25**(9): p. 2067-2078.
120. Jadhav, K.S. and R.C. Bauer, *Trouble with Tribbles-1: Elucidating the Mechanism of a Genome-Wide Association Study Locus*. Arteriosclerosis, Thrombosis, and Vascular Biology, 2019. **39**(6): p. 998-1005.
121. Liu, Q., et al., *TRIB1 rs17321515 gene polymorphism increases the risk of coronary heart disease in general population and non-alcoholic fatty liver disease patients in Chinese Han population*. Lipids in Health and Disease, 2019. **18**(1): p. 165.
122. Liu, Q., et al., *TRIB1 rs17321515 and rs2954029 gene polymorphisms increase the risk of non-alcoholic fatty liver disease in Chinese Han population*. Lipids in Health and Disease, 2019. **18**(1).
123. Dastani, Z., et al., *Novel loci for adiponectin levels and their influence on type 2 diabetes and metabolic traits: A multi-ethnic meta-analysis of 45,891 individuals*. PLoS Genetics, 2012. **8**(3).
124. Chambers, J.C., et al., *Genome-wide association study identifies loci influencing concentrations of liver enzymes in plasma*. Nature Genetics, 2011. **43**(11): p. 1131-1138.
125. Burkhardt, R., et al., *Trib1 is a lipid- and myocardial infarction-associated gene that regulates hepatic lipogenesis and VLDL production in mice*. J Clin Invest, 2010. **120**(12): p. 4410-4.
126. Avellino, R., et al., *An autonomous CEBPA enhancer specific for myeloid-lineage priming and neutrophilic differentiation*. Blood, 2016. **127**(24): p. 2991-3003.
127. Wang, N.D., et al., *Impaired energy homeostasis in C/EBP alpha knockout mice*. Science, 1995. **269**(5227): p. 1108-12.
128. Olofsson, L.E., et al., *CCAAT/enhancer binding protein alpha (C/EBPα) in adipose tissue regulates genes in lipid and glucose metabolism and a genetic variation in C/EBPα is associated with serum levels of triglycerides*. Journal of Clinical Endocrinology and Metabolism, 2008. **93**(12): p. 4880-4886.
129. Pedersen, T.A., et al., *Distinct C/EBPα motifs regulate lipogenic and gluconeogenic gene expression in vivo*. The EMBO journal, 2007. **26**(4): p. 1081-1093.
130. Matsusue, K., et al., *Hepatic CCAAT/enhancer binding protein alpha mediates induction of lipogenesis and regulation of glucose homeostasis in leptin-deficient mice*. Mol Endocrinol, 2004. **18**(11): p. 2751-64.
131. Qiao, L., et al., *Knocking Down Liver CCAAT/Enhancer-Binding Protein α by Adenovirus-Transduced Silent Interfering Ribonucleic Acid Improves Hepatic Gluconeogenesis and Lipid Homeostasis in db/db Mice*. Endocrinology, 2006. **147**(6): p. 3060-3069.

132. Mauvoisin, D., et al., *Key role of the ERK1/2 MAPK pathway in the transcriptional regulation of the Stearoyl-CoA Desaturase (SCD1) gene expression in response to leptin*. *Mol Cell Endocrinol*, 2010. **319**(1-2): p. 116-28.
133. Tsai, J., et al., *MEK/ERK Inhibition Corrects the Defect in VLDL Assembly in HepG2 Cells*. *Arteriosclerosis, Thrombosis, and Vascular Biology*, 2007. **27**(1): p. 211-218.
134. Ishizuka, Y., et al., *TRIB1 downregulates hepatic lipogenesis and glycogenesis via multiple molecular interactions*. *Journal of Molecular Endocrinology*, 2014. **52**(2): p. 145.
135. Izuka, K., *The transcription factor carbohydrate-response element-binding protein (ChREBP): A possible link between metabolic disease and cancer*. *Biochimica et Biophysica Acta (BBA) - Molecular Basis of Disease*, 2017. **1863**(2): p. 474-485.
136. Makishima, S., et al., *Sin3A-associated protein, 18 kDa, a novel binding partner of TRIB1, regulates MTP expression*. *Journal of Lipid Research*, 2015. **56**: p. 1145-1152.
137. Soubeyrand, S., A. Martinuk, and R. McPherson, *TRIB1 is a positive regulator of hepatocyte nuclear factor 4-Alpha*. *Scientific Reports*, 2017. **7**(1): p. 1-12.
138. Lau, H.H., et al., *The molecular functions of hepatocyte nuclear factors - In and beyond the liver*. *J Hepatol*, 2018. **68**(5): p. 1033-1048.
139. Yan, Z., H. Yan, and H. Ou, *Human thyroxine binding globulin (TBG) promoter directs efficient and sustaining transgene expression in liver-specific pattern*. *Gene*, 2012. **506**(2): p. 289-94.
140. Doran, D.M. and I.L. Spar, *Oxidative iodine monochloride iodination technique*. *J Immunol Methods*, 1980. **39**(1-2): p. 155-63.
141. Borén, J., S. Rustaeus, and S.O. Olofsson, *Studies on the assembly of apolipoprotein B-100- and B-48-containing very low density lipoproteins in McA-RH7777 cells*. *J Biol Chem*, 1994. **269**(41): p. 25879-88.
142. Patro, R., et al., *Salmon provides fast and bias-aware quantification of transcript expression*. *Nat Methods*, 2017. **14**(4): p. 417-419.
143. Frankish, A., et al., *GENCODE reference annotation for the human and mouse genomes*. *Nucleic Acids Res*, 2019. **47**(D1): p. D766-d773.
144. Sonesson, C., M. Love, and M. Robinson, *Differential analyses for RNA-seq: transcript-level estimates improve gene-level inferences [version 1; peer review: 2 approved]*. *F1000Research*, 2015. **4**(1521).
145. Love, M.I., W. Huber, and S. Anders, *Moderated estimation of fold change and dispersion for RNA-seq data with DESeq2*. *Genome Biology*, 2014. **15**(12): p. 550.
146. Aung, L.H., et al., *Association of the TRIB1 tribbles homolog 1 gene rs17321515 A>G polymorphism and serum lipid levels in the Mulao and Han populations*. *Lipids Health Dis*, 2011. **10**: p. 230.
147. Caviglia, J.M., et al., *Different fatty acids inhibit apoB100 secretion by different pathways: unique roles for ER stress, ceramide, and autophagy*. *Journal of lipid research*, 2011. **52**(9): p. 1636-1651.
148. Htet, L., et al., *Association of the TRIB1 tribbles homolog 1 gene rs17321515 A>G polymorphism and serum lipid levels in the Mulao and Han populations*. 2011.
149. Ostertag, A., et al., *Control of adipose tissue inflammation through TRB1*. *Diabetes*, 2010. **59**(8): p. 1991-2000.

150. Hadizadeh, F., E. Faghihmani, and P. Adibi, *Nonalcoholic fatty liver disease: Diagnostic biomarkers*. World journal of gastrointestinal pathophysiology, 2017. **8**(2): p. 11-26.
151. Spinella, R., R. Sawhney, and R. Jalan, *Albumin in chronic liver disease: structure, functions and therapeutic implications*. Hepatology International, 2016. **10**(1): p. 124-132.
152. Nagiec, M.M., et al., *Novel tricyclic glycal-based TRIB1 inducers that reprogram LDL metabolism in hepatic cells*. MedChemComm, 2018. **9**(11): p. 1831-1842.
153. Singh, A.B. and J. Liu, *Berberine decreases plasma triglyceride levels and upregulates hepatic TRIB1 in LDLR wild type mice and in LDLR deficient mice*. Scientific Reports, 2019. **9**(1).
154. Ma, D., et al., *The liver clock controls cholesterol homeostasis through trib1 protein-mediated regulation of PCSK9/Low Density Lipoprotein Receptor (LDLR) Axis*. Journal of Biological Chemistry, 2015. **290**(52): p. 31003-31012.
155. Lin, J.H., P. Walter, and T.S.B. Yen, *Endoplasmic Reticulum Stress in Disease Pathogenesis*. Annual Review of Pathology: Mechanisms of Disease, 2008. **3**(1): p. 399-425.
156. Lee, Y.-H., et al., *Disruption of the c/ebpa Gene in Adult Mouse Liver*. 1997. **17**(10): p. 6014-6022.
157. Chens, B.P.C., et al., *ATF3 and ATF3 Delta Zip. Transcriptional Repression Versus Activation by Alternatively Spliced Isoforms*. 1994. p. 15819-15826.
158. Hai, T. and M.G. Hartman, *The molecular biology and nomenclature of the activating transcription factor/cAMP responsive element binding family of transcription factors: Activating transcription factor proteins and homeostasis*. 2001. p. 1-11.
159. Hai, T., C.C. Wolford, and Y.S. Chang, *ATF3, a hub of the cellular adaptive-response network, in the pathogenesis of diseases: Is modulation of inflammation a unifying component?* 2010. p. 1-11.
160. Chen, B.P., C.D. Wolfgang, and T. Hai, *Analysis of ATF3, a transcription factor induced by physiological stresses and modulated by gadd153/Chop10*. Molecular and Cellular Biology, 1996. **16**(3): p. 1157-1168.
161. Pan, Y.X., et al., *Activation of the ATF3 gene through a co-ordinated amino acid-sensing response programme that controls transcriptional regulation of responsive genes following amino acid limitation*. Biochem J, 2007. **401**(1): p. 299-307.
162. Hayner, J.N., J. Shan, and M.S. Kilberg, *Regulation of the ATF3 gene by a single promoter in response to amino acid availability and endoplasmic reticulum stress in human primary hepatocytes and hepatoma cells*. Biochim Biophys Acta Gene Regul Mech, 2018. **1861**(2): p. 72-79.
163. Chang, Y.S., H.W. Kan, and Y.L. Hsieh, *Activating transcription factor 3 modulates protein kinase C epsilon activation in diabetic peripheral neuropathy*. Journal of Pain Research, 2019. **12**: p. 317-326.
164. Lim, J.H., et al., *Organelle stress-induced activating transcription factor-3 downregulates low-density lipoprotein receptor expression in Sk-Hep1 human liver cells*. Biol. Chem, 2011. **392**: p. 377-385.
165. Chen, B.P., et al., *ATF3 and ATF3 delta Zip. Transcriptional repression versus activation by alternatively spliced isoforms*. J Biol Chem, 1994. **269**(22): p. 15819-26.

166. Reinke, A.W., et al., *Networks of bZIP protein-protein interactions diversified over a billion years of evolution*. *Science*, 2013. **340**(6133): p. 730-734.
167. Rodríguez-Martínez, J.A., et al., *Combinatorial bZIP dimers display complex DNA-binding specificity landscapes*. *eLife*, 2017. **6**.
168. Ishibashi, S., et al., *Hypercholesterolemia in low density lipoprotein receptor knockout mice and its reversal by adenovirus-mediated gene delivery*. *Journal of Clinical Investigation*, 1993. **92**(2): p. 883-893.
169. Bauer, R.C., et al., *Therapeutic Targets of Triglyceride Metabolism as Informed by Human Genetics*. *Trends Mol Med*, 2016. **22**(4): p. 328-340.
170. Allen-Jennings, A.E., et al., *The roles of ATF3 in glucose homeostasis. A transgenic mouse model with liver dysfunction and defects in endocrine pancreas*. *Journal of Biological Chemistry*, 2001. **276**(31): p. 29507-29514.
171. Hai, T. and M.G. Hartman, *The molecular biology and nomenclature of the activating transcription factor/cAMP responsive element binding family of transcription factors: activating transcription factor proteins and homeostasis*. *Gene*, 2001. **273**(1): p. 1-11.
172. Cheng, C.F., et al., *Adipocyte browning and resistance to obesity in mice is induced by expression of ATF3*. *Communications Biology*, 2019. **2**(1).
173. Jadhav, K. and Y. Zhang, *Activating transcription factor 3 in immune response and metabolic regulation*. *Liver Res*, 2017. **1**(2): p. 96-102.
174. Jang, M.K., et al., *ATF3 inhibits adipocyte differentiation of 3T3-L1 cells*. *Biochemical and Biophysical Research Communications*, 2012. **421**(1): p. 38-43.
175. Xu, Y., et al., *Hepatocyte ATF3 protects against atherosclerosis by regulating HDL and bile acid metabolism*. *Nature Metabolism*, 2021. **3**(1): p. 59-74.
176. Yan, F., et al., *Overexpression of the transcription factor ATF3 with a regulatory molecular signature associates with the pathogenic development of colorectal cancer*. *Oncotarget*, 2017. **8**(29): p. 47020-47036.
177. Yin, H.-M., et al., *Activating transcription factor 3 coordinates differentiation of cardiac and hematopoietic progenitors by regulating glucose metabolism*. 2020.
178. Papaioannou, V.E. and R.R. Behringer, *Early embryonic lethality in genetically engineered mice: diagnosis and phenotypic analysis*. *Veterinary pathology*, 2012. **49**(1): p. 64-70.
179. Turgeon, B. and S. Meloche, *Interpreting neonatal lethal phenotypes in mouse mutants: insights into gene function and human diseases*. *Physiol Rev*, 2009. **89**(1): p. 1-26.
180. Saiz, N. and B. Plusa, *Early cell fate decisions in the mouse embryo*. *Reproduction*, 2013. **145**(3): p. R65-80.
181. Mihajlović, A.I. and A.W. Bruce, *The first cell-fate decision of mouse preimplantation embryo development: integrating cell position and polarity*. *Open Biology*. **7**(11): p. 170210.
182. Ciemerych, M.A. and P. Sicinski, *Cell cycle in mouse development*. *Oncogene*, 2005. **24**(17): p. 2877-2898.
183. Brett, K.E., et al., *Maternal-fetal nutrient transport in pregnancy pathologies: the role of the placenta*. *International journal of molecular sciences*, 2014. **15**(9): p. 16153-16185.

184. Hay, W.W., Jr., *Placental-fetal glucose exchange and fetal glucose metabolism*. Transactions of the American Clinical and Climatological Association, 2006. **117**: p. 321-340.
185. Mitanchez, D., *Glucose Regulation in Preterm Newborn Infants*. Hormone Research in Paediatrics, 2007. **68**(6): p. 265-271.
186. Hawdon, J.M., M.P. Ward Platt, and A. Aynsley-Green, *Patterns of metabolic adaptation for preterm and term infants in the first neonatal week*. Arch Dis Child, 1992. **67**(4 Spec No): p. 357-65.
187. Aronoff, S.L., et al., *Glucose Metabolism and Regulation: Beyond Insulin and Glucagon*. Diabetes Spectrum, 2004. **17**(3): p. 183.
188. Halse, R., et al., *Control of Glycogen Synthesis by Glucose, Glycogen, and Insulin in Cultured Human Muscle Cells*. Diabetes, 2001. **50**(4): p. 720.
189. Lawrence, J.C. and P.J. Roach, *New Insights Into the Role and Mechanism of Glycogen Synthase Activation by Insulin*. Diabetes, 1997. **46**(4): p. 541.
190. Dent, P., et al., *The molecular mechanism by which insulin stimulates glycogen synthesis in mammalian skeletal muscle*. Nature, 1990. **348**(6299): p. 302-8.
191. Han, H.-S., et al., *Regulation of glucose metabolism from a liver-centric perspective*. Experimental & Molecular Medicine, 2016. **48**(3): p. e218-e218.
192. Hers, H.G., *The Metabolism of Glycogen in the Liver of Foetal and Newborn Rats*, in *Metabolic Adaptation to Extrauterine Life: The antenatal role of carbohydrates and energy metabolism*, R. De Meyer, Editor. 1981, Springer Netherlands: Dordrecht. p. 3-7.
193. Girard, J., *Metabolic adaptations to change of nutrition at birth*. Biol Neonate, 1990. **58 Suppl 1**: p. 3-15.
194. Girard, J. and p. Pegorier, *Pre-and Post-Partum Nutrition and Metabolism An overview of early post-partum nutrition and metabolism*. Placenta Biol. Neonate, 1998. **18**(38): p. 635-642.
195. Girard, J., *Gluconeogenesis in late fetal and early neonatal life*. Biol Neonate, 1986. **50**(5): p. 237-58.
196. Bougneres, P.F., et al., *Ketone body transport in the human neonate and infant*. J Clin Invest, 1986. **77**(1): p. 42-8.
197. Clément, S., et al., *The lipid phosphatase SHIP2 controls insulin sensitivity*. Nature, 2001. **409**(6816): p. 92-97.
198. Cotter, D.G., et al., *Obligate role for ketone body oxidation in neonatal metabolic homeostasis*. Journal of Biological Chemistry, 2011. **286**(9): p. 6902-6910.
199. Ibdah, J.A., et al., *Lack of mitochondrial trifunctional protein in mice causes neonatal hypoglycemia and sudden death*. Journal of Clinical Investigation, 2001.
200. Kuma, A., et al., *The role of autophagy during the early neonatal starvation period*. Nature, 2004. **432**(7020): p. 1032-1036.
201. Seghers, V., et al., *Sur1 knockout mice. A model for K(ATP) channel-independent regulation of insulin secretion*. The Journal of biological chemistry, 2000. **275**(13): p. 9270-7.
202. Hussain, K., *Congenital hyperinsulinism*. American Journal Of Pathology, 2005.
203. Guan, H., et al., *Competition between members of the tribbles pseudokinase protein family shapes their interactions with mitogen activated protein kinase pathways*. Scientific Reports, 2016. **6**(September): p. 32667-32667.

204. Ginsberg, H.N. and E.A. Fisher, *The ever-expanding role of degradation in the regulation of apolipoprotein B metabolism*. Journal of lipid research, 2009. **50 Suppl**(Suppl): p. S162-S166.
205. Stanley, C.A., *Perspective on the genetics and diagnosis of congenital hyperinsulinism disorders*. 2016. p. 815-826.
206. *Diazoxide-Responsive KATP Hyperinsulinism | Children's Hospital of Philadelphia*.
207. De Leon, D.D. and C.A. Stanley, *Congenital Hypoglycemia Disorders: New Aspects of Etiology, Diagnosis, Treatment and Outcomes: Highlights of the Proceedings of the Congenital Hypoglycemia Disorders Symposium, Philadelphia April 2016*. Pediatr Diabetes, 2017. **18**(1): p. 3-9.
208. Hussain, K., *The Diagnosis and Management of Hyperinsulinaemic Hypoglycaemia*. 2015.
209. Remedi, M.S. and C.G. Nichols, *Hyperinsulinism and Diabetes: Genetic dissection of β -cell metabolism-excitation coupling in mice*.
210. Al-Nozha, M.M., H.M. Ismail, and O.M. Al Nozha, *Coronary artery disease and diabetes mellitus*. Journal of Taibah University Medical Sciences, 2016. **11**(4): p. 330-338.
211. Zhou, Y. and L. Rui, *Major urinary protein regulation of chemical communication and nutrient metabolism*. Vitamins and hormones, 2010. **83**: p. 151-163.
212. Thoß, M., et al., *Diversity of major urinary proteins (MUPs) in wild house mice*. Scientific Reports, 2016. **6**(1): p. 38378.
213. Charkoftaki, G., et al., *Update on the human and mouse lipocalin (LCN) gene family, including evidence the mouse Mup cluster is result of an "evolutionary bloom"*. Human genomics, 2019. **13**(1): p. 11-11.